^ *Written by Mr. C Y Lam*

* *Not completed*

6.1 Introduction

Each year heavy rains associated with tropical cyclones cause great loss of life and a tremendous amount of damage yet, in many places, this rainfall is necessary to maintain water supplies and sustain life. It is the potential of a tropical cyclone for causing moderate to intense rainfall over periods from ~~6 to 48 hours~~ a few hours to over one week which has to be considered as a major cause of disasters. Indeed, during the passage of many of these storms, it is only the rainfall which gives rise to significant damage and loss of life. Landslips, mud avalanches, flash floods and rapid erosion occur over hilly and mountainous terrain while over low-lying land, extensive flooding takes place because drainage systems are unable to carry away the large volume of runoff; this situation is exacerbated when a storm surge and/or a high tide reduce the fall and effectiveness of drainage systems.

Although tropical cyclones have caused world-record rainfalls in periods from 9 hours to 8 days (Fig. 6.1(1) and Table 6.1(1)) the total amount recorded can vary widely from case to case. Recorded storm rainfall has ranged from nil to ~~4 129.8~~ 5 210 mm ~~or about 6.5~~ times London's average annual rainfall of 632 mm! However, at stations without extreme oreigenic effects, the great majority of rainfalls associated with the passage of a tropical cyclone are less than 800 mm. Cases are on record of the close passages of hurricanes and typhoons causing winds of more than 34 m/s at a station with little or no accompanying rainfall, but they, of course, are exceptional.

Although this chapter deals with tropical-cyclone rainfall it must be realized at the outset that there are significant uncertainties in both measuring the rainfall when the winds are of hurricane force and of defining what is meant by the term "tropical-cyclone rainfall". The former uncertainty arises firstly because hurricane-force winds so disturb the air flow over raingauges as to reduce the catch by amounts which may exceed 80% and secondly because ~~of local~~ oreigenic ~~effects.~~ The uncertainty in defining tropical cyclone rainfall arises because both weak and intense tropical cyclones are associated with regional weather patterns which may give rise to heavy rain at distances as great as 2 000 km from the storm centre. It is usual to consider the rainfall from tropical cyclones as made up of "direct" and "indirect" components, but it is then

Table 6.1(1). World's greatest observed point rainfalls from Paulhus (1965) with additions marked + and tropical cyclone events marked c

Duration	Depth mm	Location	Date
3 s	0.58	Hong Kong	Sept 5, 1977+c
15 s	3.1	- ditto -	Aug. 17, 1971+c
1 min	38.0	Barot, Guadeloupe	Nov. 26, 1970
8 min	126.0	Füssen, Bavaria	May 25, 1920
15 min	198.1	Plumb Point, Jamaica	May 12, 1916
20 min	205.7	Curtea-de-Arges, Roumania	July 7, 1889
42 min	304.8	Holt, Mo	June 22, 1947
2 h 10 min	482.6	Rockport, W. Va	July 18, 1889
2 h 45 min	558.8	D'Hanis, Tex. (17 mi. NNW)	May 31, 1935
4 h 30 min	782.3	Smethport, Pa	July 18, 1942
9 h	1086.9	Belouve, La Réunion	Feb. 28, 1964 c
12 h	1340.1	- ditto -	Feb. 28-29, 1964 c
18 h 30 min	1688.8	- ditto -	Feb. 28-29, 1964 c
24 h	1869.9	Cilaos, La Réunion	Mar. 15-16, 1952 c
2 d	2499.9	- ditto -	Mar. 15-17, 1952 c
3 d	3240.0	- ditto -	Mar. 15-18, 1952 c
4 d	3721.0	Cherrapunji, India	Sept. 12-15, 1974 +
5 d	3853.9	Cilaos, La Réunion	Mar. 13-18, 1952 c
6 d	4055.1	- ditto -	Mar. 13-19, 1952 c
7 d	4110.0	- ditto -	Mar. 12-19, 1952 c
8 d	4129.8	- ditto -	Mar. 11-19, 1952 c
14 d	5210	Grand Ilet, La Réunion	Jan. 15-28. 1980 +c
31 d	9300.0	- ditto -	July 1861
2 mo	12766.8	- ditto -	June-July, 1861
3 mo	16368.8	- ditto -	May-July, 1861
4 mo	18737.6	- ditto -	April-July, 1861
5 mo	20411.9	- ditto -	April-August, 1861
6 mo	22454.4	- ditto -	April-Sept. 1861
11 mo	22990.0	- ditto -	Jan.-Nov. 1861
1 a	26461.2	- ditto -	Aug. 1860 - July 1861
2 a	40768.3	- ditto -	1860 - 1861
		Other tropical cyclone extreme rainfalls	
1 h	189.5	Linzhung, Honan, China	Aug. 7, 1975+c
2 h	385.6	Belouve, La Réunion	Feb. 28, 1964+c
6 h	766.1	- ditto -	Feb. 28, 1964+c

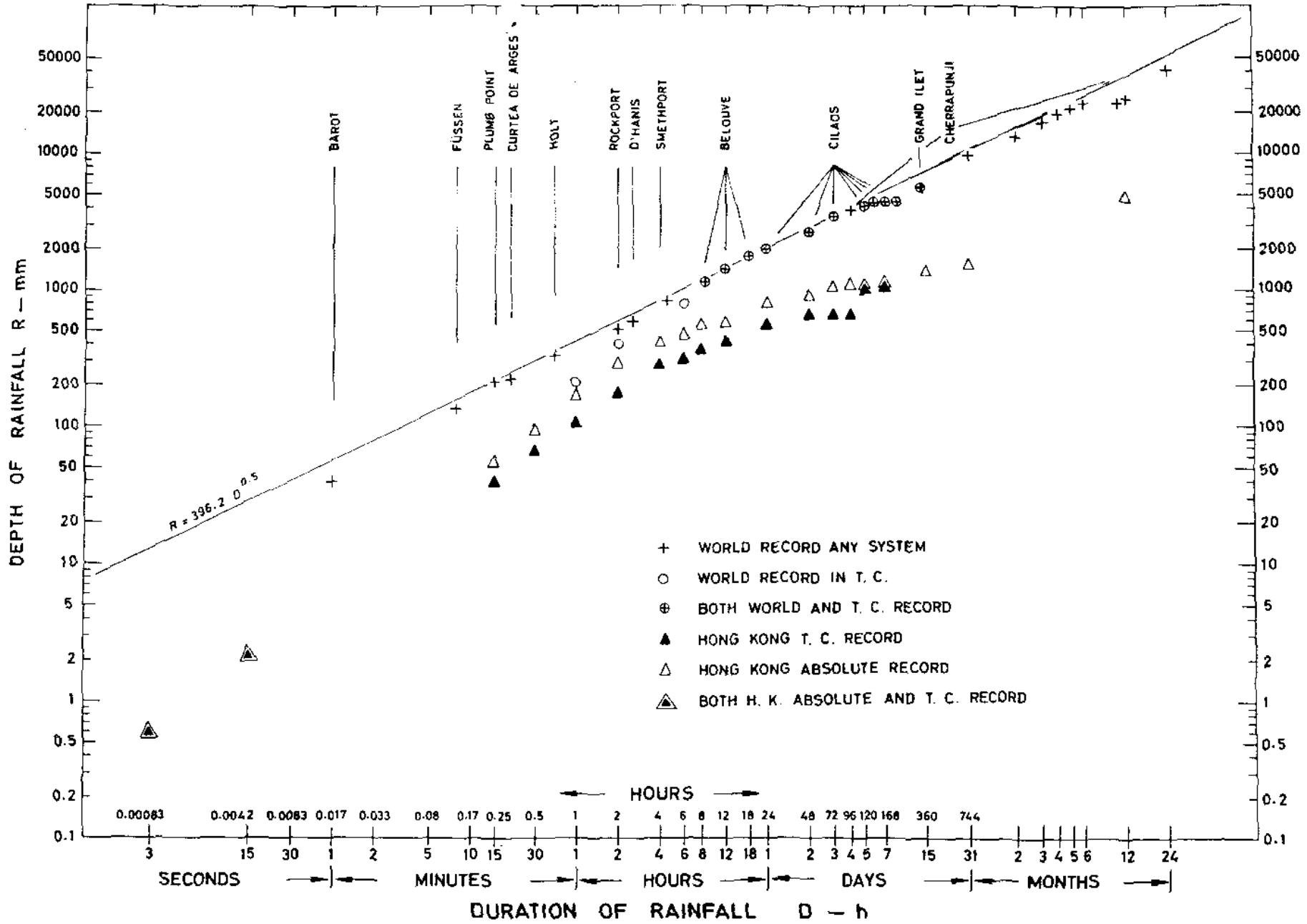

Fig. 6.1(1). World rainfall records from Table 6.1(1) plotted along with extremes from the long rainfall record of the Royal Observatory Hong Kong. The envelope to the world records is also shown.

necessary to decide where to draw the distinction between the two and, additionally, there will be cases when attribution of indirect rainfall to a cyclone cannot be positively established. The problem arises most frequently when storms ~~are near~~ approach the Asiatic mainland and interact with the monsoons or baroclinic disturbances such as waves in the westerlies and surface fronts.

It is often asked what proportion of the average annual rainfall at a station, is attributable to tropical cyclones? This question cannot be answered precisely for the reasons given above. However, the great majority of coastal stations bordering the Western Pacific between 10°N and 30°N receive between 15% and 50% of their rain from tropical cyclones and their associated rains. The percentage can rise to as much as 70% in mountainous areas favoured by a high frequency of tropical cyclones - such as in Taiwan and northern Philippines.

It is of interest to note that tropical cyclones occasionally penetrate into normally arid zones bringing more than the average annual rainfall to the affected areas. ~~several times as great as the average annual rainfall~~. This occurs particularly in the Middle East, in the arid areas of south-west North America and in parts of Australia. Such penetrations take place when the broad scale flow is such as to maintain a moist, tropical inflow to the remnant vortex (sect). A notable example of this effect arrived with a cyclone from the ~~is the~~ Arabian Sea ~~cyclone which~~ travelled along the Gulf of Aden on 27 October 1972, the first to do so for 75 years (See Fig. 11.). The storm brought 229 mm of rain to Djibouti and 152 mm to Aden; these figures are nearly twice and six times the respective average annual rainfalls of 127 and 25 mm. In the U.S.A. in October 1977 hurricane Heather brought rainfall amounts to some stations in Arizona which exceeded the normal annual average. McBride (1980) presented radar and satellite pictures of cyclone Peter-Greta on 16 January 1979 to show that the storm retained spiral rainbands at Alice Springs, in the centre of Australia, after travelling 1 400 km from the NE coast.

The greatest rates of rainfall and the worst floods associated with tropical cyclones are not necessarily due to the passage of the centre of an intense storm over or close to the area concerned. At distances of about 500 - 2 000 km from a storm centre, convective instability may be greater than that nearer the centre and, if the flow in the upper troposphere is favourable, very heavy rain may occur ~~either~~ in long inflow rainbands especially ~~or~~ at places where the local topography and airflow trigger the instability.

In addition, weakening tropical storms moving inland, particularly in the autumn, can give rise to greater flooding than is usually associated with mature typhoons. The total rainfall at a station from the passage nearby of a tropical cyclone is poorly correlated with the intensity of the storm as measured by the lowest central pressure or highest wind speed. Fast-moving intense typhoons have crossed stations without dropping significant amounts of rain whilst some slow-moving weaker storms or remnants have brought disastrous flooding.

Tropical-cyclone rainfall is a difficult phenomenon to characterise for not only is its distribution within a storm highly variable but the amount recorded at a gauging station depends additionally on a number of factors such as the speed and track of the storm, oreigenic effects, the exposure of the raingauge and wind speed.

Oreigenic effects greatly enhance tropical-cyclone rainfall. The rate of rainfall at a given location during the passage of a storm is determined by the moisture content of the low-level inflow and its rate of rise. The moisture-laden, high-speed winds in a tropical cyclone are deflected upwards by hills or mountains and thereby attain high rates of ascent. It is under such conditions that record-breaking rainfalls occur. Higher rates are recorded over shorter periods in other weather systems - such as heat thunderstorms - in which high ascent rates are caused by convective instability. For longer periods, record rainfalls are associated with oreigenic effects in mountainous areas which are subject to persistent humid winds. Two such notable areas are in the southern slopes of the Himalayas and in the mountains of Hawaii where steady southwest monsoon and trade winds blow, respectively. The highest average annual rainfall (12.5 m) occurs at a station near the peak of Kawai in the Hawaiian Islands. Intense rainfall such as is associated with reflectivities greater than 55 dBZ (see sect 10) are seldom observed in tropical cyclones. Maximum reflectivities of about 45 dBZ are more usual. These reflectivities would correspond to rainfall intensities of about 150 and 30 mm/h respectivity (but see Table 10.4(1)). Flooding may result from low rates of rainfall (10-25 mm/h) sustained over days as illustrated in Fig. 6.4.3(2) or from a shorter period of high rates of rainfall as illustrated in Fig.6.3.6(1) or from a combination of the two.

The rainfall in a tropical cyclone tends to increase at first as it enters land not only because of oreigenic effects but also because increased friction retards the low-level winds which then blow more directly across the isobars increasing the convergence and rainfall in the inner regions of the storm. The effect is usually temporary because further inland the storm's inflow will weaken and hold less moisture ~~the further the storm moves inland~~. However, rainfall may increase inland if the storm moves onto a mountain barrier or meets a cold front. The tendency for the rainfall in a tropical cyclone to increase at a coastline must be allowed for when preparing flood or landslip warnings and, in particular, the indications of the water content of a tropical cyclone over the sea, as given by radar (sect 10.4.6), may lead ~~will tend~~ to be an underestimate of the rainfall in coastal areas.

Paulhus (1965) fitted the envelope curve $R=421.6D^{0.475}$ to the observations in Table 6.1 less the more recent events marked with a $^{+}$. The envelope shown has been expressed in terms of the square root of the duration D, as originally proposed by Fletcher (1950). The extreme depth of rainfall R - in millimetres is then given in terms of the duration D - in hours - as $R=396.2D^{0.5}$.

6.2. Rainfall Models

6.2.1 Simple model

Order-of-magnitude calculations of the distribution of rainfall in a steady-state typhoon were first made on the assumption that all inflow takes place in the lowest 1 km or sub-cloud layer and all outflow takes place in the upper troposphere above 10 km as specified in Riehl's (1950) model of a tropical cyclone. The specific humidity of the inflow will be typically in excess of 16.5 g/kg while that of the outflow will be less than 1 g/kg (See Table and Fig.). The moisture loss from the top of the typhoon will therefore be less than 5% of the inflow and can be neglected along with the relatively small amounts of liquid water or ice that may be lost. On these assumptions the total amount of rainfall within a cylinder around the storm centre can be equa to the flux of moisture across its circumference in the lowest 1 km (Δp = 100 mb) layer. Horiguti (1928) made a calculation using these assumptions and inflow and humidity data from the "Okinawa" typhoon of 18 August 1924. His results were in very good agreement with the observed rainfall. Hughes (1952) made similar calculations using the inflow data from his mean over-sea typhoon (Fig. 5.3.1 (e)) which he considered to be appropriate to the lowest 1 km or 100 mb (Δp). He chose a value of 16.6 g/kg for the specific humidity $\bar{q}$ (or the nearly equal mixing ratio $\bar{w}$) from Schacht's (1946) mean hurricane sounding.

Following Hughes the mass of moist air entering a cylinder of radius r is equal to the circumference $2\pi r$ multiplied by the depth of the layer Δh, the average radial velocity $\bar{v}_r$ and the density ρ. The product of this mass flux and the mean specific humidity $\bar{q}$ gives the inflow of moisture which can be equated to the product of the rate of rainfall R per unit area and time and the total area πr^2, yielding

$$R = \frac{2\bar{v}_r}{r} \cdot \bar{q} \rho \Delta h$$

But $\rho \Delta h = \Delta p/g$ so that

$$R = \frac{2\bar{v}_r}{r} \cdot \bar{q} \cdot \frac{\Delta p}{g} \qquad (6.1)$$

Using eqn (6.1) and the values Δp = 100 mb, $\bar{q}$ = 16.6 g/kg and taking values of $\bar{v}_r$ from Fig. 5.3.(1e), Hughes obtained the results shown in Table 6.2.1(1). They show that the rate of rainfall - averaged in space and time - should decrease outwards from the inner ring. Hughes' sample consisted of large, mature typhoons moving at about 5 m/s and if his average typhoon with the characteristics given in Table 6.2.1(1) moved in a straight line directly over a low level station then the total storm rainfall would amount to 277 mm over a 48 h period. This amount is not inconsistent with the observations from the wettest storms at island stations (Table 6.3.2(1)) especially if some allowance is made for gauge loss. However, the radial distribution of the rainfall in tropical cyclones as observed at selected stations (Fig. 6.2(1)) departs considerably from Hughes' model. In particular, the rainfall in the model is higher in the inner regions and lower in the outer regions. There are three factors which can jointly cause this discrepancy. Firstly, the model is derived from large intense typhoons whereas station averages are from tropical cyclones of a wide range of sizes and intensity passing at various speeds. Secondly, gauges at observing stations suffer a large loss of catch in hurricane force winds and thirdly, the calculation ignored the contribution of water vapour from evaporation from the warm ocean . Tropical cyclones converge large quantities of water vapour and this is enhanced by increased evaporation from the warm ocean due to the high wind speeds. Some of the water vapour carried into the storm goes towards raising humidity levels in the inner storm areas but by far the greater part falls out as rain.

Evaporation from the ocean beneath a typhoon cannot be directly measured but is estimated by budget studies using the principle of the conservation of water vapour[+]. In the steady state the contribution from evaporation is taken as the difference between the convergence of water vapour into a cylinder and the rainfall there. There are considerable errors in this method as the average rainfall in a tropical cyclone is

[+] The equation for the conservation of water vapour integrated over a cylindrical volume extending from the surface to 100 mb is:-

$$\int \frac{\partial (\bar{\varrho}\bar{q})}{\partial t} = -\int \nabla \varrho v_q + \text{Evap.} - \text{Precip.}$$

For steady conditions the term on the left is zero.

Table 6.2(1) Rainfall and energy values in moving typhoons.
Calculated from data in Hughes (1952)

Radius	Total Latent Heat release inside radius	Total rainfall inside radius	Av. rainfall inside radius	Ring	Av. rainfall in ring	
^{o}Lat	10^{14} W	t/h x 10^{9}	mm/d	^{o}Lat	mm/d	mm/h
0.5	2.43	0.36	863	0.0 - 0.5	863	36.0
1.0	3.78	0.57	337	0.5 - 1.0	160	6.7
1.5	4.55	0.68	180	1.0 - 1.5	54	2.3
2.0	4.85	0.73	108	1.5 - 2.0	15	0.6
2.5	4.91	0.74	70	2.0 - 2.5	2.6	0.1
3.0	5.05	0.76	50	2.5 - 3.0	4.5	0.2
3.5	5.35	0.80	39	3.0 - 3.5	8.8	0.4
4.0	5.38	0.81	30	3.5 - 4.0	0.4	-

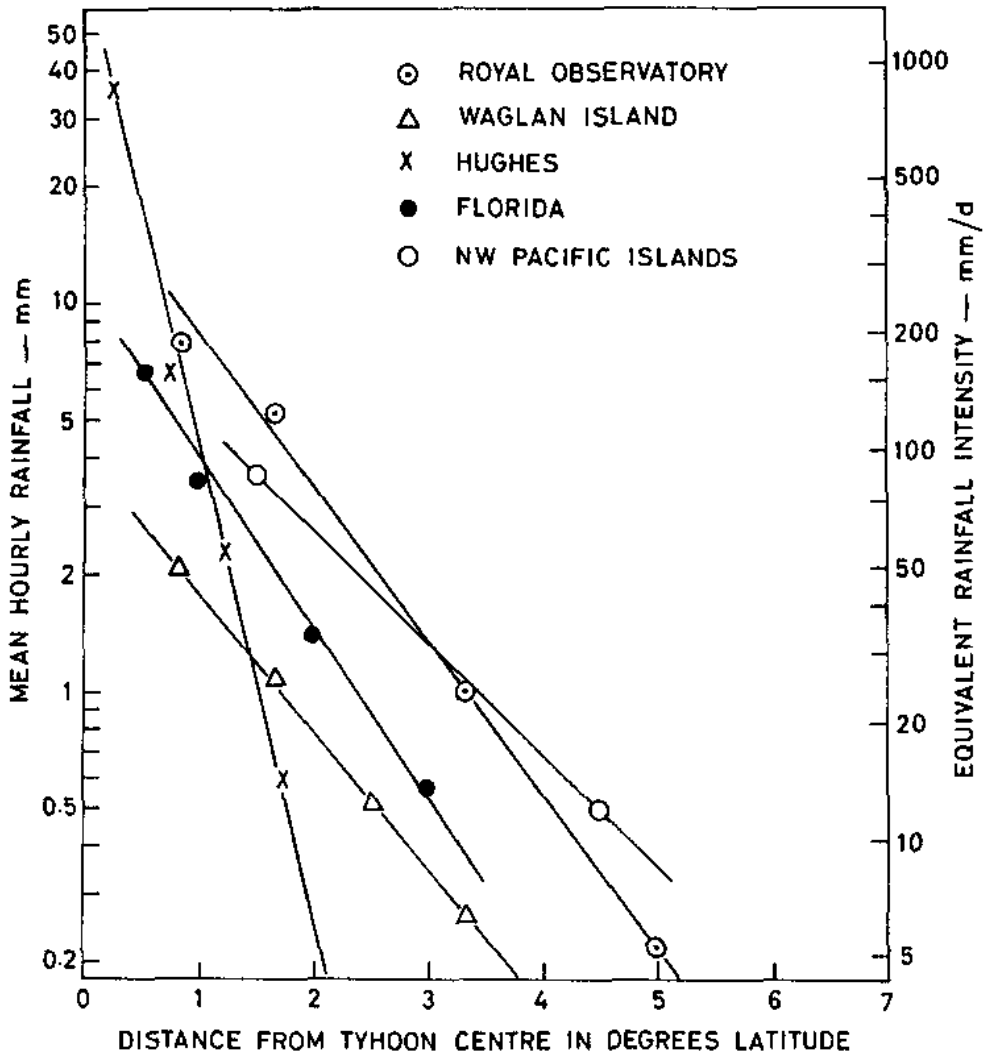

Fig. 6.2(1). Mean hourly rainfall relative to the centre of typhoons and Florida hurricanes. The hurricane data is from Fig. 6.3.3. The Pacific island data is from Frank (1976) and the rainfall at the Hong Kong stations of the Royal Observatory and Waglan Island is from Kwong (1974).

in doubt (see Fig. 6.2(1)) and the radial velocity of the wind, which greatly affects the moisture flux, is also difficult to estimate. Frank (1976) used composite rawinsonde data from Pacific stations to determine the average convergence of water vapour and the Florida and Pacific curves of Fig. 6.2(1) were used for the average profile of rainfall. Table 6.2(2) shows the average evaporation in Pacific tropical cyclones obtained by this method.

Evaporation from the ocean in a tropical cyclone falls off with distance from the centre in much the same way as does the wind speed indeed, the evaporation depends greatly on wind speed and can be estimated from the bulk aerodynamic formula Evap. = $\varrho C_E v(q_s - q)$. In this formula v is the 900 mb wind speed q_s is the saturated specific humidity of the sea surface q the specific humidity of air at the surface and C_E is an evaporation co-efficient usually found to be in the range $1.5 - 2.0 \times 10^{-3}$ for all wind speeds. Frank (1976) used 900 mb winds and a value of C_E of 1.7×10^{-3}. $(q_s - q)$ was found to be approximately constantly at 4.8×10^{-3} but would be less in the inner regions where colder water and high relative humidity will be found. The evaporation is therefore approximately proportional to wind speed and estimates made using this formula agree well with those shown in Table 6.2(2). The average summer evaporation in normal weather conditions in the tropical Pacific area is about 6 to 7 mm/d. At Hong Kong in July, for example, the average daily evaporation from a Class A pan (average temperature 30.8°C) is 5.8 mm. but over the Pacific Ocean the water is usually warmer and the wind speed greater. Heavy rainfall and wind-induced splashing invalidate pan readings in the high wind-speed areas of typhoons but, in their outer circulation and in the absence of rain, pan evaporation can be as high as 9 mm. Such a reading occurred at Hong Kong on the approach of typhoon Wanda on 30 August 1962.

The uncertainties inherent in the methods used to determine the evaporation in Table 6.2(2) have been noted. Widely different values can be obtained by using other profiles for the radial distribution of rainfall or other wind models such as, for example, the one in Fig. 5.3(1e). Nevertheless, Table 6.2(2) represents the best estimate of the average evaporation and rainfall in typhoons and helps to illustrate the importance of the former for the latter. For example, although most (75%) of the rainfall in the inner region (0-2°) of a typhoon is derived from the convergence of water vapour, about 65% of the rainfall within 0 - 6°

Table 6.2.(2)
(After Frank 1976)

Water Budget mm/d

Convergence of q	67	12	-7	1	-1	-1	
Precipitation	90	23	7	7	7	7	
Required evaporation from ocean	23	11	14	6	8	8	
Distance from T.C. centre	0^{o}	2^{o}	4^{o}	6^{o}	8^{o}	10^{o}	12

may be attributed to evaporation over that area. The area weighted evaporation within the 0 - 6° circle is about 14 mm/d or about twice the normal summer value. The excess is attributable to the high wind speeds and accounts for 33% of the total precipitation within 6° of the storm centre. If introduced into Hughes' simple model the additional rainfall from evaporation in the outer parts of the storm would raise the theoretical curve of Fig. 6.2(1) to move more into line with the distributions of observed rainfall. The reduced role of evaporation when a storm moves over extensive land areas contributes to its rapid decay.

6.2.2 Model distribution of rainfall

The idealised rainfall distribution in a tropical cyclone consists of a central rain-free eye surrounded by an annular eye wall with radial depth of about 30 km. The eye wall contains continuous and very heavy rainfall averaging 25 mm or more in one hour with the rate of rainfall over short periods of time being as high as 500 mm/h as is shown in Fig. 6.3.6(2b).

Outside the eye wall are the spiral rainbands illustrated in Fig. 1. and shown in the radar photographs in Chapter 4 and Chapter 10. In a schematic storm the bands would be well defined and evenly spaced. In practice they are variable in number and in their orientation around the eye and they may be discrete and clearly defined as shown in Alice in Fig. 10.7(5) or in Wendy in Fig.4.1 or they may be more numerous and near contiguous and embedded in less heavy rain areas as in typhoons Dot and Shirley in Fig. 4.3.

Ten typhoons for which good radar photographs of the total rain areas were available were examined to determine the extent of rain areas relative to the total storm area. The area of the typhoons was taken as being that contained within the outermost closed isobar (1 mb interval). The cloud cover, as indicated by satellite photographs, averaged 90% of this area while rain areas averaged 30%. The larger typhoons - 7.6° and 13.3° latitude in diameter - had proportionately less rainfall - less than 15% - but for the majority of storms the rain area was between 20% and 40% of the area contained within the outer isobar.

One feature occasionally found ahead of a typhoon is the precursor band. This rainband if present is found outside the spiral rainbands. It is usually less curved than normal spiral bands and advances in the direction of the typhoon and ahead of the centre. Such precursor bands consist of a narrow band of intense convection storms like a squall line, and are often accompanied by thunder. These bands as seen by radar or satellites are described and illustrated in sect 10.6.4 and sect 11.6.2 respectively.

6.2.3 Average distribution of rainfall

The average distribution of rainfall around a tropical cyclone centre has not yet been adequately described. The literature contains assertions and data analyses that are contradictory. Early observations of the distribution of rainfall in typhoons as determined from stations in the Philippines were presented by Depperman (1937). The distribution of rainfall in hurricanes was presented by Cline (1926) and, for storms over the relatively flat Florida peninsula by Miller (1958). These three studies all indicated that the rainfall maximum occured in the right front of the tropical cyclone centre as illustrated by Miller's data in Fig. 6.2.3(1). Miller considered that oreigenic effects over Florida would be minimal but, he did adjust the gauge catch for wind effects by adding 30% to 80% of the reading according to rainfall intensity. Depperman's data would have been strongly influenced by both oreigenic and wind effects. It is possible that there may be a systematic change in rainfall distribution when a tropical cyclone recurves into the westerlies. It should therefore be noted that both Cline's and Miller's data (Shields 1973) refer mainly to recurving cyclones. Dunn and Miller (1964), proposed that the precipitation pattern of low-lattitude storms is symmetrical with a right front quadrant maximum developing as hurricanes changed path to move northwards.

Frank (1977) examined 21 years of hourly data from nine small Pacific island stations and 12 years of 12 h data from four small Japanese islands. These rainfall observations were not corrected in any way for wind speed and they probably all contain significant local oreigenic contributions. The average rainfall rates for four quadrants in 2° bands and the averages for the bands themselves are shown in Fig.6.2.3(2). No striking asymmetries are shown by this analysis but, if anything, the right rear, between 2° and 4° from the centre, has rather more rain than elsewhere. The rainfall rates are higher than those observed in hurricanes by Miller (Fig. 6.2.3(1)) in spite of the latter being adjusted for wind speed. This is probably due to the larger mean size of typhoons and the islands' oreigenic contributions. It is of interest to note that a maximum of low-level convergence is indicated to the rear of the centre of the average typhoon as shown in Fig. 5.3.1(2) which is based on aircraft wind observations.

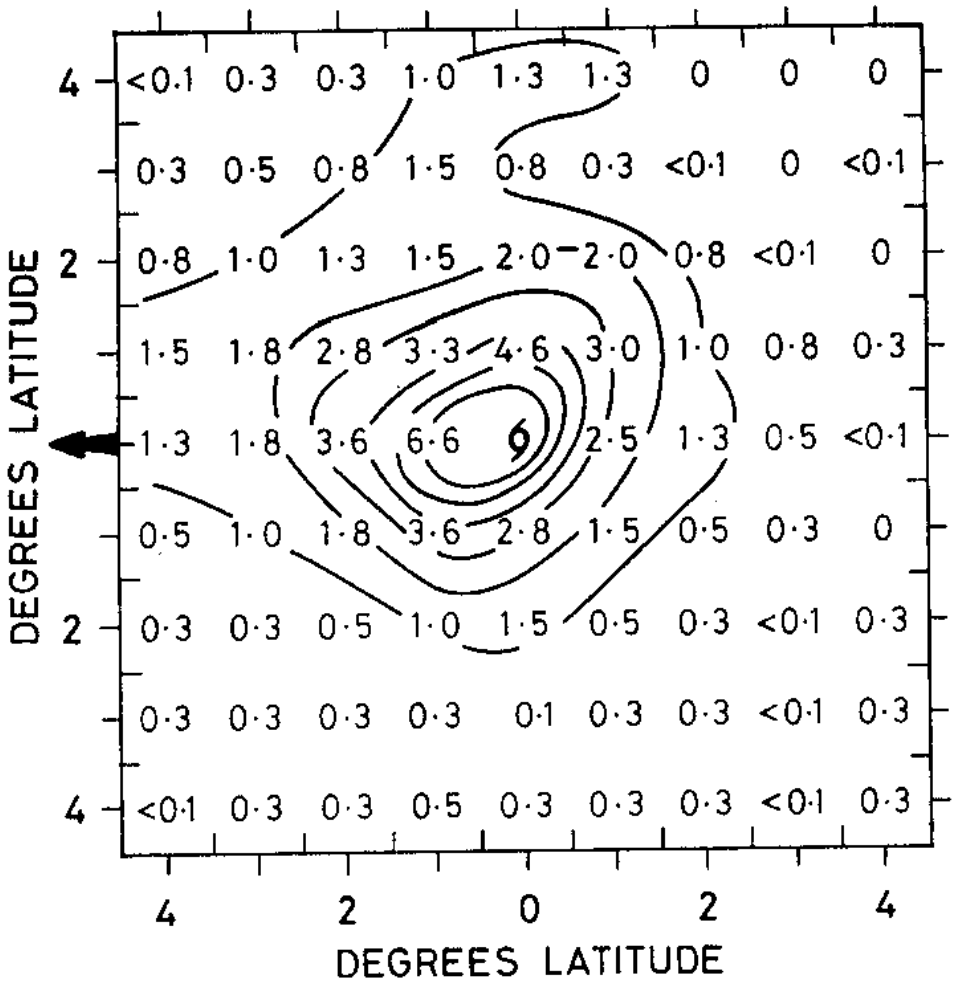

Fig.6.2.3(1)Mean hourly rainfall (mm) in one degree squares relative to the centre of 16 Florida hurricanes. The arrow indicates the direction of movement and the isohyets (see text) are drawn at intervals of 1 millimetre from 1 to 6. The rainfall in the centre square was 6.6 mm (data from Miller 1958).

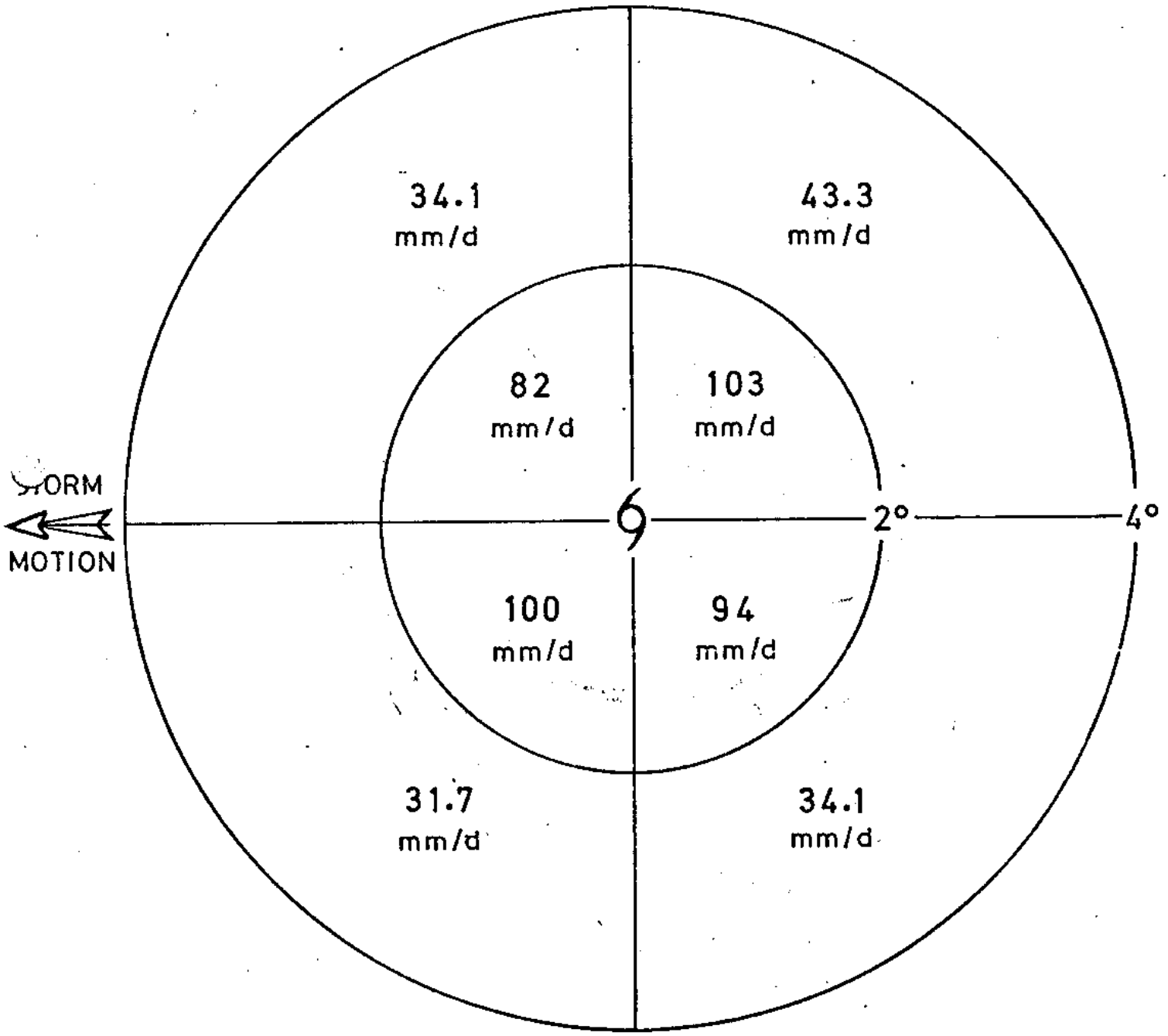

TOTALS AND AVERAGES IN BANDS

0°- 2° Band	1488 h	5.86 m	94.5 mm/d
2°- 4° Band	3499 h	5.19 m	35.4 mm/d
0°- 4° Band	4987 h	11.05 m	53.0 mm/d

Fig. 6.2.3 (2). Mean precipitation around tropical cyclones as derived from observations from 13 Pacific island stations. (After Frank 1977).

Kwong (1974) presented rainfall intensities, before and after the passage of 264 tropical cyclones whose centres passed within 185 km of the Royal Observatory, Hong Kong. Fig. 6.2.3(3) shows mean hourly rainfall over 60 h for the whole sample of 264 storms (a), and for the sub-groups whose centres passed within 28 km of the Observatory (b), and westward moving storm which passed within 185 km to the north (c), and to the south (d). All these groups show greater intensities and more rain after the passage than before the passage. The ratio of after-storm rainfall to before-storm rainfall varies from 1.29 for those passing over (within 28 km) the Observatory to 2.66 for those passing to the north. Different storm tracks will be associated with different oreigenic effects which will modify the storm rainfall as received at the Observatory. The rainfall in 13 typhoons which passed close to the small offshore island of Waglan is therefore shown, for comparison, in Fig. 6.2.3(4). This sample also shows the heaviest rain to the rear of the centre. The distribution of rainfall in the 13 storms varied greatly about the mean. Within a few hours of the passage of the centres, the standard variation of the hourly amounts is about twice the mean value; further away, the standard deviation and the mean are nearly equal. The mean storm rainfall the 13 typhoons was only 65·3mm with standard deviation 31·8mm. The typhoons had lowest pressures between 944mb and 989mb.//

Rainfall recorded at land stations is not a reliable guide to the distribution of rainfall in a storm because, apart from the instrumental uncertainties and ~~the~~ coastal and local oreigenic effects there are also effects due to drier air being drawn into a cyclone on a long land track such as, for example, across south China. Remote sensing of rainfall by radar or from satellites can be used to better determine the distribution of rainfall in these storms when they are over the oceans distant from land.

Heavy rainfall in mature tropical cyclones over the ocean is always found concentrated in a ring around the eye at the centre of the storm - the eye wall - but, the location of the area of heaviest rain outside the eye wall is variable. In addition, the location of rainbands carrying the heaviest rain is also variable. Fig. 6.2.3(5) shows the digitised rainfall depiction (see sect 10.) in hurricane Anita on 2 September 1977 as it was moving on a course to the west-soutwest across the Gulf of Mexico. The heaviest rainfall both in the eye wall - at this particular moment - and in the outer regions of the hurricane are in the right rear. On the other hand, the heaviest rainfall in the

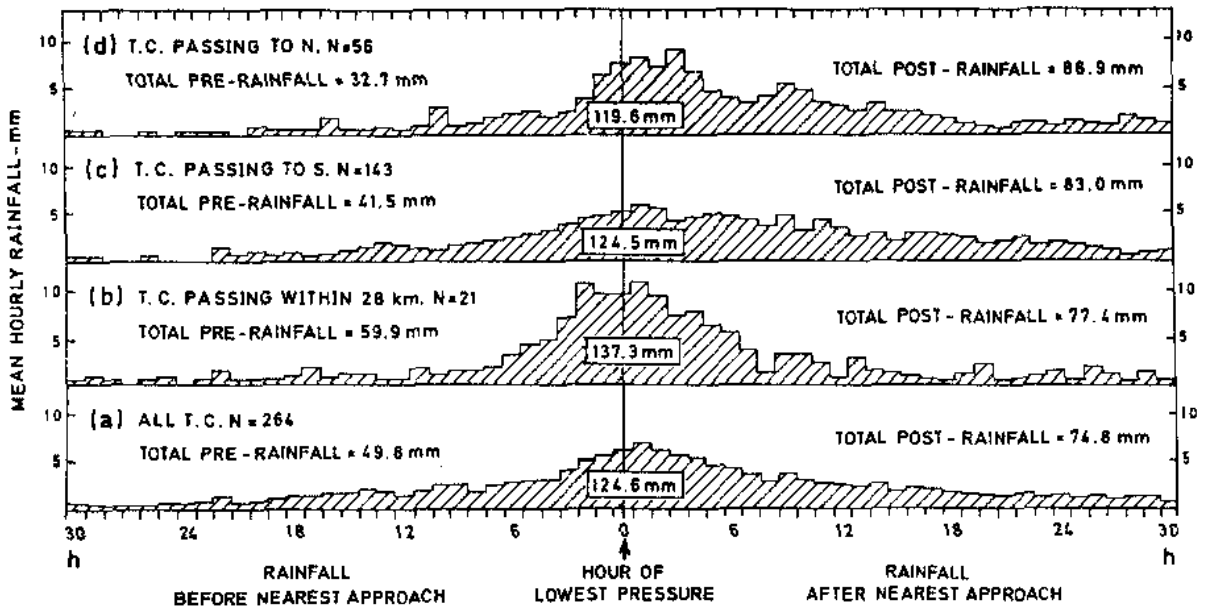

Fig. 6.2.3(3). Mean hourly rainfall recorded at the Royal Observatory, Hong Kong during the passage of tropical cyclones within 185 km, on different tracks, in the period 1884-1979, 1947-1971 (After Kwong 1974).

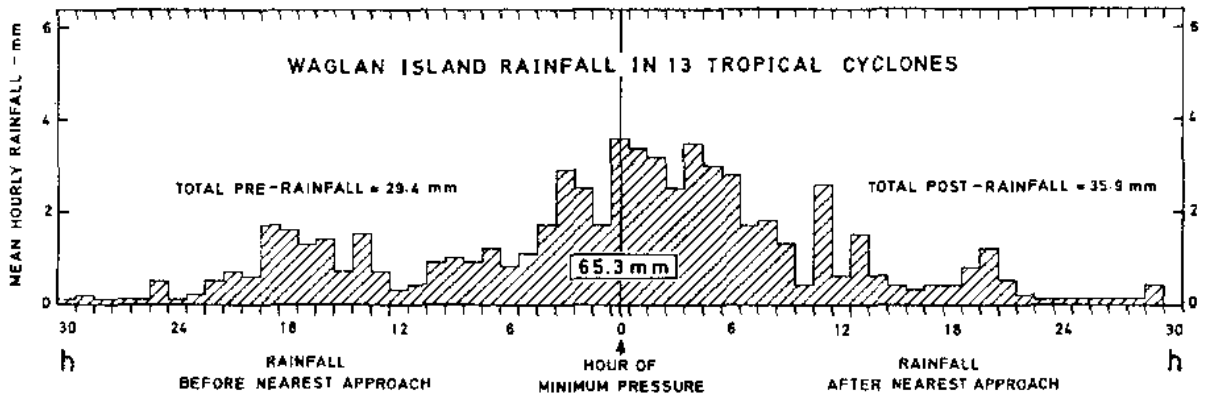

Fig. 6.2.3(4). Mean hourly rainfall at Waglan Island (18 km SE of the Hong Kong Observatory) during the passage of 13 typhoons whose centres passed within 30 km of the island in the period 1957-1978. The movement of the typhoons was between W and N and their average speed was 4.3 m/s.

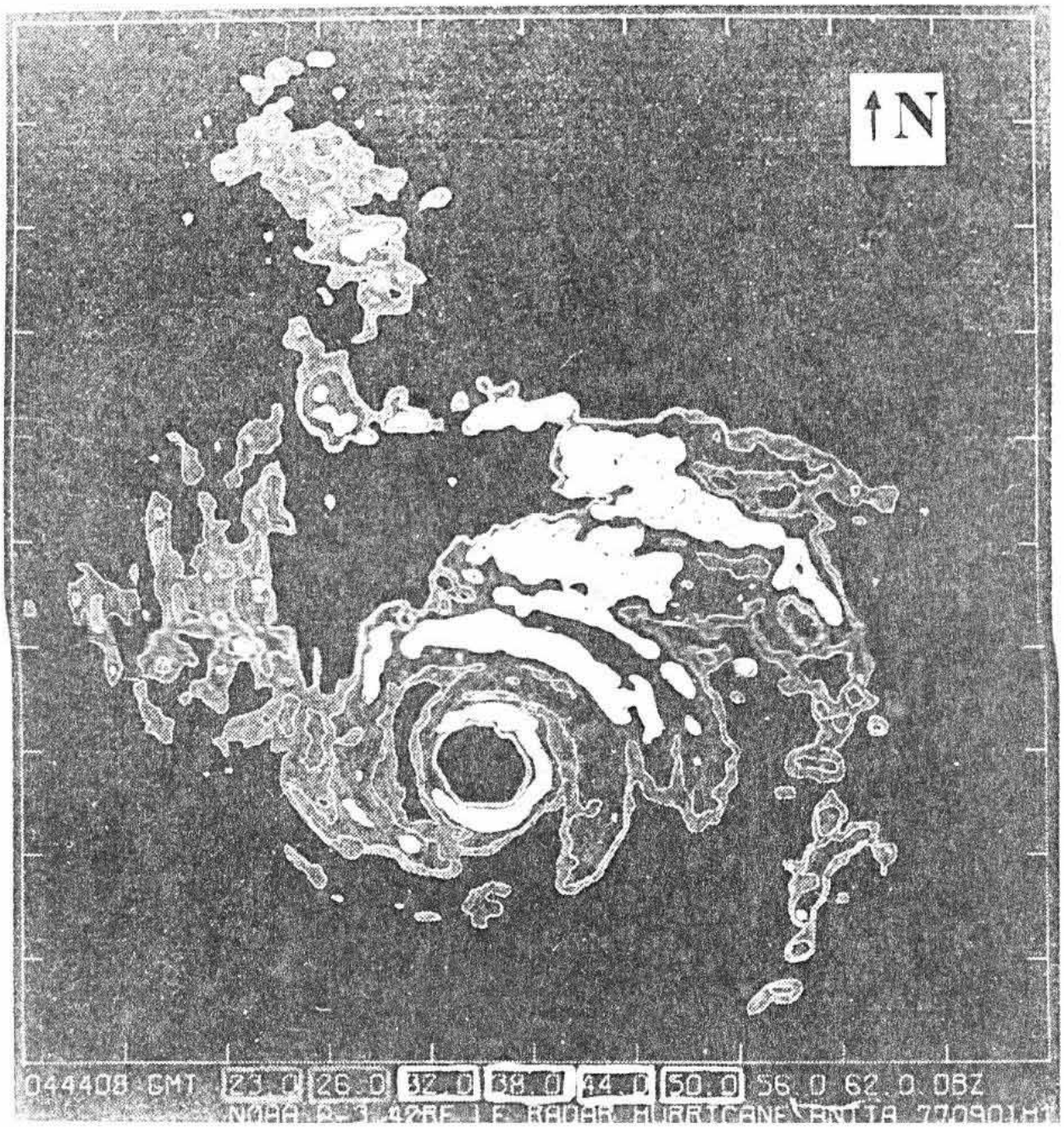

Fig.6.2.3(5).A computer-analysed depiction of the digitised 50mm-radar presentation on board a NOAA Orion (P 3) reconnaissance aircraft in Hurricane Anita at 0627 GMT on 2 September 1977. Four shades, corresponding to different values of dBZ, are shown with the highest (lightest shading) of 50dBZ corresponding to rainfall rates between 70 and 130 mm/h (From Sheets 1978).

weakening typhoon Elsie shown in Fig. 6.2.3(6) is in the front and front-right of the storm. This pattern is typical of those situations in which cold air from the NW is drawn into the circulation of a deep typhoon. The heavy rain band or bands extend towards the NW whatever the direction of storm motion.

Watanabe (1963) presented radar photographs of an intense rainband in the NW quadrant of the deep typhoon Nancy after it had recurved and was moving NE towards Japan in September 1961. The changing pattern of rain in typhoon Lucy is shown in Fig. 10.7(7) and the rapid change in rainfall distribution, over two hours, in severe tropical storm Agnes is shown on the left of Fig. 10.7(a). Satellite images of tropical cyclone rainfall as determined by microwave radiation show the same basic pattern and variability. In the intense (60 m/s winds) hurricane Ava, rainfall was heaviest to the rear of the eye with the characteristic "comma" tail consisting of a long rainband, being well shown in Fig. 11.8.2(1). This feature is more usual in weakening tropical storms. In these cases most of the outer spiral rainbands fade away to leave one or two long ones in the moist south-westerly inflow as described in section 6.4.3.

As a tropical depression intensifies into a typhoon the rain areas move in towards the centre so that the rainfall becomes more concentrated and more nearly symmetrical and the intensity of the rain increases. This is shown in Fig. 11.8.2(2) and 11.8.2(3). The outer rainbands illustrated by these ESMR images of the development of the typhoon shown near Luzon, may not be unrelated to the adjacent high mountains affecting the outer regions of the storm circulation. Fig. 11.8.2(4) again shows how well concentrated near the centre is the heavy rain. In this case, the heaviest rainfall is ahead of the eye.

Satellite and radar observations therefore suggest that outside the eye wall the distribution of rainfall in a mature cyclone over the Ocean is very variable both ~~with~~ time and in space, but there are indications that, on average, the rainfall is heaviest in the right rear sector but that it may frequently be found in the right front sector after recurvature. Intense storms which draw in colder air will often have a broad band of heavy rain in the NW sector while weakening storms over land may often retain a broad heavy rainband in the SW sector. Finally, at most stations the tropical cyclone rainfall will be heavily modulated by local oreigenic effects.

6

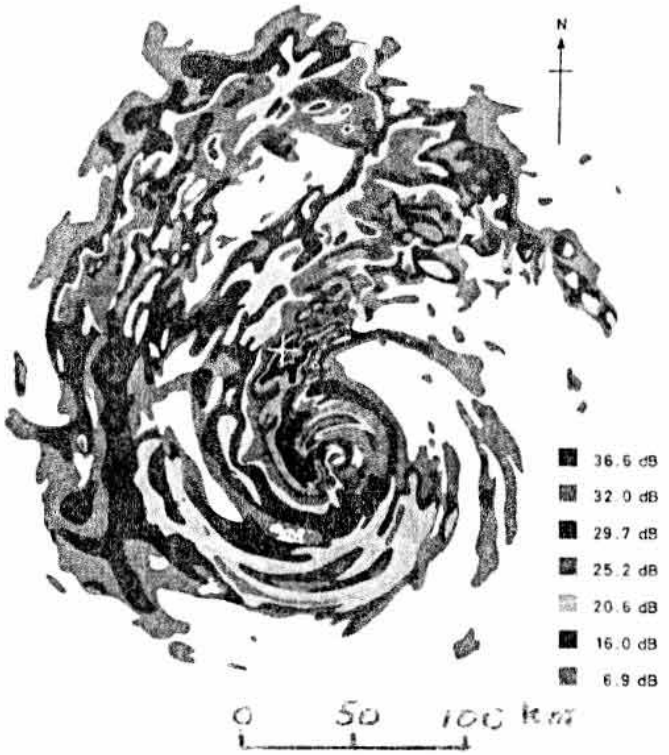

Fig.6.2.3(6).Radar reflectivities (add 15 for dBZ) in typhoon Elsie displayed on the Hong Kong 100 mm radar at 0335 GMT on 14 October 1975. The black and light green areas correspond to rainfall rates of approximately 70 and 1 mm/h respectively. The clear eye is just disappearing as cold air penetrates to the inner circulation and weakens the storm. The typhoon was moving towards the west.

6.2.4 Rainfall mechanisms

Because tropical cyclones make an inhospitable environment in which to take observations relatively little is known about their rainfall mechanisms. However, it is known that both warm rain and the Wegner-Bergeron mechanisms (see sect 3.) occur in ~~a typhoon~~ these storms. Warm ~~air~~ rain processes can be observed - visually or by radar - to play an important role because many cumulus clouds rain heavily when their tops are well below the level of the 0°C isotherm. That rain also forms from the Wegner-Bergeron process because is evidenced by the melting band which can sometimes be seen in certain parts of a tropical cyclone as described in sect 10.8.3 and illustrated in Fig. 10.8(3).

However, in the central parts of a mature typhoon the melting band does not form because the up currents there have speeds in excess of 1 m/s which carry snow crystals upwards. Further ~~away~~ out from the typhoon centre - where there may be a gentler and more general ascent - layer clouds form and may produce widespread rain by the Wegner-Bergeron process. Convective bands of heavier rainfall are usually embedded within these areas of continuous rain. Rate-of-rainfall recorders show the steady background rain with superimposed peaks associated with the passage of rainbands. Recordings illustrating this structure are shown in Figs. 6.3.6(2) and 6.4.3(2).

A further discussion of raindrop mechanisms and rain drop-size spectra is given in sect 10.4.6.

6.3 Station rainfall In Tropical Cyclones

6.3.1 Measurement of rainfall

There are many obstacles in the way of obtaining reliable measurements from conventional recording raingauges in tropical cyclone conditions. Some sources of difficulty are:-

i. Loss of catch due to the air flow over the gauge.

ii. Loss of catch during the emptying process in heavy rain.

iii. Malfunction due to inundation or storm surge.

iv. Smudging and spreading of the ink record on damp recording charts.

v. Catch of wind-borne debris and consequent malfunction.

vi. Catch of sea spray.

vii. Damage from wind-borne missiles.

viii. Lifting of surface water into the gauge by the wind.

ix. Inadequacy of gauge exposure.

A typical account illustrating some of the problems encountered is given in the report on the Darwin Christmas-day cyclone Tracy 1974: "The Dines tilting siphon pluviograph at Darwin airport was damaged and stopped recording after the passage of the eye of the cyclone soon after 0400 CST 25 December 1974. Water had previously entered the outer case and damaged the chart so that the record was faint and fragmentary after midnight." (Cyclone Tracy 1974). Fortunately, the good practice of having a standard gauge alongside the pluviograph enabled the twenty-four hour catch from 0900 CST on 25 December to be determined as 280 mm, while the maximum rate of rainfall over 15 minutes reached 105 mm/h just before the passage of the eye.

A standard raingauge looses catch in strong winds but for a variety of reasons the magnitude of this loss in hurricane conditions has not yet been adequately established. The loss comes about because the presence of the gauge affects the enveloping airflow which is deflected up over the gauge orifice and accelerated across it carrying some drops clear of gauge. Small drops are carried away more readily than large ones. The loss decreases as the rim of the gauge is lowered towards

ground level thereby reducing the gauge profile and putting the rim in a region where the wind speed is reduced. Gauges in pits with their orifice flush with the ground and fitted with no-splash surrounds have been used to assess the under reading of standard gauges in wind speeds up 15 m/s or so but, practical difficulties e.g. wind transport of ground water and debris, preclude good measurements in hurricane conditions. A pitted gauge was in use at Hong Kong for several years in an attempt to assess the loss in the nearby standard gauge. However, the only result obtained was that with winds generally of gale force (≥17 m/s) about 30% of rain was lost. (17.2 to 24.4 m/s)

Fig. 6.3.1(1) shows the effect of the wind speed at 2 m on the catch of raingauges with their rims at different heights. These measurements were made near Dunedin in New Zealand and include some snowfalls. They indicate a loss of about 30% for a standard gauge height at wind speeds of 15-20 m/s. However, it is not known how the dropsize distribution differed, if at all, from that in tropical cyclones. The effect of drop size on the catch of a standard gauge in winds up to 15 m/s has been determined in wind tunnel tests and is shown in Fig. 6.3.1(2). Note that at 15 m/s only 11% of the 1mm diameter drops are caught. In heavy rain near the centre of a tropical cyclone the median volume raindrops i.e. drops of a size such that half the total water is contained in larger drops, have diameter, around 2 mm (see sect 10.4.6). Fig. 6.3.1(2) indicates that the loss of these drops at wind speeds near 15 m/s will be about 50% with the loss of larger and smaller drops being less and more respectively. Miller (1958) quotes Hubert's correction factor of 2.5 for a shielded raingauge in light to moderate rain (< 3 mm/h) in winds of 45 m/s. For heavier rain the correction is less. Using Hubert's corrections Miller adjusted upwards, by an average of 30%, the hourly rainfalls used to construct Fig. 6.3.3(1) but in some squares with light rain and high wind speed the adjustment reached 80%.

From the foregoing it seems likely that in winds of hurricane force a well exposed standard gauge will loose 30% or more of the rainfall. However, unless the gauge is sited on well drained land several hundred metres from trees, buildings, the sea or other expanse of water there may well be a contribution from water picked up by the winds. The effect of the exposure of a gauge and its distance from the coast can also be large. The magnitude of these effects is illustrated in Fig. 6.2(1) which shows that the catch at the sheltered gauge at the Royal Observatory

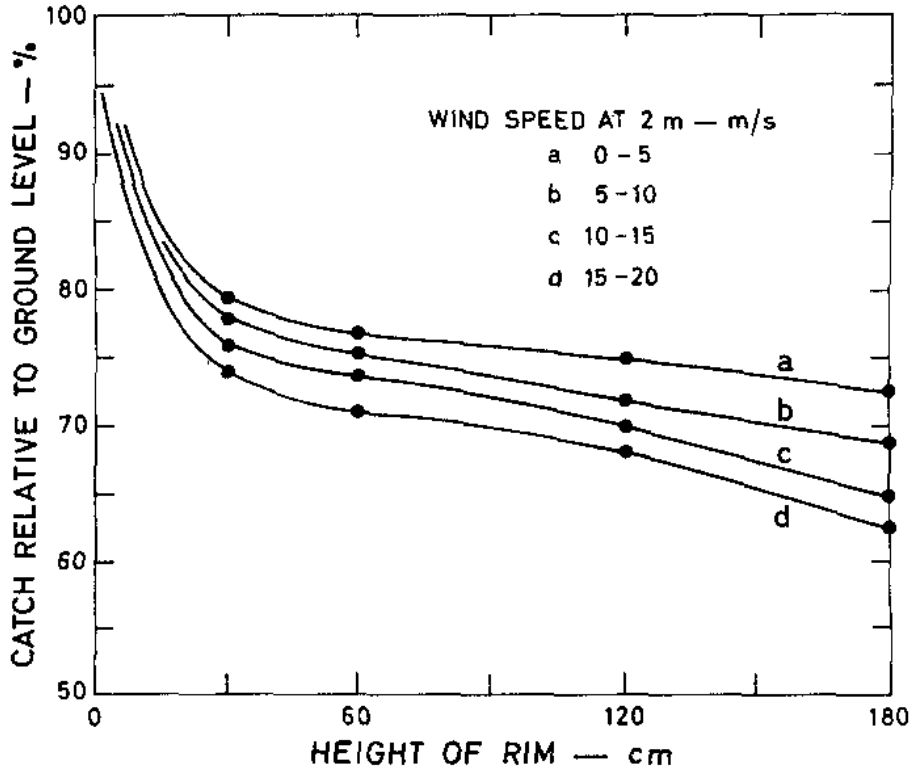

Fig. 6.3.(1) Raingauge catch deficiency in relation to rim height and wind speed. (After Dreaver and Hutchinson 1974.)

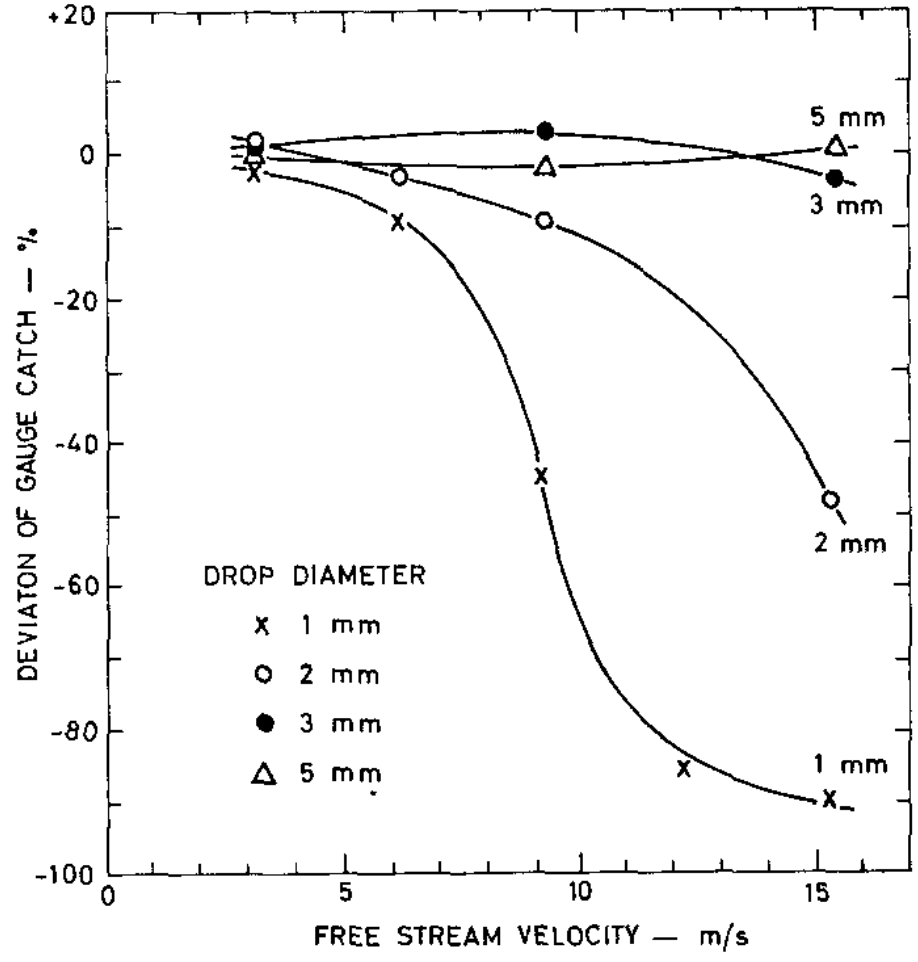

Fig. 6.3.(2) Deviation of standard raingauge catch relative to the drop diameter and the wind velocity. (After Mueller and Kidder 1972.)

Hong Kong is about 4 times that on the small but steep offshore island of Waglan only 18 km away. Both the relative exposure of the gauges and oreigenic effects due to the hills near the Observatory will contribute, in unknown proportions, to this difference.

6.3.2. T.C. rainfall at a point

The total rainfall recorded at a station during the close passage of a tropical cyclone is very variable having ranged from nil to 5 210 mm. The average tropical cyclone moving directly over a station at about 5 m/s will bring approximately 130 mm of rain over a total of 48 hours. Five average distributions of rainfall in tropical cyclones have been presented; they are for Florida hurricanes (Fig. 6.2.3(1)), Pacific typhoons (Fig. 6.2.3(2)), Hong Kong typhoons (Fig. 6.2.3(3)(b)), typhoons passing over Waglan Island (Fig. 6.2.3(4)) and for the model storm of sect 6.2.1 (Table 6.2(1)). For an average speed of movement of 5 m/s these storms would drop 128, 135, 137, 65 and 277 mm respectively. The model storm is associated with a greater total rainfall than the others because it refers to selected, large, mature typhoons and because the gauges used to determine the other totals suffer from loss of catch. The hurricane averages ~~have been~~ increased by an average of 30% to allow for wind effects. If the Hong Kong and Pacific Island values were similarly incremented they would yield average catches of about 180 mm. The actual gauge catch for an average typhoon passing at 5 m/s directly overhead a region with hills less than 1 000 m high would be about 130 mm but could be half this at exposed sites or much greater if the orography was favourable. In real terms the average total rainfall in the 24 h period would approach 200 mm.

The ~~actual~~ amounts of rainfall recorded at a station during the close passage of tropical cyclones depends on their ~~intensity~~, size, speed of movement, track and on local oreigenic effects. The observed frequency of occurrence of rainfall totals caused by tropical cyclones passing within 550 km of four stations are shown in Fig. 6.3.2(1). As is to be expected the average catch under all circumstances is about half that from average storms passing overhead at 5 m/s. On the other hand there will be a few mature storms which will move slowly (< 5 m/s) over or around a station susceptible to oreigenic effects and so give several times the rainfall of the model storm. The ten highest extreme tropical cyclone rainfalls at selected island and coastal stations are given in Table 6.3.2(1). Note that all stations have received maximum falls in excess of that of the model storm. The listed stations, with the sole exception of Tokyo, are in an area in which typhoons sometimes slow down during recurvature. Large amounts of rain can be caught at these times in spite of gauge losses in high wind speeds.

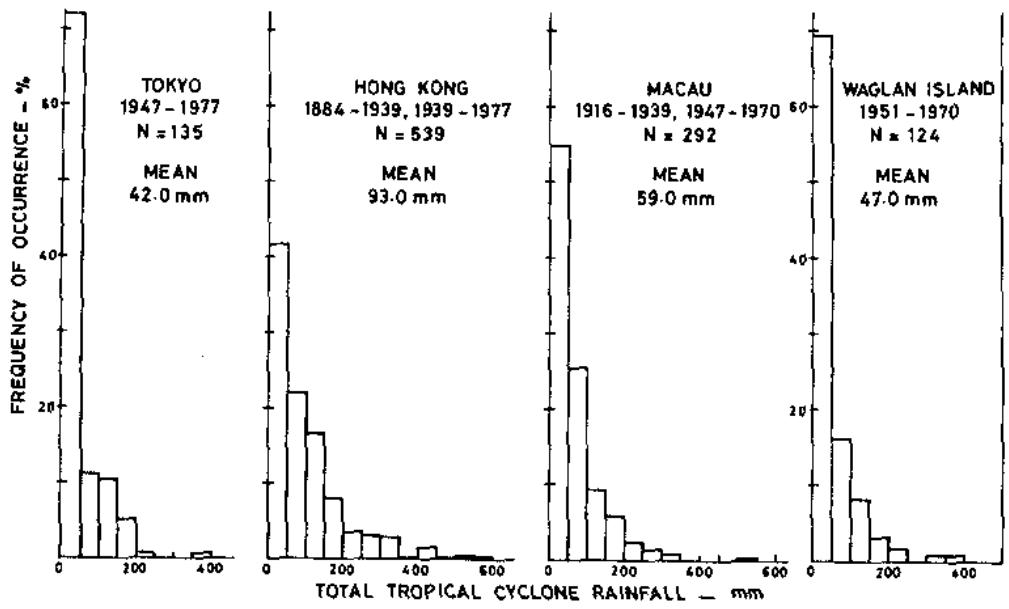

Fig. 6.3.2(1). The frequency of occurrence of total, direct and indirect (550 km radius plus 3 days after), tropical cyclone rainfall at four stations.

In Table 6.3.2(1), along with the annual extreme tropical-cyclone rainfall amounts for selected stations, is also shown the amount which would, on average, be equalled or exceeded once in fifty years at each station. The 50-year extreme ranges from 330 mm at Tokyo, where storms are less frequent and tend to be fast moving, to 963 mm at Naze where storms are both relatively frequent and often recurve. The high reading of 1040.5 mm at Naze occurred during the slow recurvature of typhoon Fran in September 1976. The track of the storm in Fig. 6.3.2(2) shows that while Fran was just north of Naze it moved very slowly. Four satellite pictures of the typhoon - and of the bright lights of some Far East cities - are shown in Fig. 6.3.2(3). Typhoon Fran moved on to cross Japan where it caused the loss of 165 persons and damage estimated at approximately \$572 x 10^6 (1976 U.S. dollars).

Table 6.3.2(2) illustrates how tropical cyclones recurving around Naze drop much more rain than do those moving on westerly or easterly tracks. It is probable that the reduced rainfall in the westward moving storms is associated with the fact that cold air can easily reach the centre of these storms. This is shown by the trajectories in Fig.5. 5.3.1(1)+(2). Eastward moving storms can maintain an input of warm air to their central regions so retaining their intensity (Snellman 1961) and rainfall. The record storm total of 5 210 mm at Grand Ilet La Réunion was also associated with a slow moving and recurving tropical cyclone as is shown in Fig. 6.3.7(1).

In Table 6.3.2(3) are given selected extreme rainfall totals from tropical cyclones at stations in S.E. Asia.

Table 6.3.2(1) The ten highest annual extreme rainfall amounts (mm) due to a tropical cyclone at selected stations and their 50-year extreme

	Island Stations				Coastal Stations				
Name	Naze	Pengohia Hau	Lan Hau	Waglan	Tokyo	Taipeh	Hong Kong	Macau	Manila
Location	28.4°N 129.5°E	25.7°N 122.1°E	22.0°N 121.5°E	22.2°N 114.3°E	35.7°N 139.8°E	25.1°N 121.5°E	22.3°N 114.2°E	22.2°N 113.5°E	14.6°N 121.0°E
Altitude	7 m	102 m	325 m	56 m	36 m	7 m	33 m	59 m	25 m
Period	1954-1977	1959-1976	1959-1976	1951-1970	1947-1977	1959-1976	1947-1977	1947-1970	1956-1970
	1040.5	418.0	519.1	385.3	371.9	483.0	527.4	539.9	629.2
	572.5	405.2	489.9	318.7	225.5	340.5	516.1	303.5	299.8
	507.0	302.2	479.8	241.8	191.0	287.3	469.3	262.0	291.1
	498.5	247.4	322.6	218.1	169.5	239.1	422.7	250.4	235.2
	452.5	235.5	188.5	181.0	161.5	227.0	408.1	250.0	228.3
	436.5	227.4	167.1	180.6	160.2	223.9	350.4	212.0	191.0
	420.5	215.5	128.0	157.9	159.5	190.2	340.9	210.6	176.3
	410.0	213.0	126.9	132.5	154.8	189.5	331.2	209.5	171.3
	385.6	206.0	123.7	128.6	148.7	187.2	323.2	191.6	169.4
	329.5	168.4	120.8	102.5	132.7	173.4	300.4	169.8	162.3
From All Annual Tropical Cyclone Extreme in the Period									
Mean	317.5	192.7	170.8	132.9	105.6	180.2	255.1	163.9	201.4
Mode	216.1	141.2	89.7	85.9	69.7	125.5	197.2	112.0	133.1
50 a Extreme	964	528	698	436	330	535	618	494	660

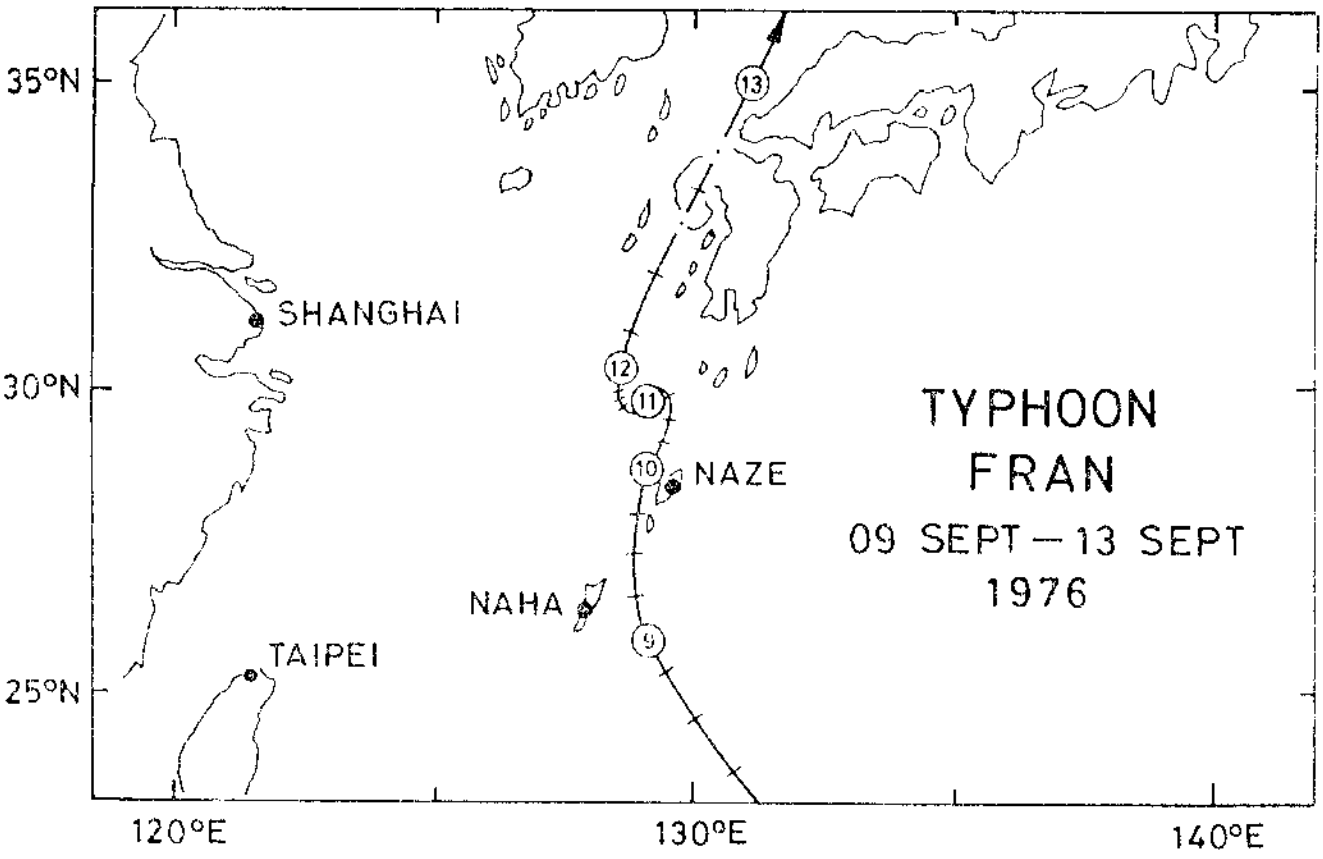

Fig. 6.3.2(2). The track of typhoon Fran in September 1976 showing the storm's slow movement during the period 10 September to 12 September which caused prolonged, heavy rainfall at Naze.

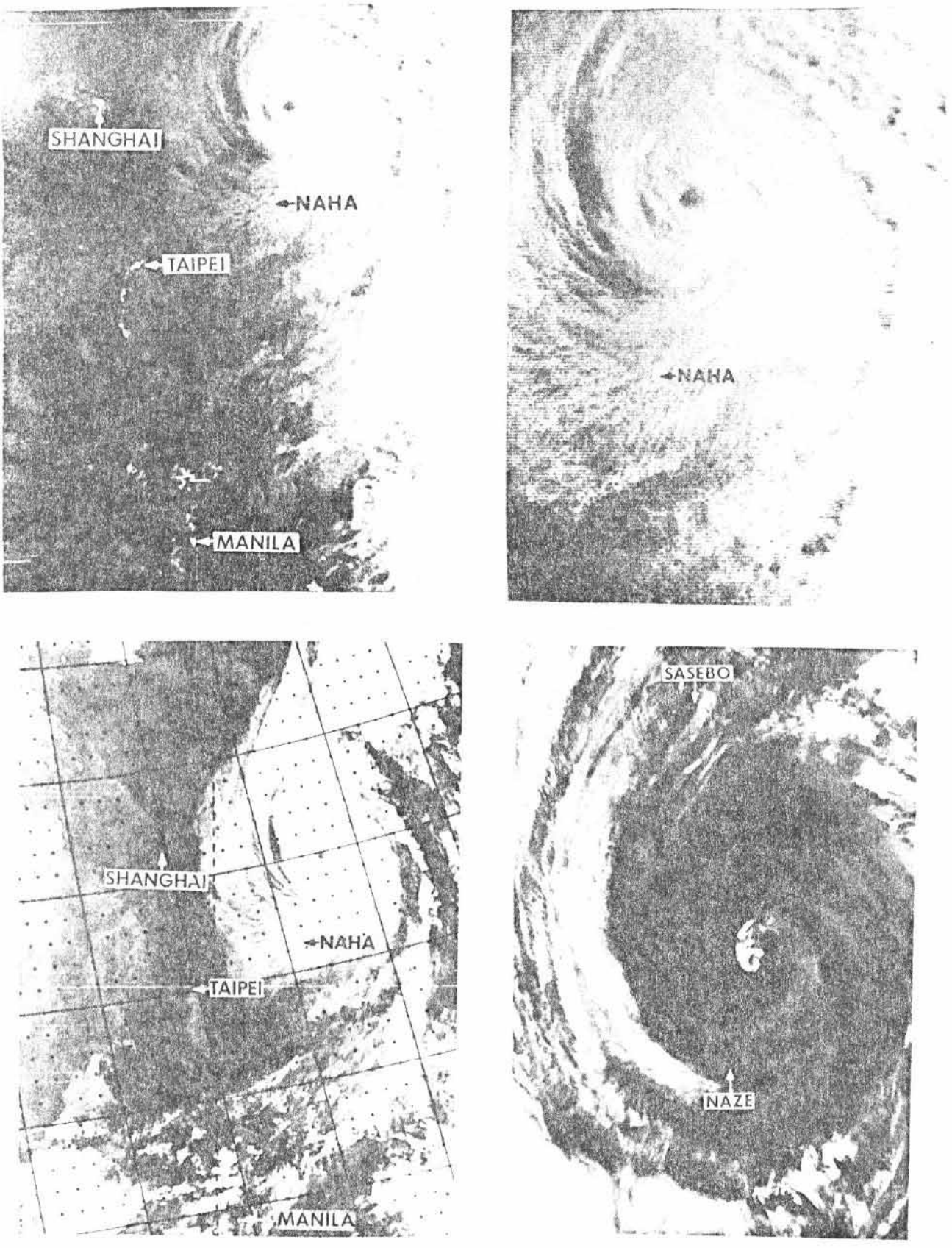

Fig. 6.3.2(3) Visual images by moonlight (upper) of typhoon Fran at 1129 GMT on 10 September 1976 and infrared images at the same time (left) and at 1116 GMT on the 11 September (right). The ~~l~~t infrared picture (right) is inverted i.e. cold areas are shown darker. The maximum surface wind speeds were about 45 m/s and the minimum pressure near 950 mb. (DMSP imagery from JTWC 1976).

Table 6.3.2(1). Rainfall at Naze on the day before and the day after the closest approach of tropical cyclones on different tracks during the period 1954-1977

Direction of T.C. Movement	Average Daily Rainfall		Total
	Before Closest Approach	After Closest Approach	
	mm	mm	mm
Westward	11.7	9.8	21.5
Eastward	34.6	30.4	65.0
Northward and recurving	55.6	77.4	133.0

Table 6.3.2(3). Selected extreme rainfall totals due to individual tropical cyclones

Place	Rainfall mm	Date	Remarks
Grand Ilet, La Réunion	5210	15-28 Jan 1980	Cyclone Hyacinthe
Hiso, Kyushu	2781	8-14 Sept 1976	T. Fran and front
Xinlino, Taiwan	2749.0	17-19 Oct 1967	T. Carla. Record not confirmed.
Anpu, Taiwan	2673.1	1- 8 Oct 1969	T. Flossie
Tapu, Taiwan	2623.0	31 Aug-6 Sept 1911	-
Taiwan	2000-2500	-	Many occasions at high level stations
Paishih, Taiwan	1684.0	9-12 Sept 1963	T. Gloria
Reunion, Mauritius	1193.8	15-21 Feb 1896	-
Taguac, Guam	838.2	20-22 May 1976	T. Pamela slow moving
Vacaos, Mauritius	749.8	17-20 Jan 1964	Cyclone Danielle
Royal Observatory, Hong Kong	597.4	17-18 July 1926	-
Naha, Okinawa	557.7	14-17 Oct 1959	T. Charlotte and front

6.3.3 Annual T.C. rainfall

At most western-Pacific stations between 10°N and 32°N, tropical-cyclone rainfall contributes more than 15% of the mean annual rainfall from all causes. This is illustrated by the data in Tables 6.3.3(1) which also show that Tokyo at latitude 35.7°N receives only 12% of its annual rainfall from typhoons. The actual amount recorded in one year at the listed stations is shown to have varied, during the respective data periods, from nil at Hong Kong in 1901 to 1 666 mm at Naze in 1976.

At some locations in this area which normally receive relatively little rain from other sources the proportion contributed by tropical cyclones can be large. For example, Shanghai with an annual rainfall of only 1 142 mm receives about 33% from typhoons.

The Philippine Islands are affected by many tropical cyclones each year - 19.3 on average - most of which cross the northern islands where the topography is severe. At stations in this area tropical-cyclone rainfall amounts to more than 60% of the annual rainfall, as is shown in Table 6.3.3(2). These islands are well placed to receive large amounts of rainfall when the flow of the monsoons is enhanced by tropical storms and typhoons (sect). Tropical cyclones are less frequent over the southern Philippines so that, for example, Davao at latitude 7.1°N receives only 14.5% of its rain from tropical cyclones. This amount is comparable to that received at Tokyo at 35.7°N.

Taiwan is also an area with severe topography and a high annual frequency of tropical cyclones; a combination which results in some stations there receiving a high proportion of their rainfall from typhoons and tropical storms. Fig. 6.4.2 shows the annual rainfall from tropical cyclones whose circulation affected Taiwan during the period 1959-1974. The island station of Makung receives 56% of its annual rainfall (1 090 mm) from tropical cyclones - on this restricted definition of typhoon rainfall - but most stations receive about 20%.

Table 6.3.3(1). Annual tropical-cyclone (T.C.) rainfall at selected stations.

	Tokyo	Naze	Hong Kong Observatory	Macau Observatory	Waglan Island
Period	1947-1977	1954-1977	1884-1939; 1947-1977	1916-1939; 1947-1970	1951-1970
Altitude a.m.s.l.	36 m	7 m	33 m	59 m	56 m
Latitude	35.7 °N	28.4 °N	22.3 °N	22.2 °N	22.2 °N
	mm	mm	mm	mm	mm
Mean annual rainfall	1493.0	3010.9	2168.8	1729.2	1215.6
Mean annual T.C. rainfall	184.4	656.1	566.9	355.6	282.9
T.C. rainfall as % of mean annual rainfall	12%	22%	26%	21%	23%
Maximum annual T.C. rainfall	651.7 (1958)	1666.0 (1976)	1235.7 (1964)	848.3 (1965)	567.3 (1965)
Minimum annual T.C. rainfall	8.5 (1976)	109.5 (1958)	Nil (1901)	Nil (1901)	26.3 (1956)
Mean rainfall from a T.C.	42.0	96.6	93.0	59.0	47.0
Maximum rainfall from a T.C.	371.9 (Sept.1958)	1040.5 (Sept.1976)	597.4 (July 1926)	593.9 (Sept.1965)	385.3 (July 1959)
Minimum rainfall from a T.C.	Nil+	Nil+	Nil+	Nil+	Nil+

+ On many occasions

Table 6.3.3(2)The contribution of tropical-cyclone rainfall to the annual rainfall at selected stations in the Philippines 1970-74. Direct rainfall is that within a storm's closed isobars (Data from Lomotan and Jose 1978)

	Altitude a.m.s.l.	Latitude	Tropical-cyclone rainfall								Average annual rainfall (1970-74)
			Direct			Indirect			Total		
			R	%	N	R	%	N	R	%	
	m	°N	mm			mm			mm		mm
Baguio	1500	16.4	1009	23.2	21	1853	42.4	92	2862	65.6	4366
Manila	25	14.6	378	18.2	18	1060	50.7	72	1438	68.9	2089
Daet	10	14.1	676	18.3	19	967	26.3	75	1643	44.6	3688
Cebu	33	10.3	176	12.0	10	416	28.4	49	592	40.4	1466
Davao	19	7.1	8	0.5	1	231	14.0	25	239	14.5	1647
Average	-	-	449	14.4	-	905	32.4	-	1355	46.8	2651

The average percentage of rainfall attributable to tropical cyclones varies from month to month within the year according to the average distribution of tropical-cyclone tracks and frequencies. This is illustrated, for the case of China, in Fig. 6.3.3(3).

Rainfall data for three Japanese islands is given in Table 6.3.3(4). The average rainfall from tropical cyclones shown there is the direct contribution only; the percentage values are therefore somewhat lower than in the other tables which consider both direct and indirect rainfall from these storms.

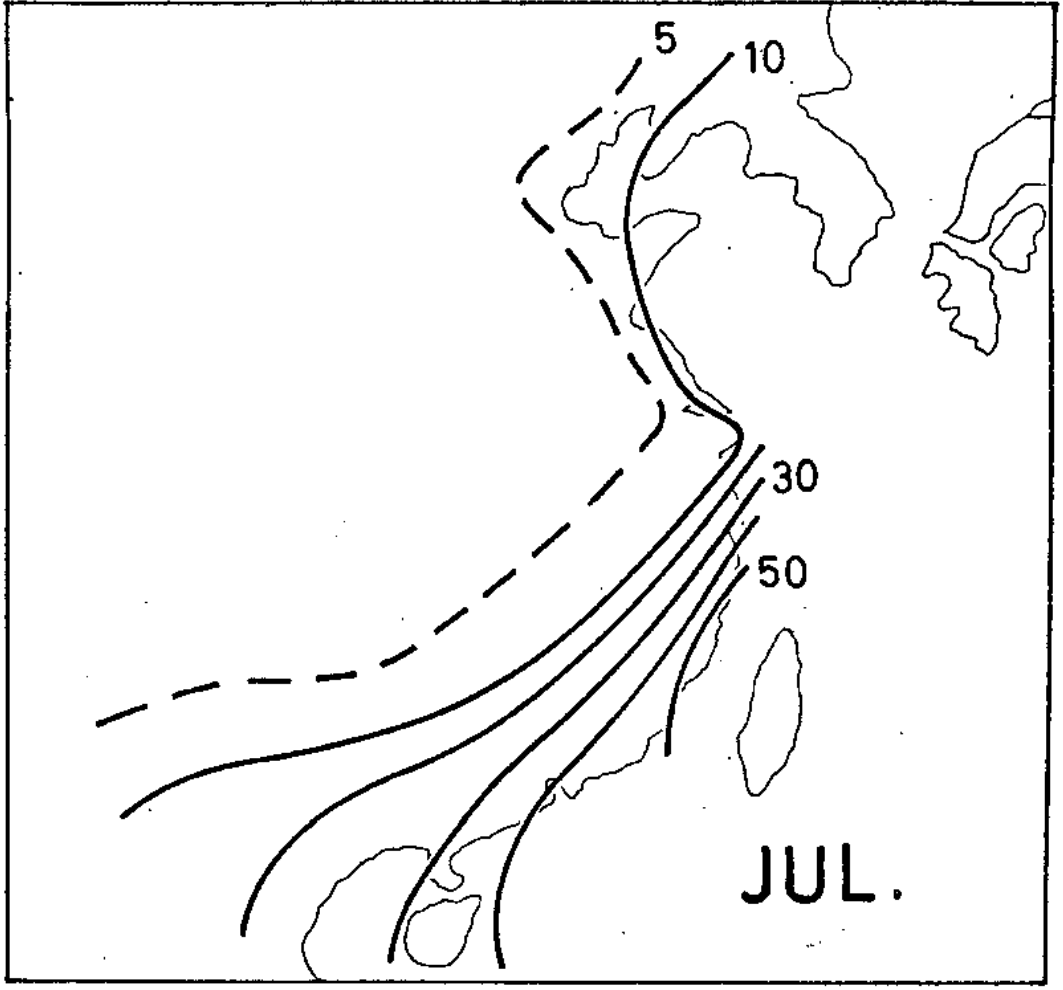

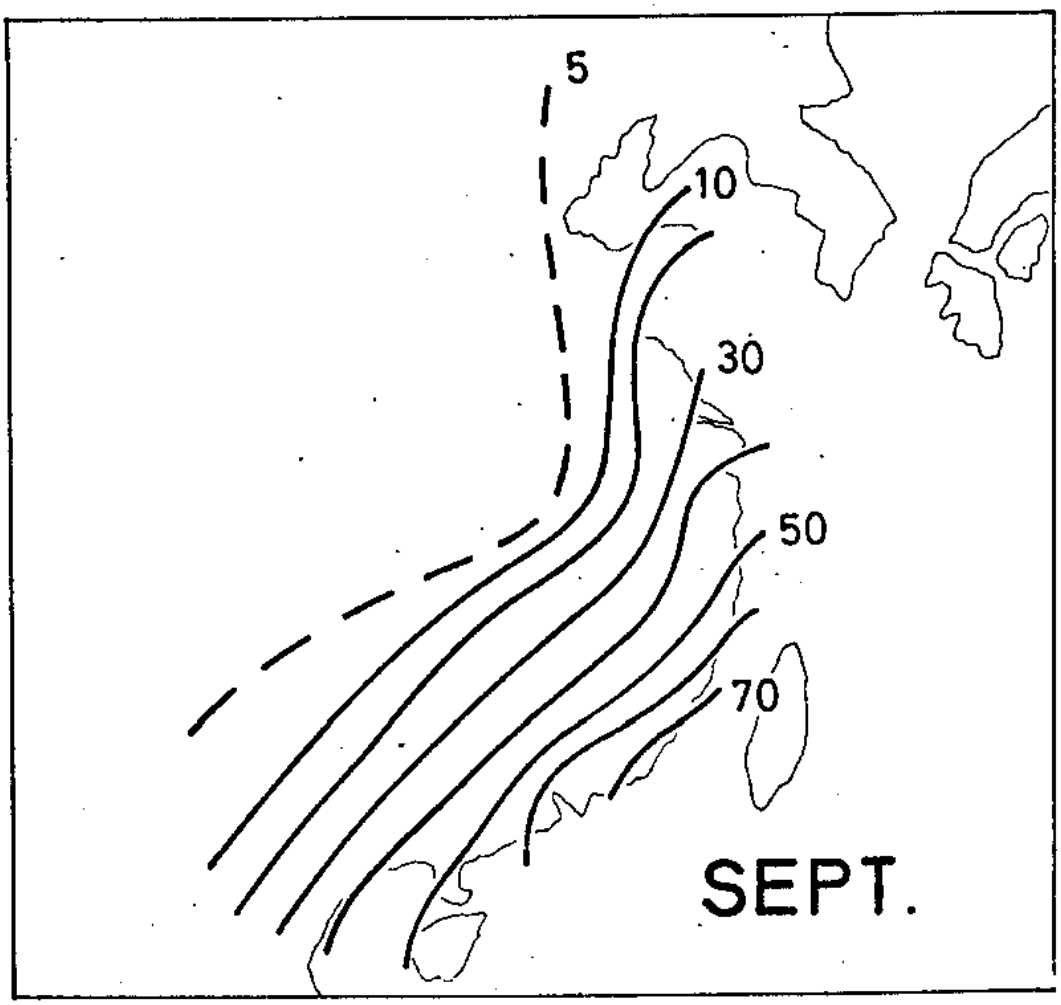

Fig. 6.3.3(3). The average percentage of rainfall caused by typhoons in July and September in China. (After Tao and Cai 1980).

(3)

Table 6.3.3. Annual tropical-cyclone (T.C.) rainfall at three island stations 1967 - 1976

Station	Ishigakjima		Naha		Naze	
Position	24.3°N 124.2°E		26.2°N 127.7°E		28.4°N 129.5°E	
Mean Annual Rainfall	1977.5 mm		2096.5 mm		3014.5 mm	
Maximum Annual Rainfall	3069.0 mm	1970	3042.0 mm	1975	3843.0 mm	1975
Minimum Annual Rainfall	1111.5 mm	1971	1402.5 mm	1968	2559.0 mm	1968
Mean T.C. Rainfall	258.0 mm		325.3 mm		547.9 mm	
Maximum T.C. Rainfall	590.5 mm	1972	748.0 mm	1969	1616.5 mm	1976
Minimum T.C. Rainfall	85.5 mm	1970	101.5 mm	1972	184.0 mm	1974
Mean Ratio T.C. rainfall / Total rainfall	13%		16%		18%	
Maximun ratio %	28%	1972	27%	1967 1971	45%	1976
Minimum ratio %	3%	1970	4%	1972	6%	1975

6.3.4 Daily T.C. rainfall

Tao and Cai (1980) defined a severe rainstorm as one in which the rainfall in a 24 h period exceeds 500 mm. They identified 57 such storms in China during the period 1953-1979 and found that 37 of them were attributable to tropical cyclones. The locations of these 37 storms are shown in Fig. 6.3.4(1) along with an indication of their severity. Three of these rainstorms produced more than 1 000 mm; they occurred in typhoons Gloria (1963), Carla (1967) and Nina (1975). Information on some of the other rainstorms is given in Table 6.3.4(1).

Tao and Cai (1980) recognised three types of tropical cyclone rainstorm:-

1) those which occur in the high energy inner regions of a cyclone
2) those on the periphery of the circulation and
3) those caused inland by a stagnant, remnant tropical cyclone.

Of the 37 severe rainstorms 24 or 65% were due to the first cause. Typhoon Gloria 1963 at Paishih, Taiwan and typhoon Emma 1963 at Kadena, Okinawa are good examples of this class of storm and they are discussed under extreme rainfalls in sect 6.3.7.

The greatest 24 h rainfall in China occurred at Xinliao near Paishih in Taiwan during the period 17-19 October 1967 in the outer circulation of typhoon Carla. At this time, the typhoon was moving slowly westward towards Hainan Island on a track about 700 km south of Xinliao. A cold front was quasi-stationary near the station as an easterly wave approached from the east. The heavy rain was associated with the interaction between favourable orography, the easterly wave and cold front and the supply of warm moist air brought by the outer circulation of Carla.

The third type of severe rainstorm - that attributable to a stagnant, remnant typhoon - is illustrated by the case of Nina 1975. When this typhoon moved inland to Honan Province a severe rainstorm occurred, rainfall amounts of 1 060 mm in 24 h, 685 mm in 6 h and 189.5 mm in one hour were recorded. The probability of the occurrence of rain of this intensity in that area is about one in 500 years. The distribution of the cumulative rainfall for the three days 5-7 August 1975 is shown in Fig. 6.3.4(2). Nina crossed the coast of China on 4 August 1975, moved

Table 6.3.4(1). Selected severe rainstorms in China due to tropical cyclones in the period 1953-1979. (After Tao & Cai 1960)

Province	Station	Longi-tude	Lati-tude	Date	Rainfall(mm)		Name
					24 hours	3-days	
Taiwan	Xinliao	24° 35′	121° 45′	17 Oct. 1967	1672	2749	Carla
Taiwan	Paishih	24° 33′	121° 13′	11 Sept. 1963	1248	1684	Gloria
Honan	Linzhung	33° 03′	113° 28′	7 Aug. 1975	1060	1629	Nina
Liaoning	Heigu	40° 34′	124° 36′	27 July 1962	657	794	Kate
Kiangsu	Chaoqiao	28° 26′	120° 56′	4 Aug. 1960	653	934	Shirle
Hupeh	Douzhenwei	30° 26′	110° 59′	9 Aug. 1975	629		Nina
Fukien	Wonchu	24° 51′	118° 16′	18 Sept. 1956	593	871	Freda
	Shanghai	31° 20′	121° 24′	21 Aug. 1977	591	593	Amy
Chekiang	Shilin	29° 48′	121° 45′	1 Aug. 1956	564	688	Wanda
Anhwei	Zilangiao	32° 40′	118° 23′	16 Aug. 1975	558	592	Ora
Hopei	Gixin	40° 02′	117° 25′	25 July 1978	534	742	Trix
Kiangsin	Dongxiang	29° 22′	110° 06′	17 Aug. 1953	500	553	Nina
Shantung	Shipozhi	36° 07′	119° 06′	12 Aug. 1974	500	572	
	Beijing	40° 22′	116° 16′	27 July 1972	500	518	Rita

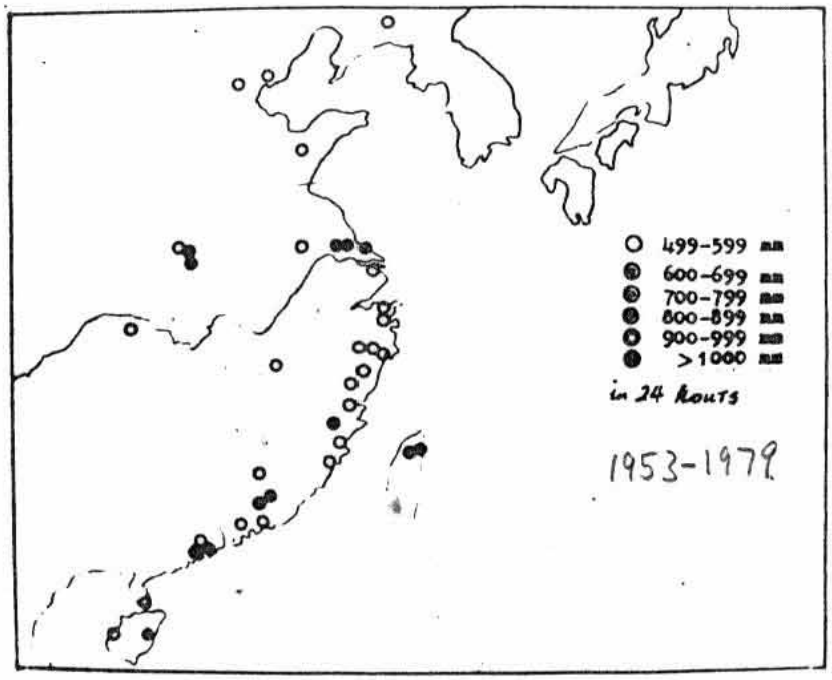

Fig. 6.3.4(1). The distribution of severe rainstorms caused by typhoons in China during the period 1953-1979. (Redrawn from Tao and Cai 1980)

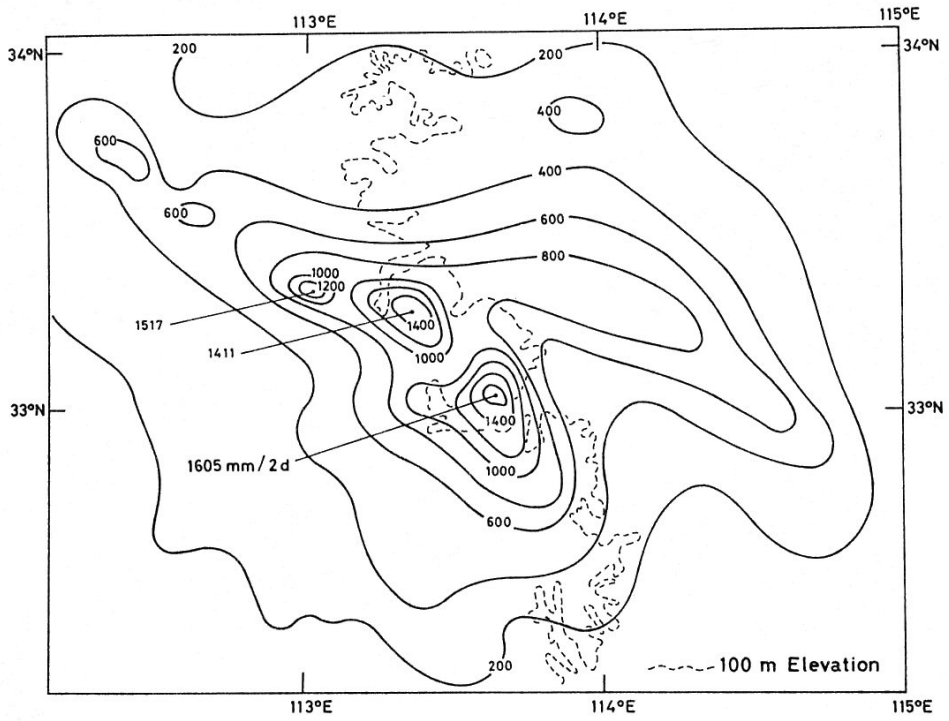

Fig.6.3.4(2). The cumulative rainfall isopleths for the three days 5-7 August 1975. The 100 m terrain contour is dashed (Redrawn from Tao & Cai 1980.

Fig. 6.3.4(3). NOAA4 nighttime I.R. satellite ~~picture~~ image of the ~~disjointed spiral~~ rainband around the weakening typhoon Nina at ~~1343 GMT on 4~~ 5 August 1975. The X on images for the 4 and 5 Aug mark the area of flooding. Times are in GMT. (Images from Golden 1980).

inland for two days, and became almost stationary on 7 August when cold air from Siberia reached the typhoon remnant. Heavy rainfall cells moved northwestward in the small spiral bands of the remnant typhoon seen in the satellite photographs in Fig. 6.3.4(3). A low level easterly jet, reaching 20 m/s in places, brought copious moisture from the East China Sea. Linzhung on the windward slope of the mountains recorded 1 600 mm while on the upwind plain and lee side of the hills the rainfall was 400 - 600 mm. The precipitation at Linzhung was three times that at stations only 30 km away. This rainstorm, analysed by Tao and Cai (1980), occurred in the east and northeast sectors of the remnant Nina as a result of the combination of convergence ahead of wind speed maxima in the low-level easterly jet, oreigenic and frontal lifting associated with a cold front (Fig. 6.3.4(4)) and convergence in the remnant typhoon Nina. Organized thunderstorms formed as potential instability in the area was repeatedly released and reformed. The strong anticyclonic outflow over the storm area is illustrated in Fig. 6.3.4(5). The importance of anticyclonic vorticity at 200 mb for heavy rain situations in or near the tropics was pointed out by Chen (1969) and Bell (1970) and will be referred to later in this chapter (see Fig. 6.4.4(3)).

On 9 August 1959 a midget typhoon landed on the southwest coast of Taiwan and brought 1001 mm of rain to Meilin in 12 hours. Isohyets for this storm are shown in Fig. 4.7. Other selected occasions when tropical cyclones brought more than 1000 mm in 24 hours are given in Table 6.3.4(2). All 24 h totals greater than 1100 mm occurred at high level stations but it is clear from the table that, in favourable circumstances, 24 h rainfalls around 1000 mm may occasionally occur over relatively low land. Although there are many occasions at which more than 1000 mm have been observed at mountain stations in Taiwan the 24 h extremes for coastal stations are much less. The greatest 24 h ~~total~~ rainfall for coastal stations is that for Kaohsiung when 576.6 mm ~~was~~ fell on 22 July 1940. 24 h extremes of 200 mm and 358.9 mm have been recorded at Tai Chung and Taipei (28 July 1928) respectively. Other selected extremes are included in Table 6.3.4(2) to give a better indication of the significance of topography for increasing 24 h rainfall.

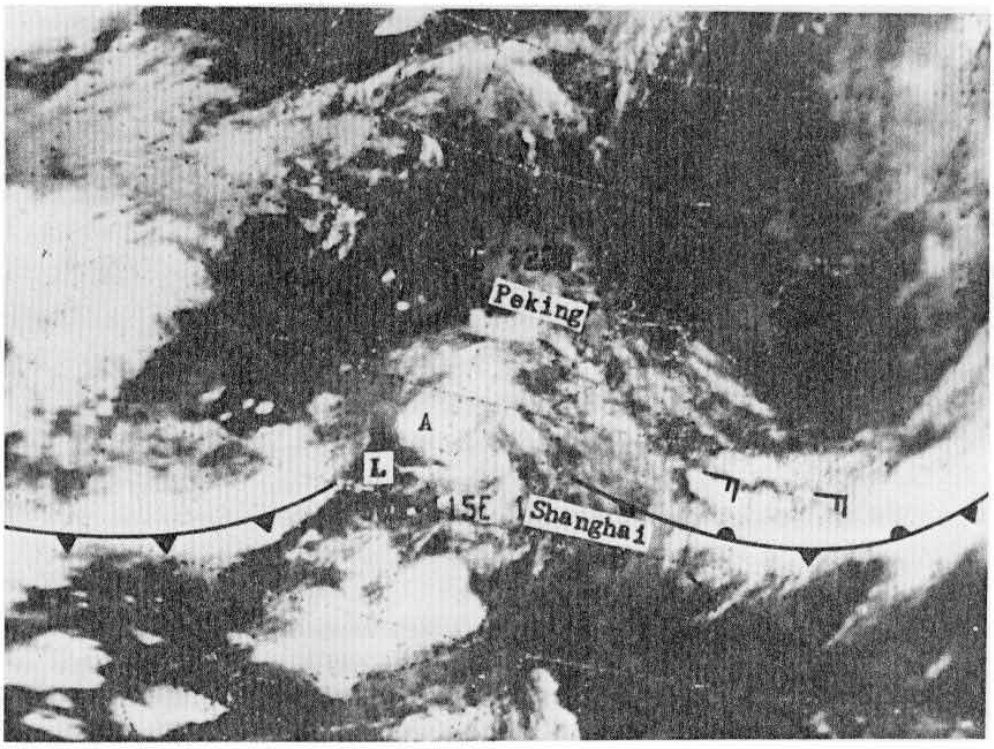

Fig. 6.3.4(4). A NOAA-4 IR image for 1200 GMT on 7 August 1975. A rainstorm (A) on the eastern side of the remnant typhoon NINA(L) caused disastrous floods in Honan province (From Tao 1978).

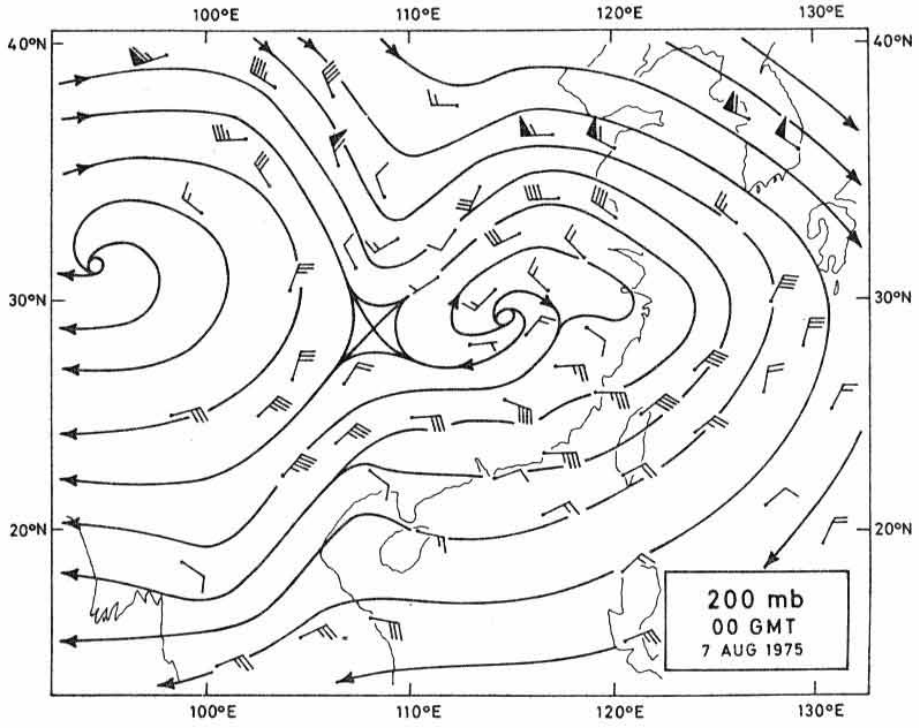

Fig. 6.3.4(5). Streamlines showing the strongly anticyclonic flow at 200 mb over the record-breaking Honan storm.

Table 6.3.4(2). Selected extreme 24 h rainfall totals due to tropical cyclones

Place	Rainfall mm	Date	Remarks
Cilaos, La Réunion	1869.9	15-16 Mar 1952	-
Xinliao, Taiwan	1672	17 Oct 1967	T. Carla
Paishih, Taiwan	1248	11 Sept 1963	T. Gloria
Taiwan	1000-1200	-	Many occasions at high level stations
Hiso, Kyushu (33.7°N, 134.1°E)	1114.0	Sept 1976	T. Fran and front
Alvin, Texas	1092.2	25-26 July 1979	Dissipating T.S. Claudette
Kadena, Okinawa	1071.9	8 Sept 1956	T. Emma
Yankeetown, Florida	983	5-6 Sept 1950	Dissipating hurricane
Baguio City, Philippines	979.4	17 Oct 1967	T. Carla
Owase, Honshu	806.0	26 Sept 1968	T. Della
Taguac, Guam	686	21 May 1968	T. Pamela slow moving
Royal Observatory, Hong Kong	552.2	19 July 1926	-
Vacoas, Mauritius	494.7	17-20 Jan 1964	Cyclone Danielle
Manila	410.0	19 May 1976	T. Olga
Pratas Reef	294.1	24 Apr 1978	T. Olive

6.3.5 Hourly T.C. rainfall

The frequency of hourly rainfall amounts within about 185 km of the centre of tropical cyclones as observed in typhoons at Waglan Island and the Royal Observatory and in hurricanes over Florida, is shown in Table 6.3.5(1). The relative infrequency of hourly falls in excess of 50 mm at Waglan and Florida when compared to their occurrence at the Royal Observatory is apparent. The higher frequency of all hourly rainfalls in excess of 50 mm at the Royal Observatory reflects both the sheltering of the gauge from extreme winds there and the increased oreigenic effects.

Frank (1977) presented hourly rainfall amounts observed at Pacific islands (see sect 6.2.3) in the form shown in Table 6.3.5(2) in which the frequencies of hourly rainfall amounts are related to the distance of the observing station from the typhoon centre and the total storm passing time. The table shows the heaviest rainfall to be concentrated within 2° of the centre of the typhoon. The incidence of heavy rainfall in the 2° - 4° band is only slightly greater than was found by Ruprecht and Gray (1976) for cloud clusters in the northwest Pacific. The frequencies of rainfall amounts $>$ 2.5 mm agree relatively well with the convective cloud cover, within 370 km, of $\sim$ 5% cumulonimbus and $\sim$ 25% total cumulus cloud cover as reported by Malkus et al (1961) and Gentry (1964).

The spatial distribution of average hourly rainfall rates in hurricanes and typhoons is shown in Figs. 6.2.3(1) and 6.2.3(2). The heaviest hourly rainfalls in tropical cyclones most frequently occur near high ground in the outer parts of a storm circulation where greater instability and interaction with cold fronts can occur. In the 90-year rainfall record at Hong Kong, for example, the highest 60-minute rainfall in a tropical cyclone is only 100.7 mm whereas 157 mm has been recorded in more unstable weather systems (Table 6.3.7(4)). An extreme rainfall of 189.5 mm occurred in the Honan Province storm during the interaction of remnant typhoon Nina and a cold front (sect 6.3.4) and 176.0 mm fell in Taiwan during the interaction of an upper westerly wave and the midget typhoon which landed on mountains there in 1959 (Fig. 4.7 and sect 6.3.7). The greatest hourly rainfall total in a tropical cyclone in Japan is 138.0 mm this occurred on the island of Okinoerabujima (Kagoshima prefecture) on 5 August 1965 in typhoon Jean. These and other extreme rainfalls during one hour are listed in Table 6.3.5(3).

6.3.5(1).

Table 6. Frequency distribution of hourly rainfall amounts from 13 typhoons centred within 185 km of Waglan Island and Hong Kong. The distribution of hourly rainfall amounts at Florida stations within about 185 km of the centre of 16 hurricanes is from Miller 1958.

TYPHOONS			HURRICANES	
Rainfall Range mm	Waglan Island %	Royal Observatory %	Rainfall Range mm	Florida Stations %
> 50	-	1.2	> 51	0.2
45 - 50	-	0.3	45 - 51	0.2
40 - 45	-	0.3	38 - 45	0.1
35 - 40	-	-	32 - 38	0.6
30 - 35	-	1.2	-	-
25 - 30	0.3	2.6	26 - 32	0.7
20 - 25	0.3	2.9	19 - 25	2.3
15 - 20	0.6	6.9	13 - 19	4.8
10 - 15	2.9	14.7	7 - 13	12.2
5 - 10	6.6	20.7	-	-
0.1 - 5	56.2	42.7	0.3 - 7	47.1
<0.05	33.1	6.6	<0.3	31.7

Table 6.3.5(2). Frequencies of hourly rainfall totals expressed as a percentage of total storm-passage time (After Frank 1977)

Hourly Total mm	Band radii - deg. lat. 0 - 2°	2 - 4°	4 - 6°	6 - 8°	8 - 10°	10 - 12°	12 - 14°
0 - Trace	30	59	80	87	89	89	90
0.2 - 2.5	35	24	14	10	7	7	7
2.55 - 7.6	19	11	4	2	3	2	2
7.6 -22.9	13	5	2	1	1	2	1
≥ 23.0	3	1	<1	<1	<1	<1	<1

Table 6.3.5(3). Selected extreme one hour rainfall totals due to tropical cyclones

Place	Rainfall mm	Date	Remarks
Linzhung, Honan	189.5	7 Aug 1975	Nina
Mt. Tahu, Taiwan	176.0	7 Aug 1959	Midget typhoon
Okinoerabujima Kagoshima, Japan	138.0	5 Aug 1965	Jean
Pratas Reef	109.0	1 July 1961	T. depression
Royal Observatory, Hong Kong	100.7	19 July 1926	-
Taguac Guam	87.1	13 Sept 1965	T.S. Virginia
Vacoas, Mauritius	75.0	3-7 Feb 1975	Cyclone Gervaise

6.3.6 Short-period T.C. rainfall

High rates of rainfall over brief intervals of time are of interest not only from the meteorological point of view but also because of their relevance to a number of practical problems in fields as diverse as satellite communication and landslips. However, ordinary recording raingauges do not adequately measure such short-lived peaks in rainfall rate. In order to measure these high rates several Jardi rate-of-rainfall gauges have been in use in Hong Kong since 1952. They have provided valuable and unique information on the very heavy bursts of rainfall which occur in the humid tropics in general and in tropical cyclones in particular. It is frequently claimed that the Jardi gauge gives the instantaneous rainfall rate. However, this is only true if the rainfall is steady because, the instrument needs time to fully respond to any change in rate. Cheng (1971) determined that a Jardi gauge registers 95% of a change in rainfall rate in about 9 seconds with the full rate being indicated if it is sustained for about 15 seconds. It was early found that the rate of rainfall in Hong Kong occasionally exceeded the 320 mm/h full-scale reading appropriate to Jardi gauges with a 686 mm diameter collecting funnel. A smaller collecting funnel of 559 mm diameter was therefore used to permit rates of rainfall up to 540 mm/h to be recorded. Records from gauges using different funnels are shown in Fig. 6.3.6(1).

A Raymond-Wilson gauge (Raymond and Wilson 1974) has a much faster response time of about 3 seconds. Since 1975 one of these gauges has been in use at the Royal Observatory Hong Kong alongside a Jardi gauge. On average, the peaks on the Raymond-Wilson (R-W) gauge are about 1.75 times greater than those recorded by the Jardi gauge but the exact ratio varies greatly as it depends on the variations of rainfall rate with time. For example, the peak rate indicated by the Jardi in tropical storm Ellen was 216 mm/h whereas 415 mm/h was registered by the R-W gauge as is shown in Fig. 6.3.6(2). The ratio of the two rates in this case is 1.92 or rather more than average. Other simultaneous recordings are shown in Fig. 6.4.3(2).

The passage across these gauges of both rainbands and convective cells within the rainbands are often clearly depicted. For example Fig. 6.3.6(1b) shows the rate of rainfall associated with an intense rainband containing very active convective cells. The wind speed at the time of the

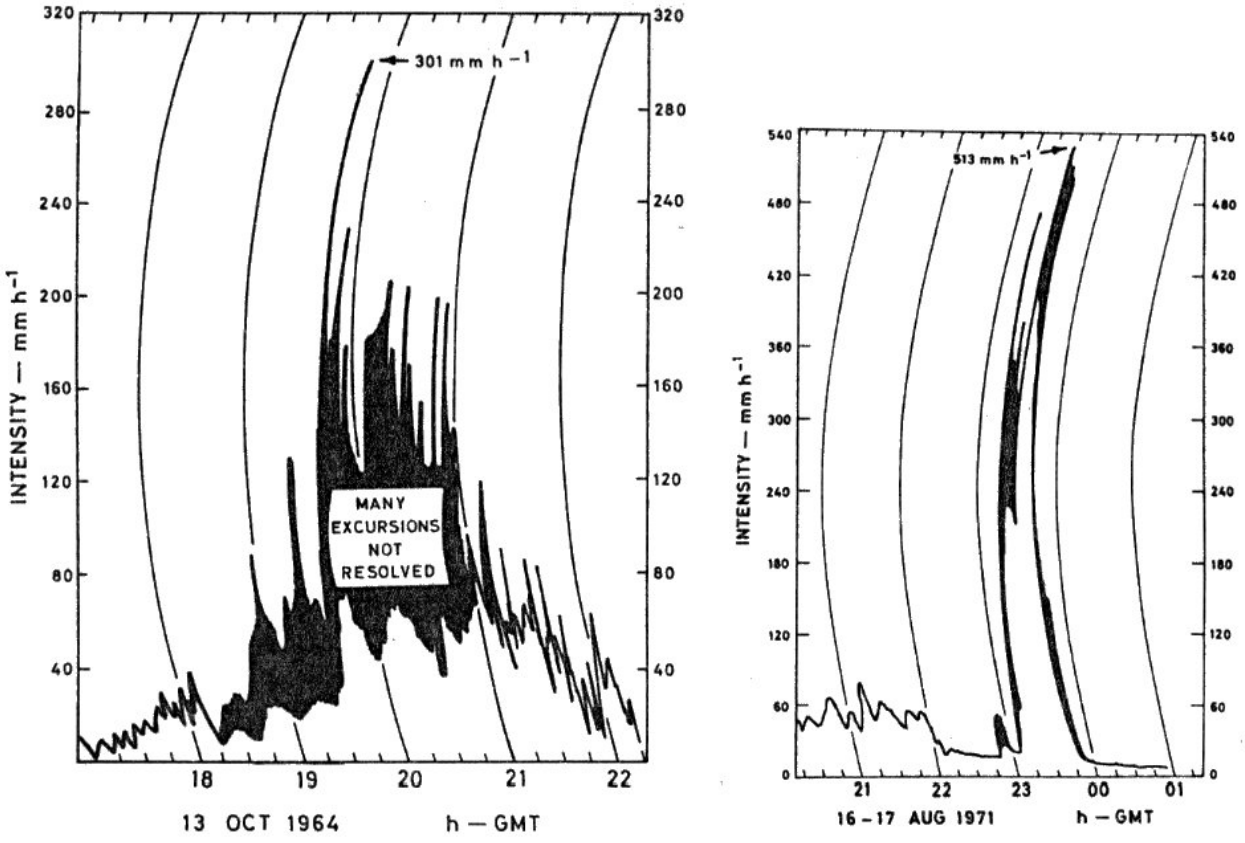

Fig.6.3.6(1) Traces from Jardi rate-of-rainfall recorders in Hong Kong (a) at King's Park during typhoon Dot and (b) at Tate's Cairn during typhoon Rose. The rate of rainfall in typhoon Rose remained above 200 mm/h for 26 minutes.

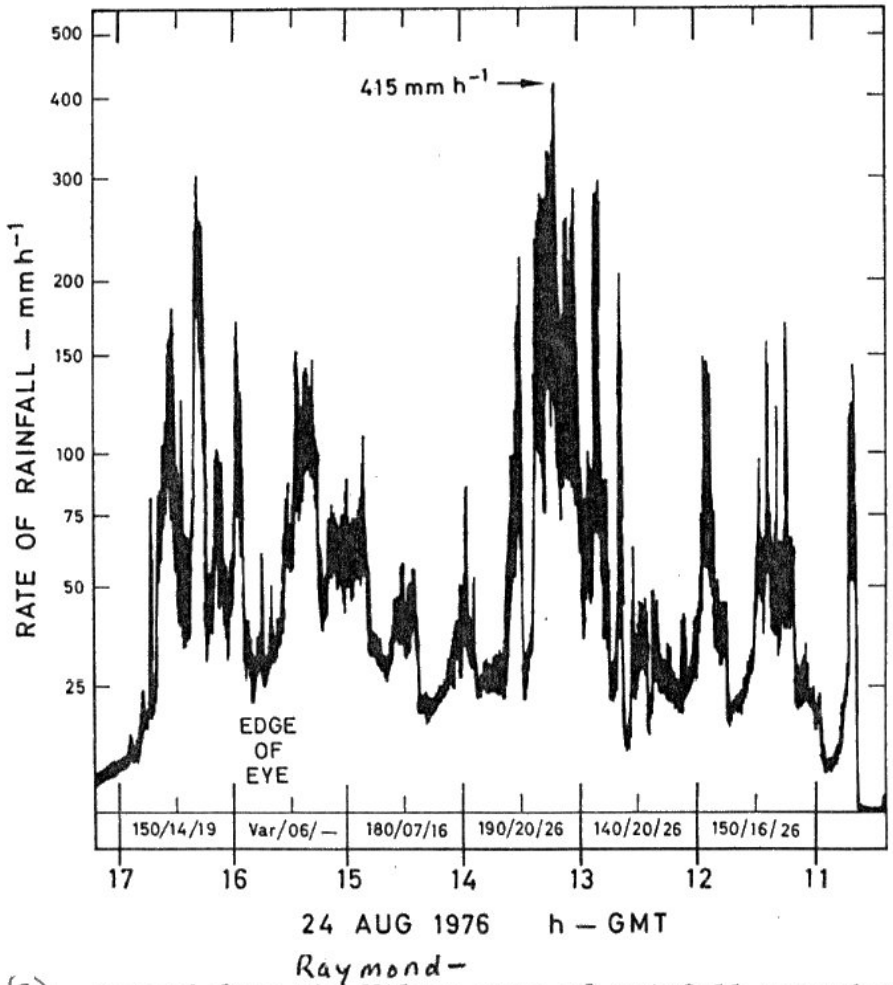

Raymond-

Fig. 6.3.6(2). Record from the Wilson rate-of rainfall recorder at the Royal Observatory, Hong Kong during tropical storm Ellen. Wind direction, mean speed and maximum gust in m/s are also indicated for each hour.

recording was generally of gale force with gusts to 25 m/s however, during the passage of the rainband the wind speed at the gauge site fell temporarily to only 7 m/s. In contrast, although typhoon Dot 1964 was a very wet storm as is indicated in Fig. 4.3 and Table 6.3.7( ), discrete rainbands were less marked and were embedded in an area of move widespread rain. The traces in Fig. 6.3.6(1a) show how the rapid passage of individual rain cells kept the recorder pen in constant motion yet the background rainfall was sufficient to keep the rate above 40 mm/h over a period of about two hours.

The annual maximum instantaneous rate of rainfall as recorded by the Jardi gauge at Kings Park, 1 km north of the Royal Observatory, Hong Kong, in each of the 29 years 1952-1980 are listed in Table 6.3.6(1). The two top ranking values were in excess of the maximum recordable rate with that instrument (320 mm/h). These and other observations at Hong Kong (Bell & Chin 1968) indicate that the Jardi readings corresponding to return periods of one hundred and one thousand years are about 470 and 600 mm/h respectively. The highest rate recorded by any Jardi gauge in Hong Kong in the same period (1952-1980) was 513 mm/h in typhoon Rose on 16 August 1971. This record (Fig. 6.3.6(1b)) was obtained at Tates Cairn, a hill top 568 m above sea level and 8 km northeast of the Royal Observatory. The highest reading of the Raymond-Wilson gauge during the period 1975-1981 was 700 mm/h in an outer rainband of typhoon Carla on 5 September 1977. The centre of the typhoon was 1200 km away over Indo China at this time and its active rainband remained near Hong Kong for two days.

It is sometimes necessary to estimate the rainfall over a short period of time given the catch over some longer period. The long series of observations at the Royal Observatory Hong Kong were used to obtain some average ratios of long to short period rainfall amounts in heavy rain episodes due to both tropical cyclones and other systems. Table 6.3.6(2) shows the ratio of the 60 min catch, on occasions with 25 mm or more, to that caught over shorter periods within the 60 minutes and to the clock hour catch. The maximum 60 min values are, on average, some 16% greater than those tabulated for clock hours. Table 6.3.6(3) extends the analysis and shows that the ratio of the maximum 24 h rainfall to that of the nearest civil day is 1.21 on tropical cyclone occasions and that, for example, the ratio of the 24 h rainfall ($\geqslant$ 90 mm) to the maximum 15 min catch within the 24 h is 15.1. The average ratios for non-tabulated period can be obtained

Table 6.3.6(1). Annual maximum instantaneous rate of rainfall recorded on a Jardi gauge at King's Park (1952-1980)

Rank	Rate mm/h	Year	Date & H.K.Time	Weather due to T.C. or not	Rank	Rate mm/h	Year	Date & H.K. Time	Weather due to T.C. or not
1	320*	1955	3 Aug 0858		16	242	1959	12 Jun 0912	
2	320*	1972	11 May 0337		17	241	1968	13 Jun 0232	
3	314	1973	3 Sep 0440	T.C.	18	233	1957	2 Jun 1225	
4	307	1958	30 Sep 1135		19	232	1977	19 May 0602	
5	302	1967	14 Jul 0544		20	226	1963	6 Sep 2048	T.C.
6	301	1964	13 Oct 0346	T.C.	21	216	1961	1 Jul 1940	T.C.
7	300	1965	27 Sep 0635	T.C.	22	208	1952+	23 Sep 1105	
8	286	1953	14 Aug 1105	T.C.	23	206	1978	1 Jun 0243	
9	286	1971	16 Aug 1014	T.C.	24	204	1976	24 Aug 2114	T.C.
10	284	1970	2 Aug 1757	T.C.	25	202	1969	26 May 2302	
11	282	1956	15 Sep 0307		26	187	1979	11 Jun 0953	
12	282	1974	18 Jun 1236		27	172	1960	25 Jun 1005	
13	281	1966	29 Apr 1950		28	154	1962	10 Aug 0438	T.C.
14	270	1975	30 Apr 1131		29	152	1954	8 Jul 0313	
15	246	1980	5 Aug 1244						

*Upper limit of recorder

+June - December only

from Fig. 6.3.6(3) which also shows that the ratios are larger in tropical cyclones than in other systems. This is due to the maximum short-period rainfall - excluding Jardi & R-W readings - in tropical cyclones being less than comparable readings in other systems. The reason for this was discussed in sect 6.1. It is of interest to note that the world record rainfalls, plotted in Fig. 6.7(1) or given by the square root relationship, yield ratios similar to those in Table 6.3.6(3) down to the one hour catches. For shorter periods the absence of relatively high rates of rainfall particular in typhoons - gives larger ratios for the Hong Kong data in Table 6.3.6(3) than are indicated by the square root relationship.

It is not often that heavy rainfall persists long enough to enable a worthwhile analysis of the frequencies of peak rainfall rates to be obtained. However in the exceptionally wet month of July 1972 at Baguio City - see sect 6.4.4 - only nine days received less than 100 mm of rain. The frequency of occurrence of peak rates of rainfall during successive intervals of 15 min throughout the month are listed in Table 6.3.6(5). The high frequency of rainfall peak rates between 21 and 40 mm - even greater than that for lesser rates - is noteworthy.

Table 6.3.6(2) Ratios of maximum 60 mm rainfall amounts to the maximum catch over shorter periods of time on occasions when the 60 min rainfall was 25 mm or more in the period 1968-1976

Averaging Period	Clock Hour	15 min	15 s
1. All Occasions	1.16	2.38	61.6
N	116	116	124
σ	0.20	0.64	21.3
2. T.C. Occasions	1.16	2.96	71.2
N	28	28	32
σ	0.23	0.55	22.9
3. Other Occasions	1.16	2.20	58.2
N	88	88	92
σ	0.19	0.55	19.7

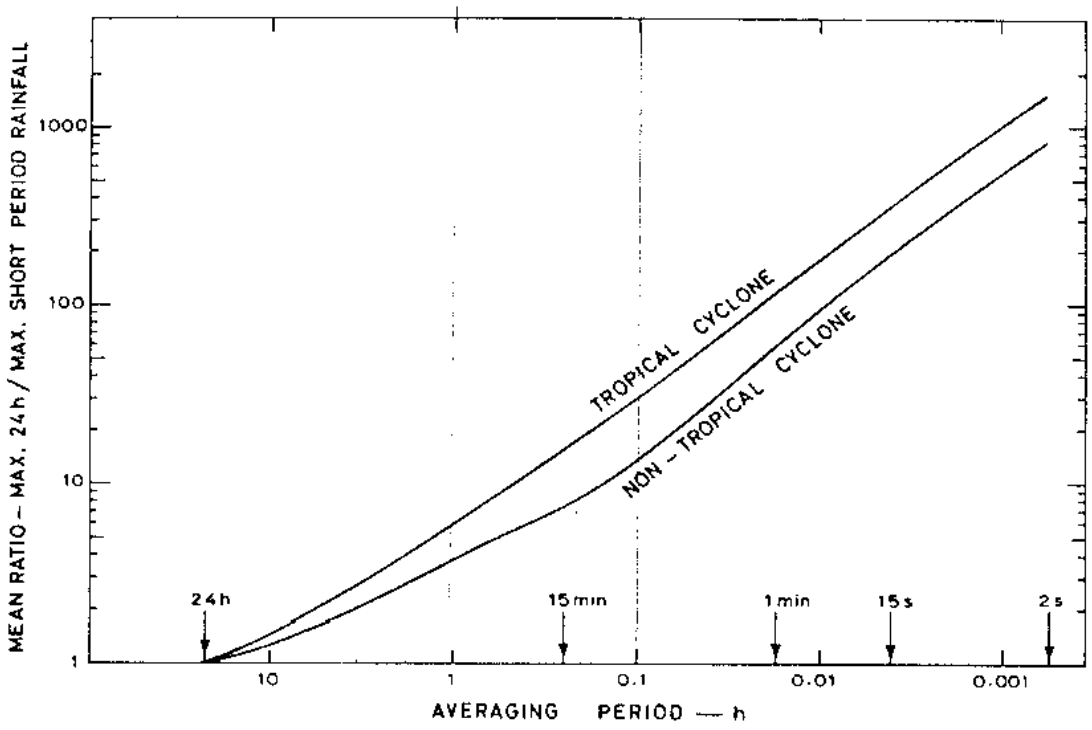

Fig. 6.3.6(3). The ratio of the maximum 24-hour rainfall, when $\geqslant$90 mm, to the maximum catch over shorter periods, within the 24 hours, in tropical cyclones and other systems at Hong Kong.

Table 6.3.6(3) Ratios of maximum 24 h rainfall amounts to the maximum catch over shorter periods of time on occasions when the 24 h rainfall was 90 mm or more

Averaging Period	Civil[1] Day	8 h[1]	1 h[1]	15 min[2]	15 s[2]	2 s[2]
1. All Occasions	1.17	1.49	4.62	9.5	245	1051
N		318	318			
σ		0.67	3.95			
2. T.C. Occasions	1.21	1.63	5.91	15.1	363	1555
N		112	112			
σ		0.37	2.35			
3. Other Occasions	1.15	1.41	3.92	7.4	197	843
N		206	206			
		0.54	227			

Notes: 1. Period 1884-1939; 1947-1975. 2. From Table 6.3.6(2) Period 1968-1976.

Gilmour and Bonnell(1979) listed the six-minute rainfall totals at a station near Cairns, northeast Australia, as cyclone Ted moved inland on a southeasterly track from the Gulf of Carpentaria on 20 December 1976. A total amount of 464 mm of rain were recorded that day. The rainfall was heaviest during the hour 0407-0506 (EST) when 101.09 mm were recorded with the greatest six-minute catch being 14.4 mm. The ratio of the 24 h total to those for 1 h and six minutes are 4.6 and 32.2 respectively as compared with 5.9 and 30.0 as indicated in Fig. 6.3.6(3). The frequencies of six-minute totals during the period of heaviest rainfall are given in Fig. 6.3.6(4). They show that six-minute totals between 4 and 5.99 mm (40-59 mm/h) are more frequent than those of 2 to 3.99 (20-39 mm/h).

Table 6.3.6(4). The frequency distribution of six-minute rainfall totals for the period 0136-0854 EST, 20 December 1976 in cyclone Ted (from Gilmour & Bonnell 1979)

Frequency categories (mm)	Total no. of events	Percentage of total
0–1·99	19	25·68
2–3·99	13	17·57
4–5·99	17	22·98
6–7·99	11	14·86
8–9·99	3	4·05
10–11·99	6	8·1
12–13·99	4	5·4
14–15·99	1	1·35

Table 6.3.6(5). Percentage frequency of peak rates of rainfall during successive intervals of 15 min in Baguio, July 1972

Peak rate of fall in an interval of 15 min mm h^{-1}	Frequency (2 976 cases) %
0 - 20	23.21
21 - 40	36.38
41 - 60	17.60
61 - 80	7.14
81 - 100	5.64
101 - 120	4.00
121 - 140	2.60
141 - 160	1.77
161 - 180	1.09
181 - 200	0.38
201 - 220	0.10
221 - 240	0.06
241 - 260	0
261 - 280	0
281 - 300	0.03

Maximum value 288 mm/h

6.3.7 Extreme tropical cyclone rainfalls

~~The earlier section of this chapter suggest that~~ For a tropical cyclone to produce extreme rainfall totals at a station three requirements should be met: 1) the storm should be over extensive areas of warm ocean to provide an adequate supply of air of high specific humidity 2) the topography should be as mountainous as possible but without being so extensive as to destroy the organization of the storm inflow and 3) the storm should be slow moving or near stationary. Many tropical islands meet the first criterion but most do not have mountains much above 1 000 m. The movement of tropical cyclones is most frequently quasi-stationary in the region between the tropical easterlies and temperate latitude westerlies. It is also in this area - around latitude 20 N or 20 S that storms frequently recurve, stall or loop as they become temporarily cought up in passing waves in the westerlies. It is not surprizing therefore that record rainfall totals from tropical cyclones are observed primarily in La Rēunion (Fig. 6.3.7(1)) and secondarily in Taiwan - both places being surrounded by warm oceans and having mountains reaching 3 000 m or more above mean sea level.

Table 6.1(1) and Fig. 6.1(1) show that tropical cyclones near La Rēunion have accounted for world record rainfalls over periods from 9 h to 15 d . The instability in tropical cyclones is adequate to generate fast rising currents through deep layers of the troposphere such as are required to obtain high rainfall rates over short-periods of time, in addition, the strong winds in typhoons keep intensive rain cells in motion and so prevent the catch accumulating in any particular gauge. At the other end of the time scale tropical cyclones have not caused record rainfalls for periods much in excess of 15 d because they would usually move clear of an area in this period or dissipate as they cool the upper levels of the underlying ocean.

The greatest recorded rainfall total from a tropical cyclone is 5210 mm. This total was recorded on the island of La Rēunion at the station Grand-Ilet during the passage of cyclone Hyacinthe during the fouteen days 15 to 28 January 1980(WMO 1980). This storm moved slowly, looped and recurved around La Rēunion as shown in Fig. 6.3.7(1).

Another station on the island, Plaine des Palmistes recorded 4 193 mm. Hyacinthe reached its greatest intensity - 965 mb - as it passed La Rēunion on 27 January. The sea temperature during this period was about 29°C or 3°C greater than normal (Sok Appardu 1981). Nearby Mauritius also received damaging rainstorms and floods during this period. The greatest rainfall total recorded there was 1 604 mm. The mountains in Mauritius reach to a little over 800 m above sea level.

Paulhus (1965) examined the rainfall record from stations in La Rēunion during the 13-year period 1952-1964. It was within this period that the listed (Table 6.1(1)) world record rainfalls for periods between 9 h and 15 d were found. Details of these extreme Rēunion rainfalls are given in Tables 6.3.7(1) and 6.3.7(2). The daily total of 1 688.8 mm recorded in cyclone Gisele at Belouve and shown in Table 6.3.7(1) actually fell in 18.5 h as shown in Table 6.3.7(2). Rainfall rates from this series of observations constitute world records for periods from 9 hours to 15 days (Fig.6.1(1)) not only for tropical cyclone rain but for all rainstorms. Paulhus (1965) was not sure that tropical cyclones caused the rainfall recorded at Aurere and Belouve. However, the cyclone tracks of the Mauritius Meteorological Service indicate that all three occasions were due to intense cyclones (those having wind speeds greater than 34 m/s) moving southward and passing within 140 km to the west of the island. La Rēunion is only about 56 x 56 km in size but it has high mountains which reach up to a little over 3 000 m. Belouve and Cilaos are located on the northern slopes of these mountains and would receive heavy oreigenic rainfall from cyclones centred to the west of the island because of the clockwise rotation of winds in Southern Hemisphere cyclones.

The cyclone season in the Indian Ocean near La Rēunion runs from November to May but January to April is the most favourable period at which time the surrounding ocean may reach temperatures close to 29°C. Mauritius records show that cyclones with central pressures lower than the 942 mb found in cyclone Carol 1960 have not been encountered during the past 160 years although 933 mb was recorded at Rodrigues in cyclone Monica on 29 March 1968 and the central pressure may have been lower than 930 mb. On 8 March 1973 cyclone Lydie passed over Tromelin where 932 mb were recorded. Mauritius does not experience such heavy rains as at La Reunion because the island high ground there does not rise above 800 m.

Table 6.3.7 (1). Rainfall maxima at La Reunion+

Storm Name*	-	Gisele	-
Intensity*	> 34 ms^{-1}	> 34 ms^{-1}	> 34 ms^{-1}
Station	Aurere	Belouve	Cilaos
Lat. and Long.	21°00'S 55°26'E	21°03'S 55°33'E	21°07'S 55°29'E
Elevation	940 m	1500 m	1200 m

Duration Days	Amount mm	Date	Amount mm	Date	Amount mm	Date
1	1583.2	7-8 Apr 1958	1688.8	27-28 Feb 1964	1869.9	15-16 Mar 1952
2	2466.8	7-9 Apr 1958	2415.3	27-29 Feb 1964	2499.9	15-17 Mar 1952
3	3129.5	6-9 Apr 1958	2689.9	26-29 Feb 1964	3240.0	15-18 Mar 1952
4	3422.4	5-9 Apr 1958	2781.3	26 Feb - 1 Mar 1964	3503.9	14-18 Mar 1952
5	3475.5	4-9 Apr 1958	2799.6	25 Feb - 1 Mar 1964	3853.9	13-18 Mar 1952
6	3475.5	4-9 Apr 1958	2808.7	24 Feb - 1 Mar 1964	4055.1	13-19 Mar 1952
7	3475.5	4-9 Apr 1958	2845.8	26 Feb - 4 Mar 1964	4110.0	12-19 Mar 1952
8	3475.5	4-9 Apr 1958	3010.9	26 Feb - 5 Mar 1964	4129.8	11-19 Mar 1952

+ Rainfall figures from Paulhue (1965)

* From the cyclone tracks of the Mauritius Meteorological Service, Gisele passed over Belouve moving to the SW, the 1958 cyclone passed 111 km to the west of the island moving SSW and the 1952 cyclone passed 139 km to the west moving towards the SSE.

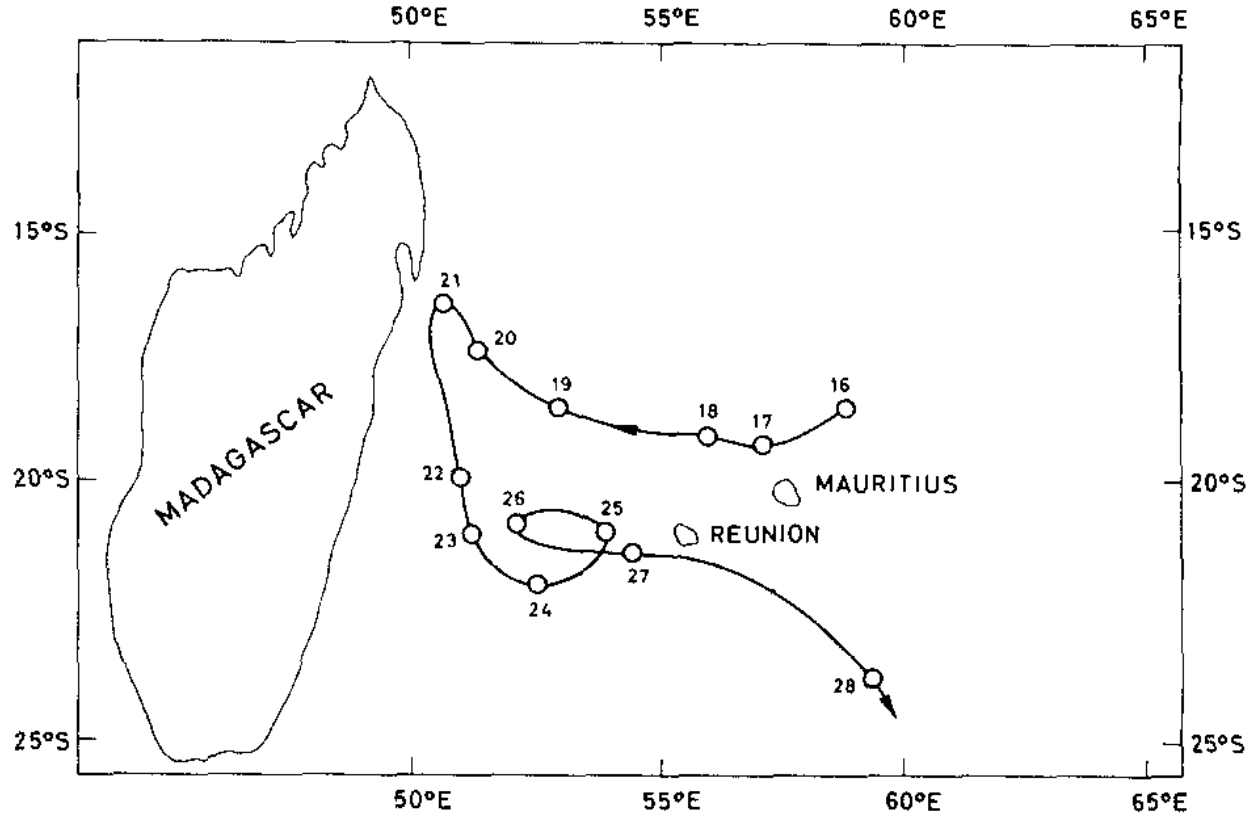

Fig. 6.3.7(1). The track of cyclone Hyacinthe during the record-breaking rainfalls at La Réunion from 15 to 28 January 1980 (After Sok Appardu 1981).

Table 6.3.7(2). Belouve rainfall during the wettest day in intense cyclone Gisele (After Paulhus 1965)

Duration h	Amount mm	Time LST	Date Feb 1964
2	385.6	1300 - 1500	28
6	766.1	1300 - 1900	28
9	1086.9	1300 - 2200	28
12	1340.1	1300 - 0100	28 - 29
18.5	1688.8	1300 - 0730	28 - 29

Before the La Réunion observations were noticed the world record rainfalls from all cuases for periods from 15h to 24h were attributed to the falls recorded at Paishih and Halaho in Taiwan on the 9 - 12 September 1963 during the passage of typhoon Gloria. This strom passed just to the north of the island on a course towards the northwest at 4.2 m/s. The central pressure of Gloria at the time of closest approach was about 930 mb. Paishih and Halaho are at elevations of 1 636 m and 1 160 m respectively on the north-facing end of a ridge which rises to over 2 100 m. Very deep typhoons with central pressures as low as 900 mb approach the island from the east where mean sea temperatures rise to over 29°C but exceed 30°C to the eastward in August (Fig. 14.). The maximum rain falls recorded at Halaho and Paishih during typhoon Gloria are given in Table 6.3.7(3) and are seen to be about 40% less than those recorded at La Reunion. The Halaho and Paishih records were obtained from autographic instruments so that curves of rainfall accumulation - shown in Fig. 6.3.7(2) - could be prepared.

Taiwan is visited by deeper typhoons than La Reunion and has slightly warmer seas - factors favouring heavy orographic rainfall - but the low level inflow into typhoons there is usually disrupted by the more extensive mountain ranges. Nevertheless, it is probable that the upper reaches of some Taiwan watersheds, favourably placed to receive enhanced oreigenic upflow from typhoon winds, may receive rainfalls approaching those at La Réunion. In this context Paulhus (1965) reports that for the period 9 - 12 September in typhoon Gloria, a total of 1 785.9 mm - or about 100 mm more than the Paishih total - was recorded at Paling.

A fall of 1 001 mm in 12 h due to a midget typhoon impinging on southern Taiwan from the southwest is illustrated in Fig. 4.6 . During this storm, on 7 August 1959, a ~~fall of~~ 176.0 mm of rain was recorded at Mt. Tahu (23·5°N 120·6°E) in one hour. ~~During the period~~ From 1911 to 1963 (inclusive) seven typhoons ~~have~~ caused daily rainfall amounts of over 1 000 mm at ~~different~~ stations in Taiwan (three of which received ~~Many stations have recorded more than 1 500 mm in a single typhoon and there have been three when~~ more than 2 000 mm ~~has been recorded~~. The latter readings were at Ta-pu (2 623.0 mm) and Feng-chi-hu (2 021.0 mm) in the typhoon of 31 August - 6 September 1911 and at Feng-chi-hu again (2 210.5 mm) in the typhoon of 17 - 21 July 1913.

Table 6.3.7 (3) Maximum rainfall amounts for durations to 48 hours at Halaho and Paishih (after Paulhus 1965)

Station	Halaho (24°38' N, 121°24' E) elev. 1160 m		Paishih (24°33' N, 121°13' E) elev. 1636 m	
Duration h	Amount mm	Date (Sept. 1963) and Time (120th E.Mer.)	Amount mm	Date (Sept. 1963) and Time (120th E.Mer.)
1	78.2	11/0800-0900	90.9	11/0700-0800
3	207.0	11/0800-1100	231.9	11/1000-1300
6	389.4	11/0300-0900	436.9	11/0700-1300
12	700.8	11/0300-1500	770.9	11/0200-1400
18	954.5	10/1900-11/1300	1050.0	11/0100-1900
24	1193.3	10/1700-11/1700	1247.9	10/2000-11/2000
30	1359.7	10/1400-11/2000	1431.0	10/1400-11/2000
36	1490.7	10/0900-11/2100	1524.0	10/0900-11/2100
48	1603.8	9/2100-11/2100	1620.0	9/2300-11/2300

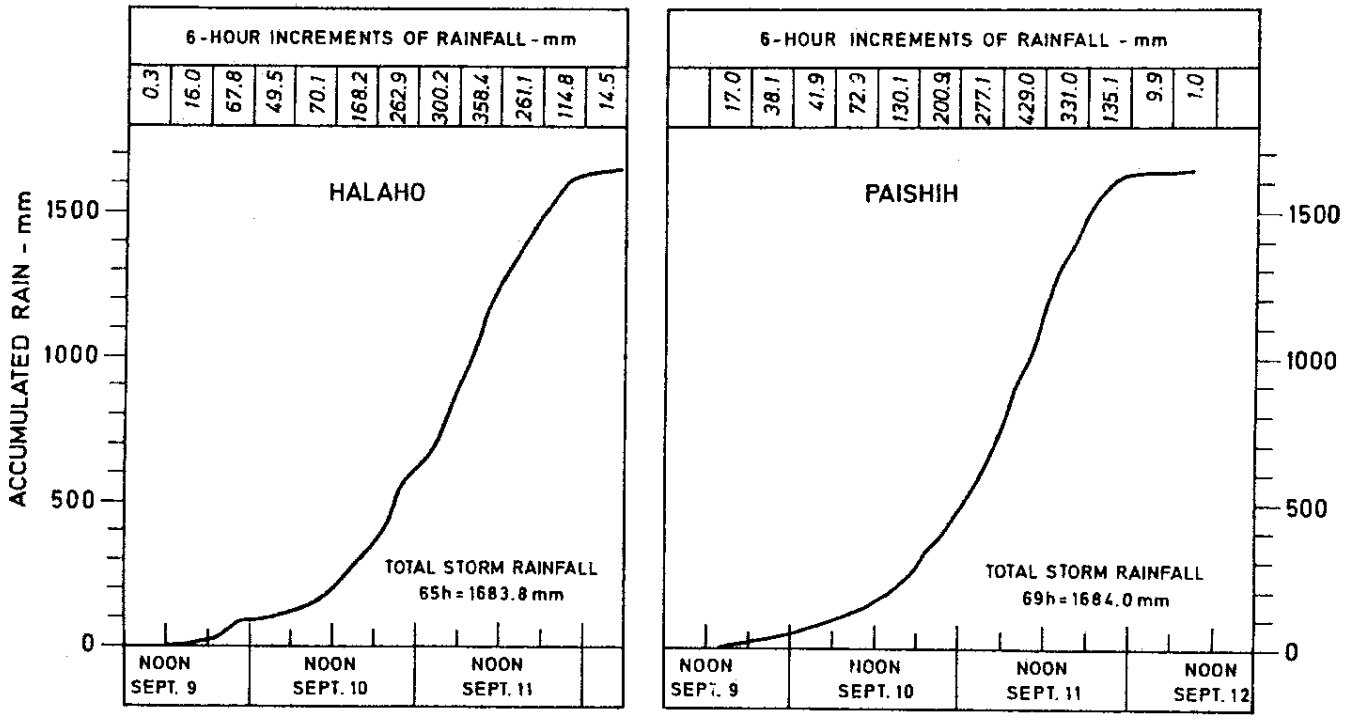

Fig.6.3.7(1) The accumumulation of rainfall (mass rainfall curves) at Halaho and Paishih in typhoon Gloria in September 1963. (Redrawn after Paulhus 1965).

Table 6.3.7(4). Greatest point rainfalls in tropical cyclones and other systems at stations in Hong Kong (Periods of observation differ between stations).

Duration	Other Systems			Tropical Cyclone		
	Depth mm	Rate mm/h	Date	Depth mm	Rate mm/h	Date
3 s	0.46	555	23/6/77	0.58	700	5/9/77
15 s	1.6	378	17/7/70	2.1	513	17/8/71
15 min	51.0	204	12/6/66	38.0	152	2/8/70
30 min	85.0	170	12/6/66	64.0	128	25/8/76
60 min	157.0	157	12/6/66	100.7	100.7	19/7/26
1 h	140.0	140	12/6/66	100.7	100.7	19/7/26
2 h	277.0	138.5	12/6/66	174.4	87.2	19/7/26
4 h	375.0	93.7	12/6/66	292.4	73.1	19/7/26
6 h	408.5	68.1	12/6/66	430.6	71.8	19/7/26
8 h	415.7	52.0	12/6/66	505.1	63.1	19/7/26
12 h	454.8	37.9	30/5/1889	526.7	43.9	19/7/26
24 h	716.5	29.9	22/5/57	552.2	23.0	19/7/26
1 d	672.7	28.0	12/6/66	534.1	22.3	19/7/26
2 d	841.2	-	30/5/1889	635.6	-	24/8/76
3 d	988.8	-	18/6/72	635.6	-	24/8/76
4 d	1014.6	-	19/6/72	635.6	-	24/8/76
5 d	1025.5	-	19/6/72	977.6	-	26/8/78
7 d	1025.9	-	20/6/72	986.8	-	26/8/78
15 d	1238.4	-	2/6/1889	-	-	-
31 d	1404.9	-	18/6/1889	-	-	-
1 a	4462.3	-	1975	-	-	-

Jordan and Shiroma (1959) investigated a large catch of rain at Kadena airfield Okinawa during the passage of typhoon Emma on 8 September 1956. The rainfall that day totalled 1071.9 mm with 1059.8 mm and 965.2 mm falling in 21 hours and 18 hours respectively. The record is of interest for two reasons. Firstly, Okinawa has relatively low relief with no point higher than 600 m and no hills higher than 240 m within 15 km of the airfield. Secondly, the case illustrates how localised can be record rainfall catches in tropical cyclones. Other rainfall stations recorded much less rain; one gauge only 30 km to the north of Kadena received only one tenth of the catch at the latter station. Jordan and Shirona (1959) accounted for ~~the discrepancies~~ this distribution by showing that Kadenna was under the eye wall for an extended period while stations further south entered the large rain-free eye - diameter 100 km - and those further north were outside the eye wall. Emma was moving WNW at 4 to 5 m/s with a central minimum pressure of 938 mb. Kadena recorded a minimum pressure of 944.3 mb and a Dines anemometer gust of 73.6 m/s. Winds at Kadena were over 25 m/s for more than 22 hours and it was possible that for part of the time water from a flat roof about 30 m away could have been blown into the gauge however, there would also have been considerable losses at other times due to wind speed.

Tropical cyclone rainfall at Hong Kong is typical of that of many other places on the south China coast where hills range up to 1 000 m or so. Table 6.3.7(4) shows the greatest point rainfalls recorded at stations in Hong Kong regardless of their height or record length. The twenty five cyclones which caused most rainfall at the Royal Observatory in 89 years are listed in rank order in Table 6.3.7(5). The return periods of tropical cyclone rainfalls are given in sect 6.10.

Table 6.3.7(5). The twenty five wettest tropical cyclones at Royal Observatory, Hong Kong, 1884-1939; 1947-1979

Rank	Period when tropical cyclone was within 555 km of Hong Kong		Name of tropical cyclone	Total tropical cyclone rainfall * mm
1	17 - 18	Jul. 1926	-	597.4
2	1 - 3	Jun. 1916	-	559.8
3	26 - 27	Sep. 1965	T.S. Agnes	527.4
4	24 - 30	Jul. 1978	S.T.S. Agnes	519.0
5	23 - 24	Aug. 1976	T.S. Ellen	516.1
6	17 - 19	Oct. 1974	T. Carmen	469.3
7	23 - 28	Aug. 1904	-	447.0
8	3 - 5	Aug. 1911	-	437.9
9	4 - 6	Oct. 1894	-	427.4
10	14 - 15	Jul. 1925	-	423.2
11	7 - 9	Jun. 1960	T. Mary	422.7
12	14 - 16	Oct. 1978	S.T.S. Nina	420.2
13	28 - 30	Jun. 1910	-	419.5
14	13 - 14	Sep. 1952	-	408.1
15	26 - 28	Aug. 1923	-	405.7
16	21 - 24	Sep. 1979	S.T.S. Mac	361.3
17	11 - 12	May 1891	-	353.0
18	13 - 14	Jun. 1918	-	349.4
19	15 - 17	Aug. 1971	T. Rose	340.9
20	2 - 3	Aug. 1902	-	338.4
21	14	Jul. 1917	-	332.4
22	11 - 13	Oct. 1964	T. Dot	331.2
23	18 - 20	Jul. 1920	-	327.7
24	19 - 20	Oct. 1909	-	323.9
25	22 - 23	Sep.. 1957	T. Gloria	323.3

* Defined as the rainfall recorded during the period when the tropical cyclone was centred within 555 km of Hong Kong and during the following 3 days.

6.4 Synoptic and Mesoscale Phenomena

6.4.1 Diurnal variation of rainfall

It has long been known that the incidence of heavy rainfall at many stations in the tropical western Pacific region is greatest at the time when most people are on their way to work that is, between about 5 a.m. and 9 a.m. This feature was evident in early climatological studies (eg. Claxton 1931) and is illustrated in the upper part of Fig.6.4.1(1) for the case of Hong Kong. In 1955 the time of reading of the Hong Kong daily raingauges was changed from 8 a.m. H.K. Standard Time (00GMT) to 4 p.m.H.K. Standard Time (08GMT) in order to avoid the frequent reading of gauges during heavy rainfall. Of the 29 annual maxima instantaneous (15 s) rainfall rates at Hong Kong listed in Table 6.3.6(1) 23 or 79% occurred within six hours of 8 a.m. The morning maximum pattern of diurnal variation is only characteristic of heavy rainfalls from convective clouds and is not found in the light rain which falls from stratus clouds.

The occurrence of a summertime morning maximum of rainfall is widespread over South-east Asia and the western Pacific and, in addition, an afternoon maximum occurs at locations which favour afternoon heating of the surface as at stations inland or on large islands (Ramage 1952, Gray and Jacobson 1977). Ramage (1952) could find no synoptic reason for the morning maximum and proposed that it was due to existing cumulus clouds becoming more unstable due to the nocturnal cooling of their tops and the relative warmth of the surface beneath the clouds where nocturnal radiation loss is inhibited.

In a study of cloud clusters over the western Pacific Ocean Ruprecht and Gray (1976) found that the mean hourly rainfall during the five-hour period around 00GMT (07 - 12LT) at Pacific islands and atolls below clusters was more than twice that in the five-hour period around 12GMT (19 - 24LT). Rain heavier than 25 mm/h was three times as prevalent in the morning. They also determined the average cloud cluster divergence at 00GMT and 12GMT from rawinsonde soundings. Their results are similar to those in Fig. 6.4.1(2) for cloud clusters. These show an increased lower tropospheric convergence with a deeper and more intense outflow layer at 00GMT than in the evening. These features were attributed to radiation losses in the surrounding clear atmosphere. There is no solar heating at night in these clear areas to counteract

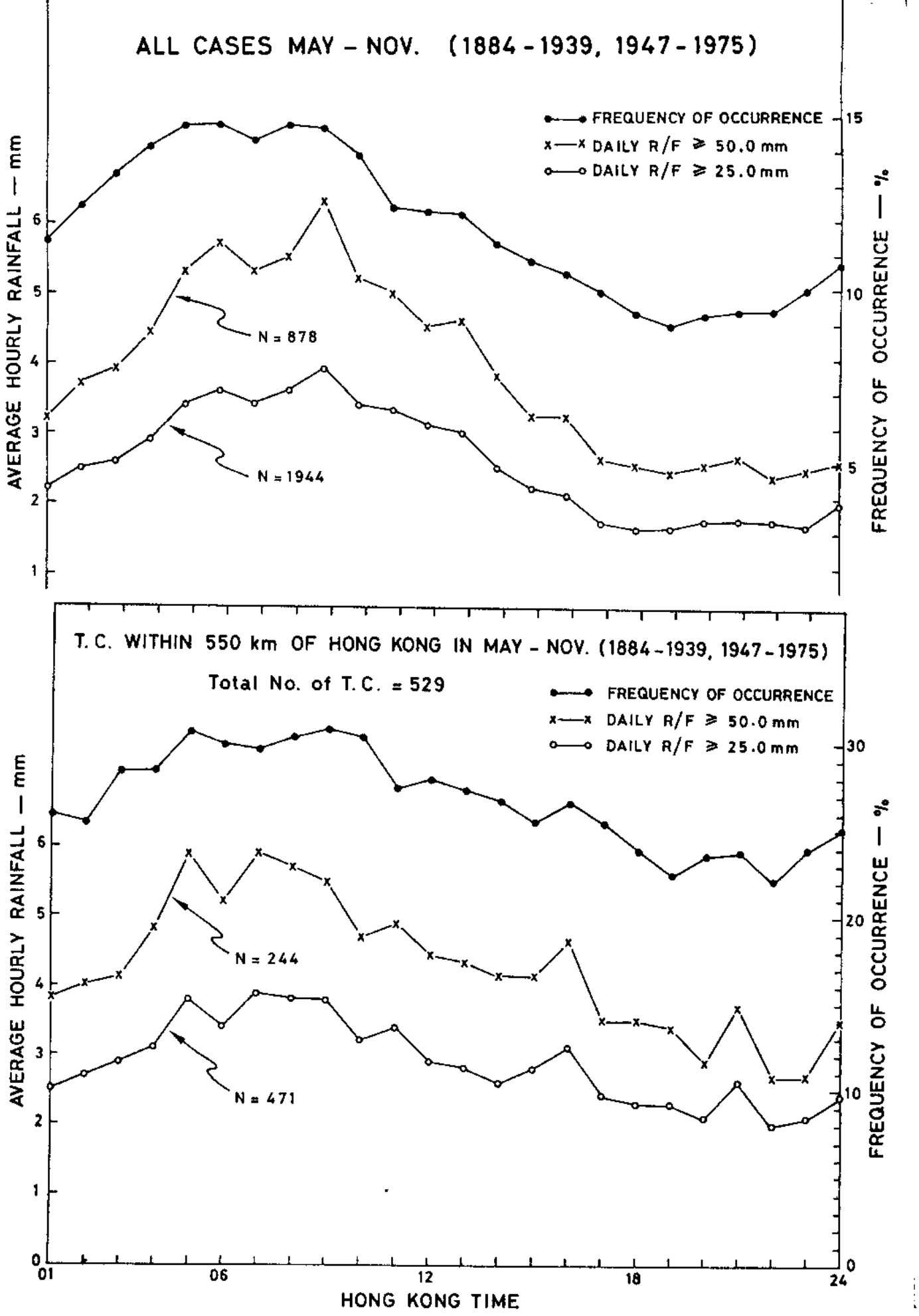

Fig. 6.4.1 ~~6.3.8~~(1). The diurnal variation of rainfall at the Royal Observatory Hong Kong on days when more than 25 mm and 50 mm were recorded. The upper graph refers to all such days and the lower figure to tropical cyclone days. The upper curve in each graph gives the percentage frequency of occurrence of rain hours ($\geq$0.1 mm).

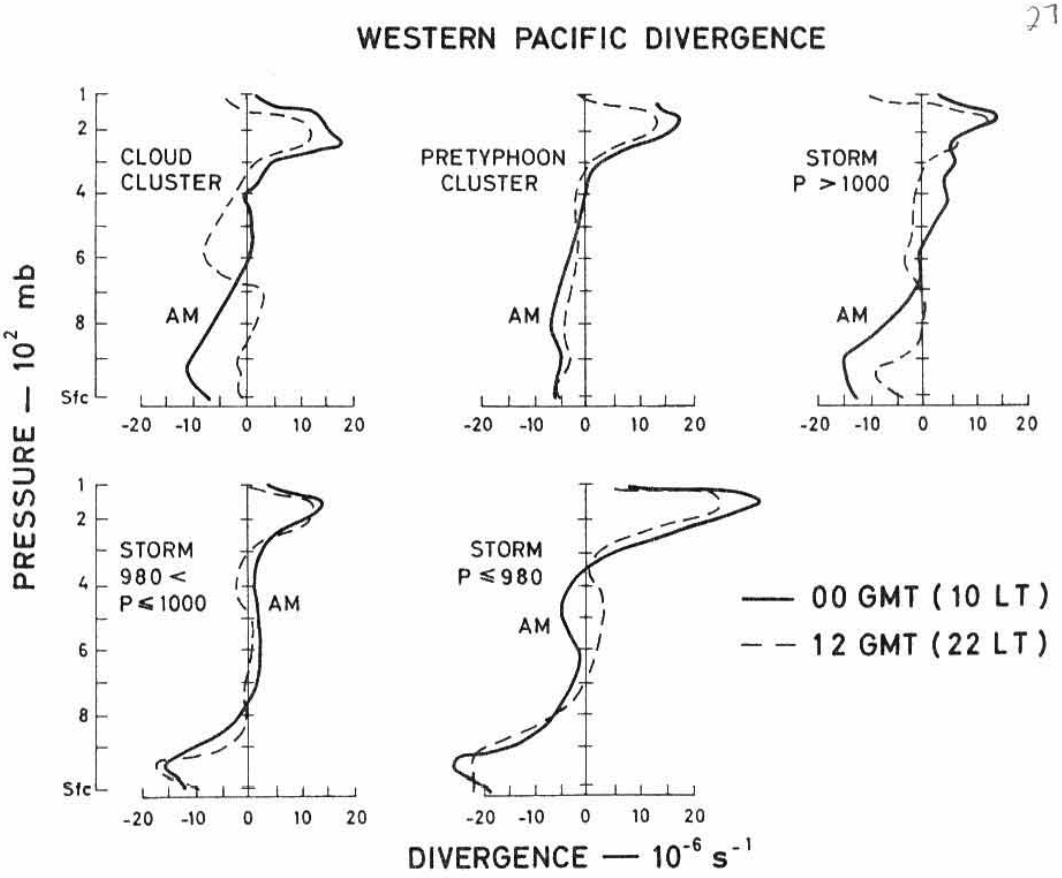

Fig.6.4.1(2).Mean divergence within 3° latitude of the centre in five Western Pacific composite weather systems. (After McBride and Gray 1980).

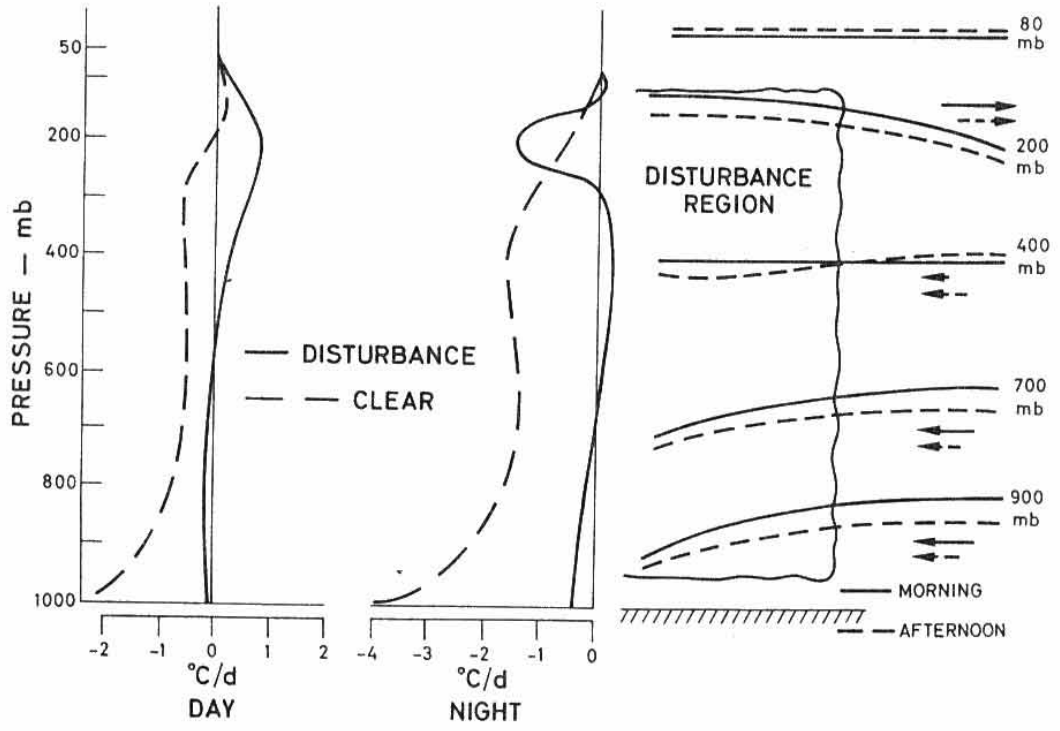

Fig. 6.4.1(3). Estimated typical day and night rates of radiation and condensation temperature change within 3° latitude of the centre of a tropical disturbance and its surroundings (left). The full line represents the net radiative-convective heating rate in the cloud cluster. The dashed line is the radiative heating rate in surrounding relatively clear region. On the right is shown the idealised slope of the pressure surfaces at different times and the corresponding down-the-pressure-gradient radial wind patterns which become established. (Redrawn from McBride & Gray 1980).

the infrared long wave cooling of about 1.8°C/d which goes on continually in the tropical lower troposphere (Cox 1971). During the day solar heating of about 0.8°C/d reduces the net cooling in the lower half of the clear troposphere to about 1°C/d. This cooling is not directly observed in the atmosphere which probably adjusts with compensating subsidence. The surrounding subsidence results in increased convergence into the disturbed area and causes enhanced upward motion there.

The differences between the radiation regimes found within a cloud cluster or tropical cyclone with a thick cirrus shield and that within the surrounding cloud-free region were studied further by Gray and McBride (1980). The cirrus canopy is largely opaque to infrared (IR) radiation and prevents the upward loss of energy at these wavelengths from lower clouds. In addition, condensation and evaporation resulting from upward vertical motion slightly warm the upper-troposphere and cools the lower troposphere of a typical tropical weather system. By contrast, cloud-free areas cool radiatively by IR energy loss at significantly greater rates than those at the same level under the cirrus canopy. By day, solar energy is absorbed and acts to increase the temperature of the cloud free areas throughout the troposphere but in the cluster or tropical cyclone it acts primarily to raise the temperature within the upper cloud layers. Gray and McBride (1980) estimated the rates of change of temperature due to radiation and convection, by day and by night, to be as shown in Fig. 6.4.1(3). The diurnally varying radiative-heating differences between disturbances and their relatively cloud-free environment cause changes in the pressure gradients around the disturbances (Fig. 6.4.1(3)). Because geostrophic control is weak at tropical latitudes the gradients lead to significant ageostrophic flow and large diurnal mass convergence and vertical velocity differences (Fig. 6.4.1(4)). Maximum accumulated night-time cooling effects should occur 1-2h after sunrise and a maximum solar warming effects should occur near sunset. If the wind adjustment lags on the changes in pressure gradients by a few hours then the maximum and minimum convergence would occur in the late morning and late afternoon as observed.

This radiative-heating forcing of morning convergence in tropical weather systems has been shown to occur in all areas of the tropics(Gray and MacBride 1980). However, this does not necessarily imply that a morning maximum of rainfall occurs in all areas. The diurnal variation

of rainfall can be quite different from that of the mass and moisture convergence because the magnitude of other relevant factors vary from one region to another. For example, the greater thermal stability and low-level wind shear found in the eastern Atlantic (GATE area) causes the convection initiated there in the morning to take 4-8 hours to become organized into rain producing systems. The rainfall maximum in this area therefore occurs in the early afternoon (McBride & Gray 1980).

Analyses of soundings from both the Western Pacific and the Western Atlantic showed the following consistent features (Gray and McBride 1980):-

(i) The low level convergence in the layer from the surface to 850 mb is greater in the morning (7 - 10 a.m.) than in the evening (7 - 10 p.m.)

(ii) There is convergence in the evening in the middle troposphere near 450 mb.

(iii) In the morning the upper level outflow extends through a deeper layer of the atmosphere than it does in the evening.

(iv) The mean tropospheric upward vertical motion is greater in the morning than in the evening.

Typhoon and hurricane analyses show only the features (iii) and (iv). The diurnal forcing described above is equally applicable to these storms and small differences between day and night convergence and vertical velocity patterns are evident in Figs. 6.4.1(2) and 6.4.1(4). However, the changes observed are less marked than in weaker disturbances because the radiational-convection pressure gradients are over shadowed by the much larger gradients which exist in the cyclones. Nevertheless, the changes are of a sufficient magnitude to modulate the intensity of storm rainfall.

The lower graph in Fig. 6.4.1(1) shows that rain is more frequent and heavier during the morning in tropical cyclones which affect Hong Kong. The rainfall recorded at nine island stations in the Western Pacific when they were within 4^{o} latitude (444 km) of a tropical cyclone is shown

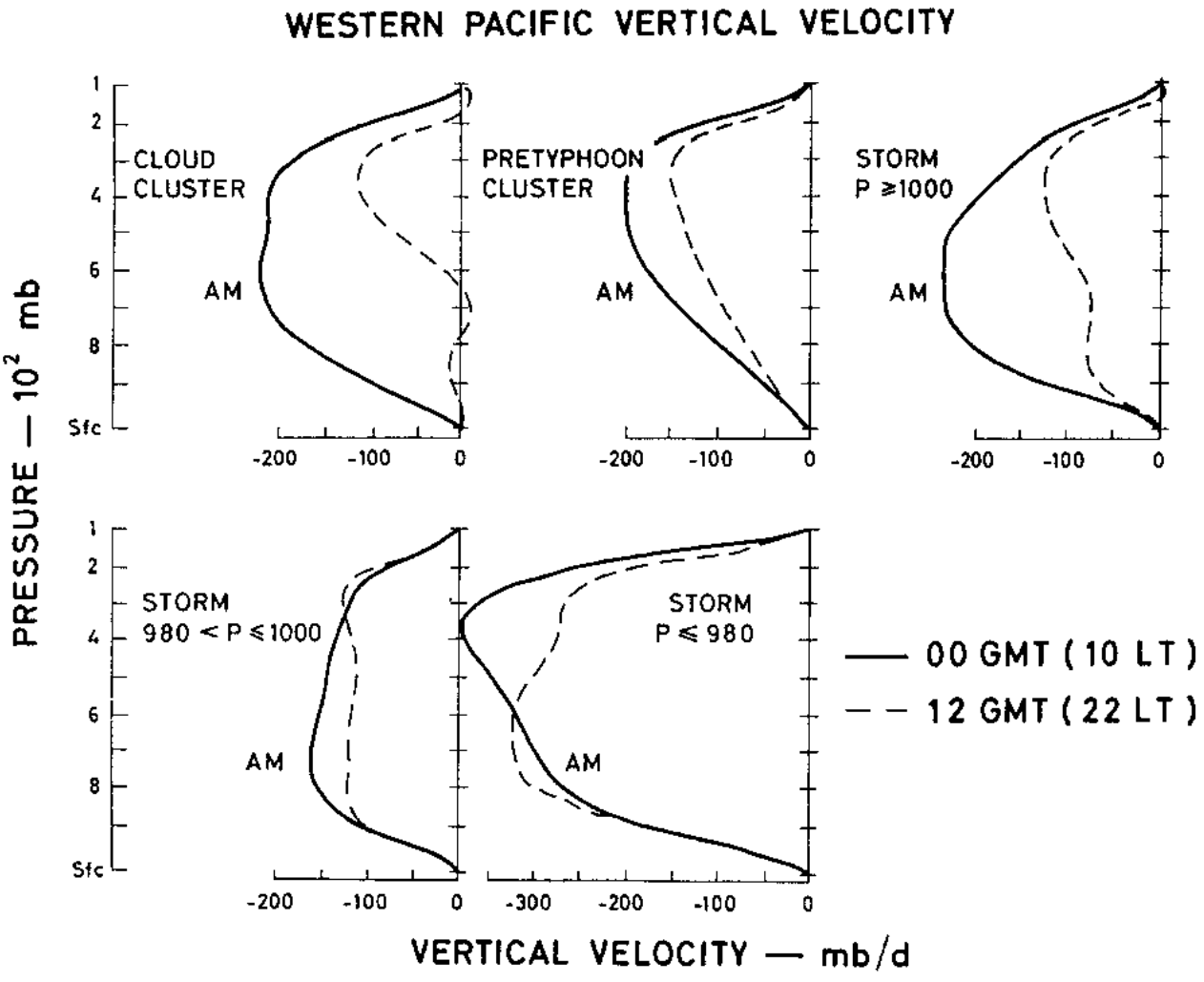

Fig. 6.4.1(4). Mean vertical velocity within 3^{o} latitude of the centre of five Western Pacific composite weather systems. (After McBride and Gray 1980).

in Fig.6.4.1(5). The rainfall used in this study (Frank 1977) fell from 248 tropical cyclones 143 of which attained a central pressure of 980 mb or less. The fact that the diurnal forcing is evident only in the heavier rain, typical of deeper convection, is well illustrated in this figure. There are two practical aspects of the diurnal variation of heavy rain in tropical cyclones. The first is that an intensification of tropical cyclone radar echoes should be expected around dawn; this will make lesser storms stronger and better defined by radar. The effect is more noticeable in the limited echo coverage of tropical storms than in the more extensive area of echoes in mature typhoons. Secondly, flash-floods and landslips are more likely to occur in the morning hours if moderate and intermittent rainfall in the outer parts of a tropical cyclone has brought the soil to near saturation and the centre of the storm is expected to move closer overnight.

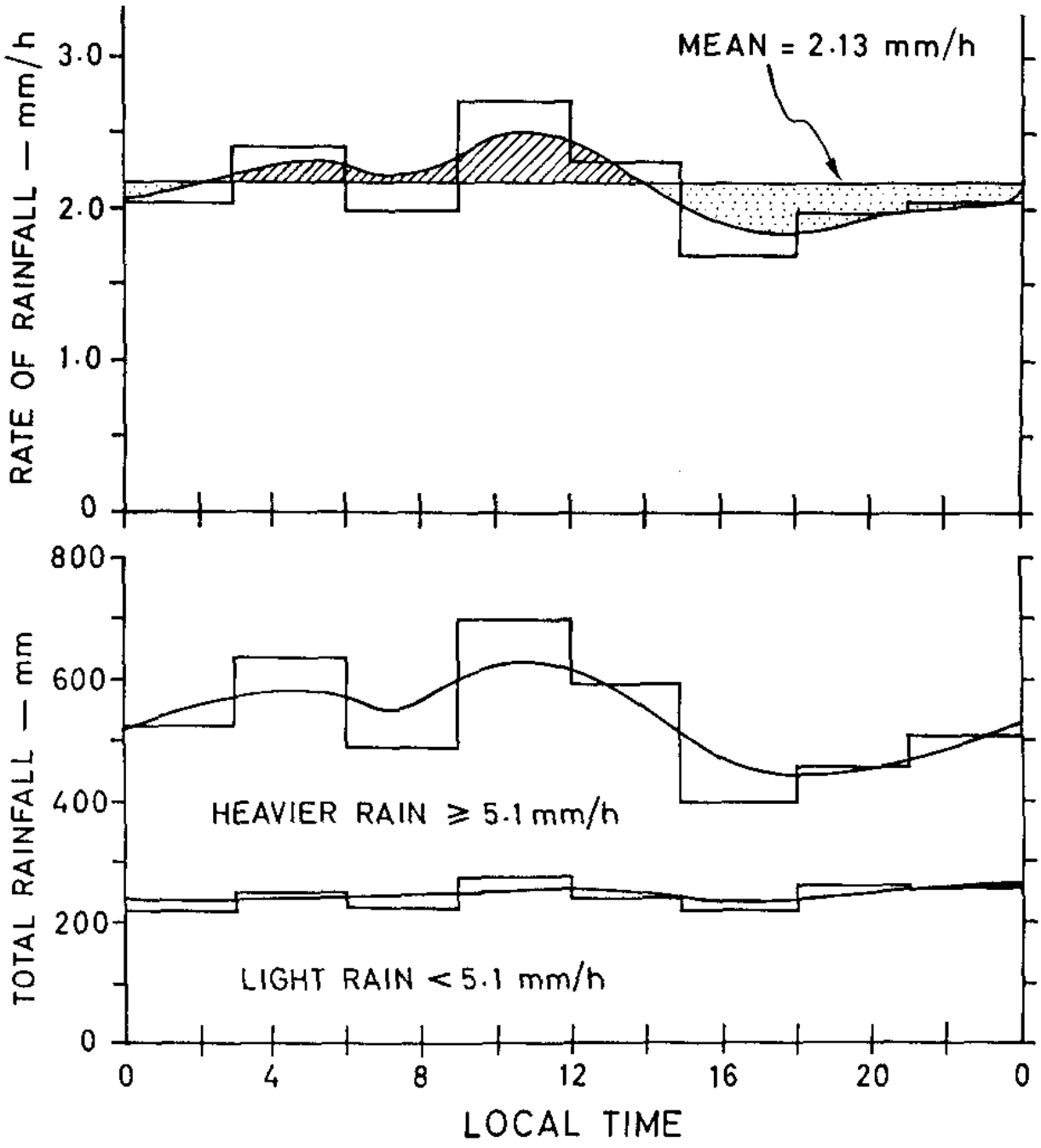

Fig.6.4.1(5) . Diurnal variation of the total rate of rainfall (the total rainfall divided by the time that the storm was within 4° latitude of the station) for nine Pacific island stations(top). The lower graph shows the diurnal variation of total rainfall during heavier rainfall episodes (≥ 5.1 mm/h) and light rain (< 5.1 mm/h) episodes for the same stations. (Redrawn from Frank 1977).

6.4.2 Oreigenic[+] effects

The rainfall in tropical cyclones is greatly enhanced in the vicinity of high ground. Fig. 6.4.2(1) clearly demonstrates this effect for the large and mountainous island of Taiwan while Table 6.4.2(1) and Fig. 6.4.2(2) show that the phenomenon is also important over lesser hills. Three general features of oreigenic rainfall associated with tropical cyclones are illustrated in Fig. 6.4.2(1). Firstly, typhoon rainfall on the east coast of Taiwan facing the ocean and exposed to the direction from which typhoons most frequently approach is greater than at stations, at a similar altitude, on the more sheltered west coast secondly, the rainfall generally increases with altitude reaching a maximum around 2 000 m and thirdly, above this level the rainfall decreases, at least in the mean, as indicated by the rainfall at Yushan (Fig. 6.4.2(1)).

The rainfall at hill stations during tropical cyclone conditions does not vary uniformly with their height because gulleys, passes and the basic wind direction all affect the airflow in a complicated way. However, it is clear from Table 6.4.2(1) and Figs. 6.4.2(1) and 6.4.2(2) that, in general in typhoons, stations at levels around 1 000 m receive about four to five times as much rain as falls on offshore islands and about twice as much as falls on coastal plains. These ratios often apply also to individual storm cases such as that shown in Fig. 6.4.2(2) but changes in storm motion and consequent wind changes can give more complicated results. Table 6.4.2(1) shows that the average tropical cyclone rainfall at the three stations Waglan Island(50 m), Tates Cairn(575 m) and Tai Mo Shan(950 m) increases almost linearly with height at a rate of about 1 mm more rain per metre of height. These three stations are well exposed and distant from higher ground but, the other stations situated within the hills in valleys or gulleys have more rain than a simple linear relationship would indicate.

Up to some height near 1 000 m the total rainfall, from all causes, tends to be greater at high level stations in the tropics than at lower stations. Above this level near 1 000 m the rainfall decreases with altitude because of the lower temperature and consequent lower water

+ oreigenic means caused by mountains. Orographic, a word sometimes used in this context has to do with the description of mountains.

there.
content of the atmosphere ~~at these higher levels~~. However, the level of reversal may be higher in tropical cyclone conditions. Eqn (6.1) shows that rainfall is a function not only of water content but also of the inflow rate and therefore the rate of ascent of the atmosphere. Depending on wind speed and local topographic conditions the rate of ascent near high mountains in high wind speed conditions may well go on accelerating up to mid-tropospheric levels. Doppler radar (sect 10.8.4) measurements in typhoon conditions have shown up-drafts accelerating with height above 3 km in quite modest topographic conditions (Fig. 6.4.2(3)) while the water content at these heights in deep typhoons can be much greater than is found in the average tropical atmosphere (Table 4.)

The rate at which tropical cyclone rainfall increases with distance in the direction from the coast to the upper slopes of nearby mountains can be remarkably high. Although this feature is shown on charts of average tropical cyclone rainfall e.g. Fig. 6.4.2(1), it is also a feature of the distribution of rainfall from individual storms as illustrated, for example in Figs. 6.4.2(2) and 6.8.1(3). Indeed, the steepest gradients occur in individual storms when the exposure favourable.

Table 6.4.2(1) Variation of mean annual rainfall and mean annual tropical cyclone rainfall with height at stations in Hong Kong 1968-76

Station Name	Height a.m.s.l.	Mean Annual T.C. Rainfall	Mean Annual Rainfall	% Rainfall Due To T.C.
	m	mm	mm	%
Royal Observatory	32	724.5	2428.9	29.8
Waglan	50	259.0	1300.2	19.9
Aberdeen Upper	120	702.9	2306.7	30.5
Tai Tam	155	769.1	2568.0	29.9
Jubilee	200	850.6	2682.7	31.7
Tate's Cairn	575	790.5	2833.5	27.9
Tai Mo Shan Farm (1968-73)	640	954.3	2879.5	33.1
Tai Mo Shan	950	1118.9	3161.2	35.4

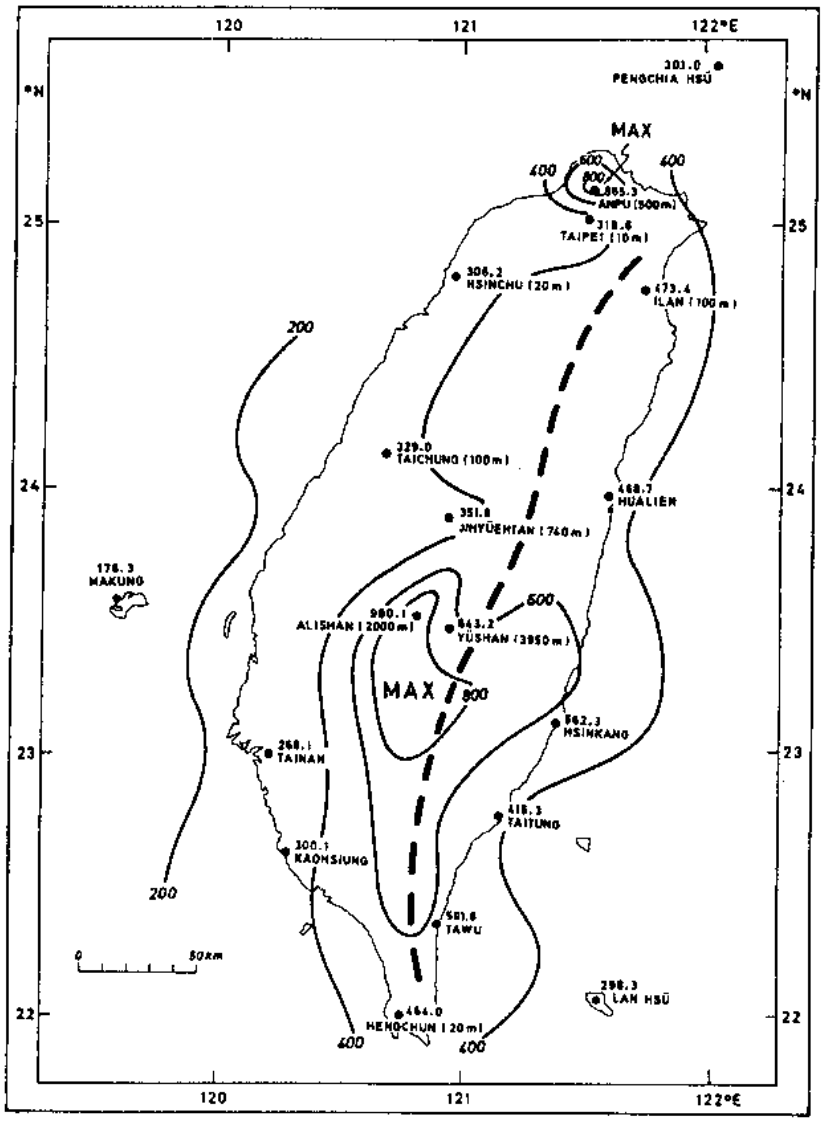

Fig.6.4.2 (1) Average annual rainfall from tropical cyclones whose circulation affected Taiwan during the period 1959 to 1974. The main mountain range containing peaks to over 3 000 m is indicated by the heavy dashed line.

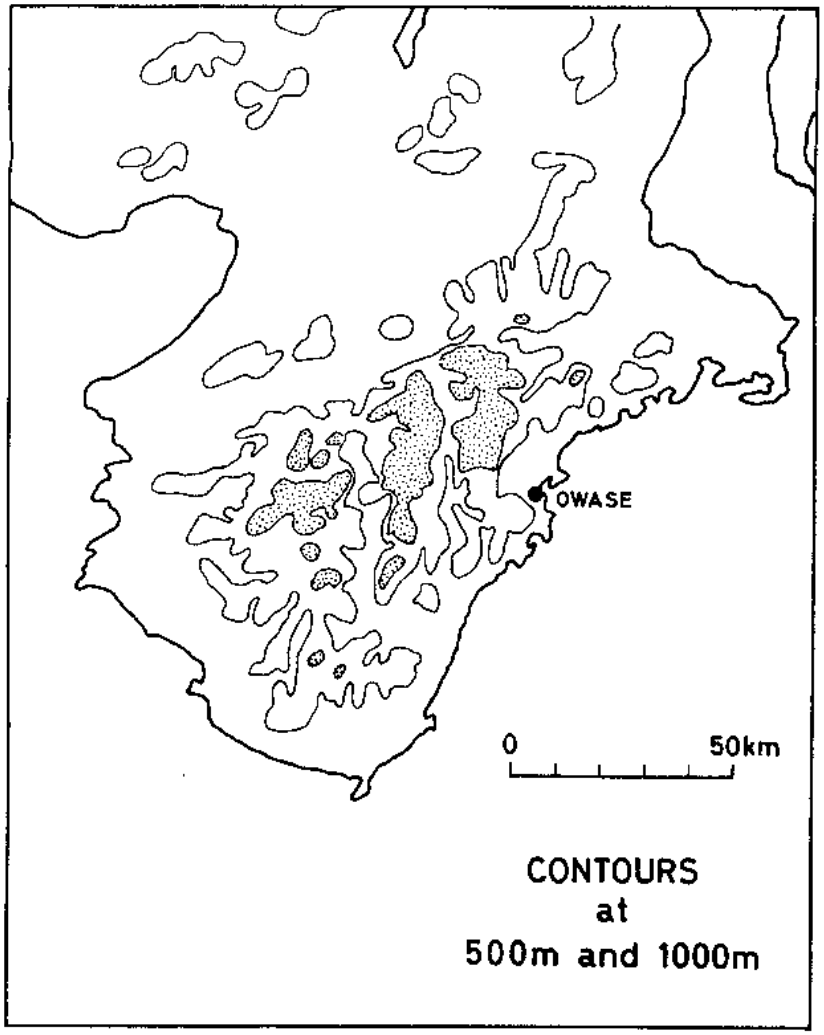

Fig. 6.4 [2(2)]. The topography of the Kii Peninsula, Honshu (left) and the 24-hour rainfall distribution there, caused by the passage of typhoon Olga. Reading from about 100 recording-raingauge stations were available. (After Sakakibara and Takeda 1973.)

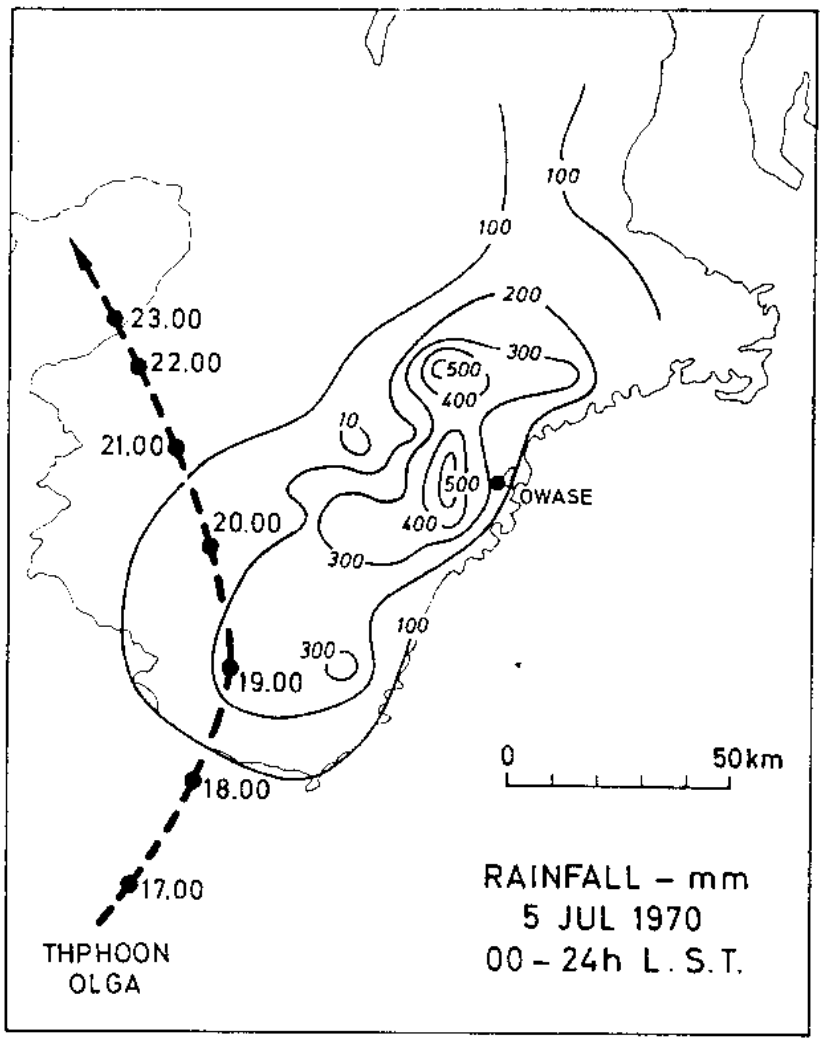

for high rainfall at upper stations is sustained. Table 6.4.2(1) shows more In Hong Kong the average tropical cyclone rainfall received on the off-shore island Waglan is less than one quarter of that received at the hill station Tai Mo Shan, 32 km away, ~~Table 6.3.1~~ . This is equivalent to an average gradient of 27 mm/km. For the case of an individual storm The distribution of 24-hour rainfall in the 1959 midget typhoon at Taiwan (Fig. 4.7) showed a gradient from the coast in excess of 40 mm/km.

The dynamics and cloud-physics processes involved in the enhancement of tropical cyclone rainfall by high ground are complex and not yet fully understood. Much good work on these problems, based on observations with sophisticated instruments, has been carried out in Japan. The Staff Members of Tokyo University (1969 and 1970) studied the rainfall due to typhoon Vera (1959). They showed that although the total amount of rain falling at Japanes stations during the passage of the typhoon was very much controlled by ~~the~~ topographic features, the variation of rainfall with time was controlled by the passage across the hills of typhoon rainbands and organized convective systems. ~~In addition, they found that the time change of rainfall amount at~~ The magnitude of the change in hourly rainfa as rainbands passed. a station was dependent on its elevation. These observations suggest that there ~~was~~ is an interaction between the intrinsic typhoon rainfall and that due to the associated oreigenic effects.

At Owase, on the Kii Peninsula to the southwest of Nagoya, the mountains range to over 1 000 m (with a peak at 1 965 m) and receive much more rain from typhoons, on certain tracks, than do surrounding districts, Fig. ~~6.3.2~~ 6.4.2(2) . Sakakibara amd Takeda (1973) showed that the rainfall which would have been caused at a station by typhoon Olga (1970) in the absence of hills, was enhanced by an amplification factor which depended upon the topographic features around the station and the wind velocity. The enhanced rainfall near high ground was not simply the sum of the undisturbed, intrinsic typhoon rainfall and the oreigenic rainfall from low level clouds which could be expected from mechanical lifting. There was a complicated interaction between the convective systems of the tropical cyclone and the oreigenic rainfall such that the total rainfall was greater than the sum of two components. The 24-hour rainfall distributions ~~due to the typhoons~~ from individual typhoons such as those in Figs. ~~6.3.2~~, ~~6.10.2~~ 6.4.2(2) and 4.7 show that the rainfall at some hill stations can be 3 to 10 times greater than that on off-shore islands, ~~or low-lying coastal stations~~.

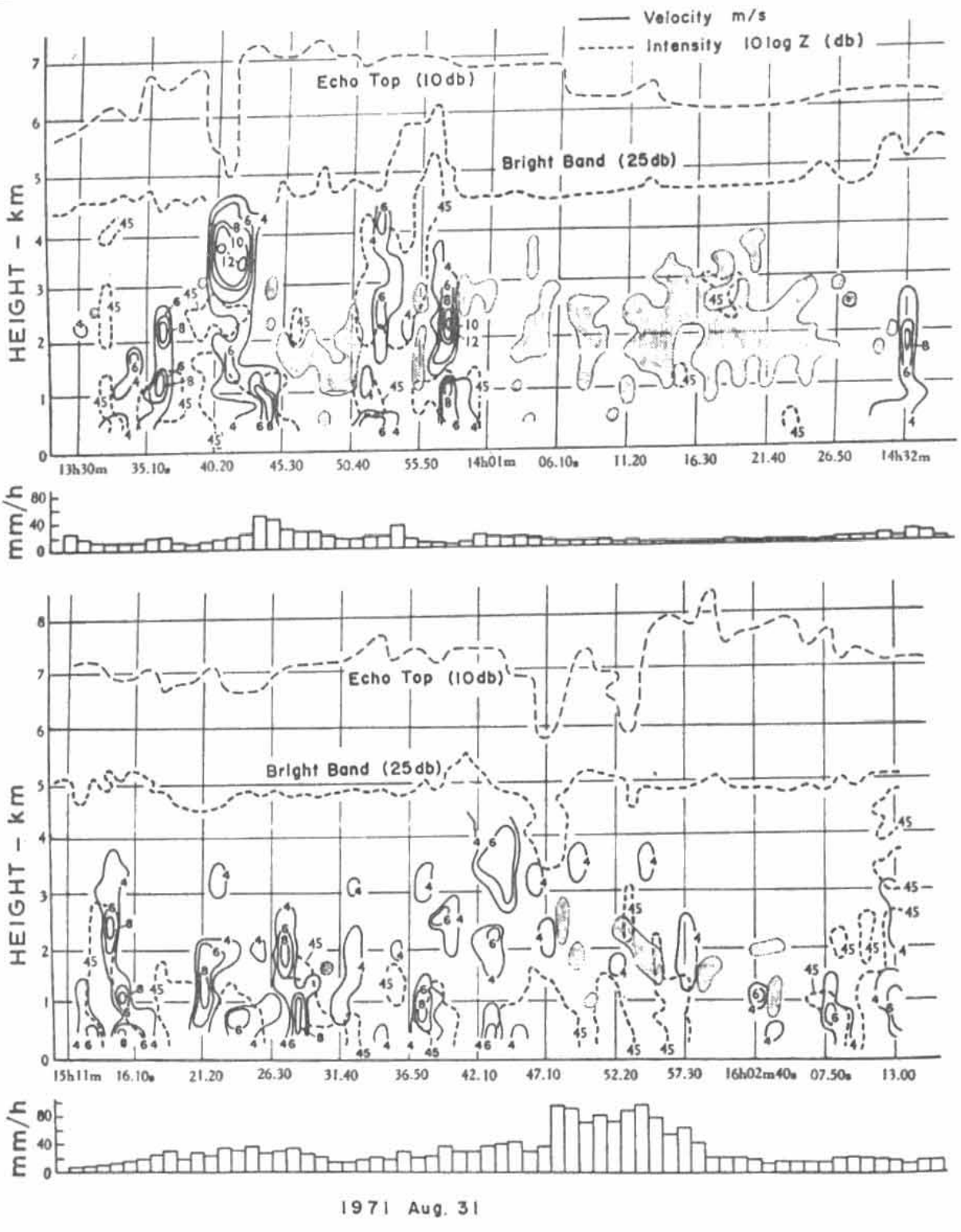

Fig. 6.4.2(3) Time-height cross section of the intensity of radar returns, vertical air velocity and rainfall rate at the ground at Owase during typhoon Trix. Updrafts of 4 m/s or more are indicated by the solid lines whilst regions containing downdrafts (<1m/s) are shaded. (After Yanagisawa et al 1974.)

Takeda and Motoda (1965) reported that, when a typhoon moves over high ground, radar observations show that the number or area of rainfall echoes increases but that the enhanced intensity of the rainfall is not detected by the radar. Other workers have also observed this effect in tropical cyclones (see sect 10.4.6.) and, in particular, Murayama and Fukatsu (1969) found that the enhanced intensity of tropical cyclone rainfall over Owase was not detected by radar. They concluded that the increased rainfall intensity ~~at Owase~~ was caused by typhoon raindrops falling through, and growing in, the many undetectable (by radar) small raindrops of diameter 1 - 2 mm in low-level oreigenic clouds. In support of this hypothesis they showed that raindrop spectra (sect 10.4.6) at Owase had a greater number of drops between 1 and 2 mm diameter than had spectra from stations on the nearby plain.

Yanagisawa et al (1974) investigated the conditions in heavy rain around Owase during the passage of typhoon Trix (1971). The central pressure of the storm was down to 980 mbar as it approached the station on the 30th August with southerly winds of 40 m/s at 850 mb~~ar~~. Rain began at 0700 h (J.S.T.) on that day and more than 500 mm were recorded before midnight with 200 mm being recorded between 1500 and 1800 h. The rain was also observed with a vertically pointing 32 mm Doppler radar, ~~(see Chap. 10.2.4 on radar)~~ a 32 mm RHI radar, and 8.6 mm cloud detecting radar, a standard 56 mm meteorological radar and a rain drop recorder. The usual spiral bands were observed, with widths about 50 km, containing many intense convective cells which were observed to grow and intensify as they moved towards the coast and hills. The RHI radar showed that there was a bright band at a height of 4-5 km in the rainbands, indicating that the upper parts of spiral bands were formed of snow crystals and that up currents were less than 1 m/s. Most updrafts were restricted to the layer below the bright band and only a few intense convective towers penetrated the bright-band level as thunderstorms (Fig. 6.4.2(3)). The updrafts ($\geq$ 4 m/s) were less than 4.5 km in height and about 2 km in width and were distributed at intervals of the order 5 km. The maximum updraft in Fig. ~~6.14~~ 6.4.2(3) is 12 m/s at a height between 3 and 4 km. Many updrafts were confined to the lowest 1 km and these relatively steady low-level updrafts of 1-2 m/s in oreigenic cumuli were always present, in combination with updrafts at higher levels, during periods of intense rain. The average updraft velocity in the lowest 1 km was greater than at higher levels but the frequency of strong updrafts was greatest near 2 km and their occurrence corresponded with periods of heavy rain.

During periods of rain from stratiform cloud in which a radar bright band was observed, the rainfall rate was of the order of 10 mm/h. However, when a large cumulonimbus approached and joined with the low level oreigenic cumuli the rainfall rate rose to the order of 100 mm/h and would persist at this intensity while moving over areas with oreigenic updrafts.

6.4.3 Quasi-stationary Rainbands

Torrential, damaging rainstorms can occur in association with tropical cyclone rainbands at distances as large as 1 000 km or so from the cyclone centre. Such inundations are particularly likely when the movement of a tropical cyclone centre away from an area under a rainband is balanced by the centrifugal motion of the rainband (Fig. 10.22). This condition occurs most frequently in the rear quadrants of tropical cyclones whatever their direction of motion. The phenomenon is usually of less significance in mature typhoons which tend to be compact with almost circular spiral bands (sect 10.6 and Fig. 10.) and have widespread heavy rain. However, the condition may assume great significance in weaker tropical cyclones with "long tail rainbands" such as those in tropical storm Judy 1966 shown in Fig. 4.2. Such long quasi-stationary rainbands feeding into westward moving storms can cause persistent heavy rain at a station. The rainfall may be further enchanced by oreigenic effects. Outer rainbands are frequently broken i.e. rainfall, or indeed cloudiness, may not be continuous along the band (Fig. 6.4.3(1).

The phenomenon is well illustrated for the case of inner rainbands by the radar photographs of typhoon Shirley 1968 shown in Fig. 6.4.3(1). The remnant of the typhoon centred overland was moving away from Hong Kong towards the northwest at 5.7 m/s. Two rainbands near Hong Kong and distant 120 km and 180 km from the storm centre moved away from the centre at about the same speed as the centre moved away from Hong Kong. These rainbands therefore remained quasi-stationary with respect to the ground. No rainfall was recorded at the island station at Waglan - located near the point marked "x" between the rainbands - during the four hour period (1600 - 2000 GMT) determined by the photographs. However, 48.7 mm were recorded at the Royal Observatory, under the inner rainband, where the instantaneous (15 s mean) rate of rainfall attained 200 mm/h. Under similar circumstances one station may receive minimal amounts of rain whilst others a few tens of kilometres away are inundated.

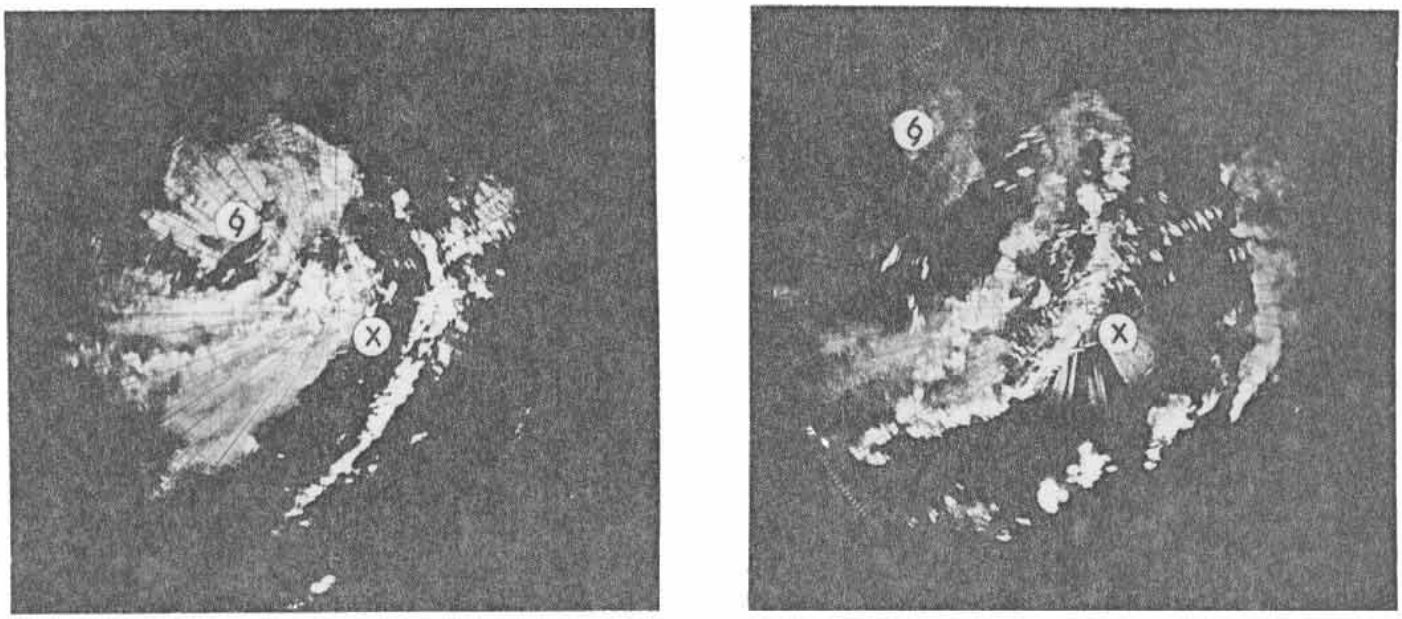

(a) (b)

Fig. 6.4.3(1). Photographs of the Hong Kong radar PPI showing the remnant of typhoon Shirley centred overland at 6 to the northwest at 1620 GMT (a) and 2000 GMT (b) on the 21 Aug. 1968. The point marked "x" remained between rainbands throughout the period. Range rings are at intervals of 74 km.

The weak tropical storm Ellen 1976 provides an impressive example of the mechanism at work in outer rainbands. Over 416 mm of rainfall fell in a 24 h period at Hong Kong when the centre of Ellen was more than 400 km distant with a minimum pressure of about 1 000 mbar. Radar photographs illustrating the near stationary rainbands are shown in Fig. 6.10.3. In tropical storm Carla 1977 a rainband remained close to Hong Kong for two days whilst the storm centre moved westward at about 5 m/s from Hainan to Indo China. On the 5th September when the storm was more than 1 000 km away 119.7 mm of rain were recorded at the Royal Observatory, Hong Kong with the instantaneous intensity (3 s mean) reaching over 700 mm/h as shown in Fig. 6.4.3.2.

Heavy rain fell for more than two days from an outer rainband of severe tropical storm Mac in September 1979. The storm passed to the SW of Hong Kong moving in a general WNW direction at 2-5 m/s towards Macau. This slow movement is close to the average centripetal motion of spiral rainbands accordingly, the heavy rainband shown about 75 km east of the Hong Kong radar in Fig. 6.4.3(3) remained quasi-stationary with respect to the ground while the storm centre moved slowly towards the WNW. Between 00 GMT on 23 September and 06 GMT and 25 September 477.0 mm of rainfall were recorded at Shanmei (station 59501) while only 11.2 mm were recorded at Waglan. During the same period the rainfall at the Royal Observatory Hong Kong was 231.6 mm. The central pressure of Mac was about 995 mb for most of the period of interest - 995.3 mb were recorded at Macau - but rain clouds near the centre were very deep with echo tops to 16.75 km.

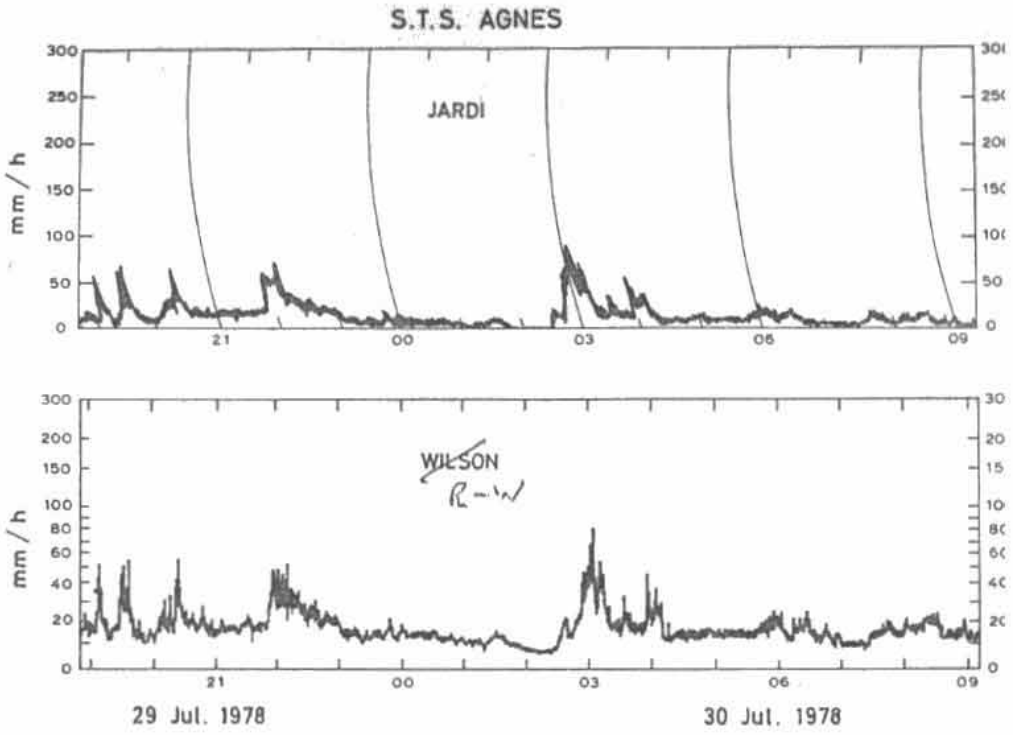

(a)

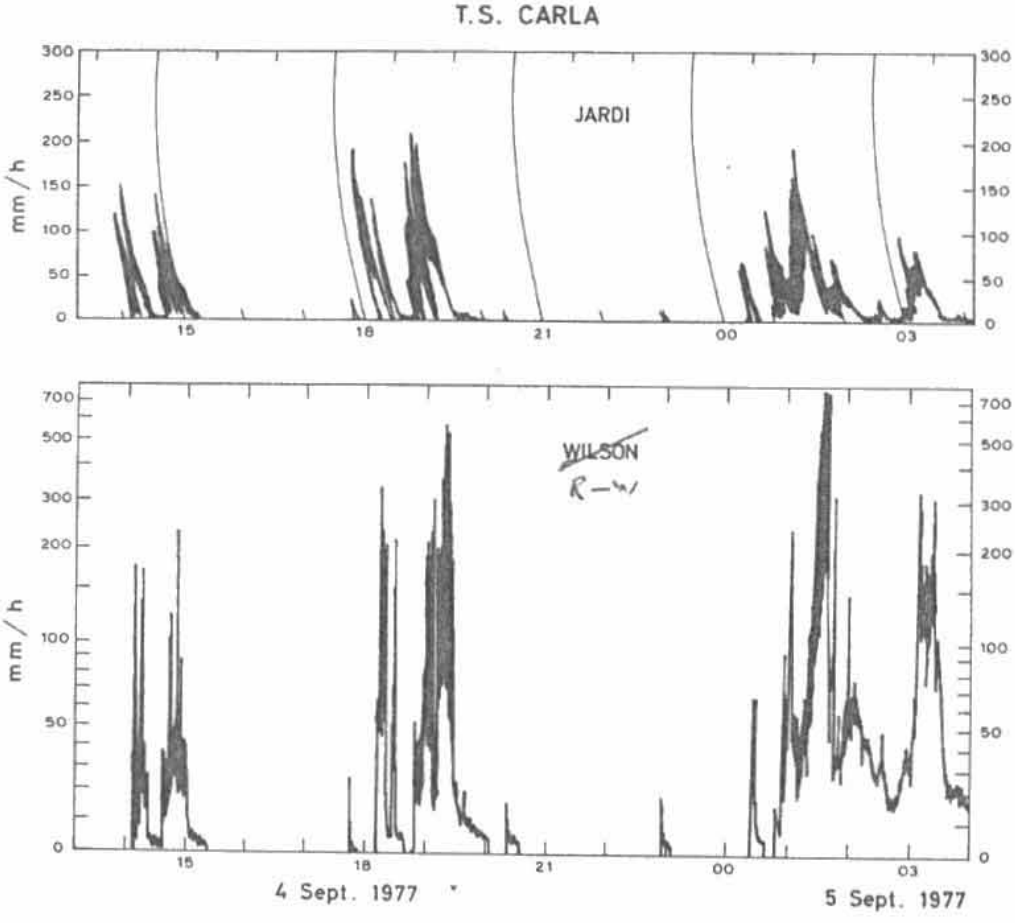

(b)

6.4.3(2)

Fig. (a) Steady rain at Hong Kong with relatively weak embedded rainbands as severe tropical storm Agnes passes about 70 km southeast of Hong Kong and (b) very heavy rain in discrete outer rainbands, without background rain, as tropical storm Carla moved westward across the southern tip of Hainan Island about 740 km southwest of Hong Kong. Time shown is Hong Kong Time (GMT + 8).

Fig. 6.4.3(3). Severe tropical storm Mac seen about 120 km west of the Hong Kong radar at 20 GMT on 23 September 1979 with an associated intense rainband about 70 km to the east of the radar station. Range rings are at intervals of 74 km.

6.4.4 Associated rain areas

In sect 6.3.4 it was stated that severe rainstorms ($\geq$ 500 mm/d) associated with tropical cyclones occur in the inner and outer regions of a tropical cyclone circulation and in stagnant tropical cyclone remnants over land. Heavy rainstorms, usually less than 500 mm/d, also form at distances from the storm centre as great as 1 500 km or more. In higher latitudes these storms are associated with interaction between the tropical cyclone's outer circulation and surface cold fronts and upper westerly waves. In lower latitudes they occur in the enhanced southwest monsoon flow on the storms periphery. Both cases are usually accompanied by an oreigenic contribution and a divergent flow at 200 mb. One favoured area for such storms is the south coast of China where heavy rain falls when a typhoon enters the mainland in the summer months. Lam (1972) analysed two such occasions which caused daily rainfalls of 220.0 mm and 189.3 mm at Hong Kong. Another favoured area is Luzon. Heavy rain falls there when there is a tropical cyclone within about 2 000 km on a bearing in the NE quadrant. The islands of Japan can experience heavy rain falls ahead of a typhoon approaching from the SW.

Of the three situations described, the rainfalls over Luzon are perhaps the most remarkable. Satellite photographs of rain clouds there in association with typhoons Irma 1978 and Rita 1972 are shown in Figs. 6.4.4(1) and 6.4.4(2) respectively. Over the period 17-21 July Rita gave rise to one of the worst floods ever observed in Luzon. Some 775 persons died and damage amounting to over US$120 million (1972 dollars) was sustained, yet Rita was about 1 700 km away at the time as is illustrated by the satellite images in Fig. 6.4.4(2) and the surface chart in Fig. 6.4.4(3). The four features favouring heavy rain were well marked in this case:- 1) a typhoon was centred on a bearing in the NE quadrant 2) the SW monsoon was turned into a more westerly current which impinged on 3) the high ($>$1 500 m) mountains of north Luzon at a time when there was 4) an anticyclonic outflow area in the upper troposphere as shown in Fig. 6.4.4(3).

Gordon (1973) has described some features of this storm and given daily rainfall figures at selected stations. At Manila airport, the five day rainfall in the period 17-21 July amounted to 1 014.9 mm. Many daily totals in the area were in excess of 250 mm. Further north, in the mountains, Baguio City (1 501 m) received 1 296.9 mm in the five

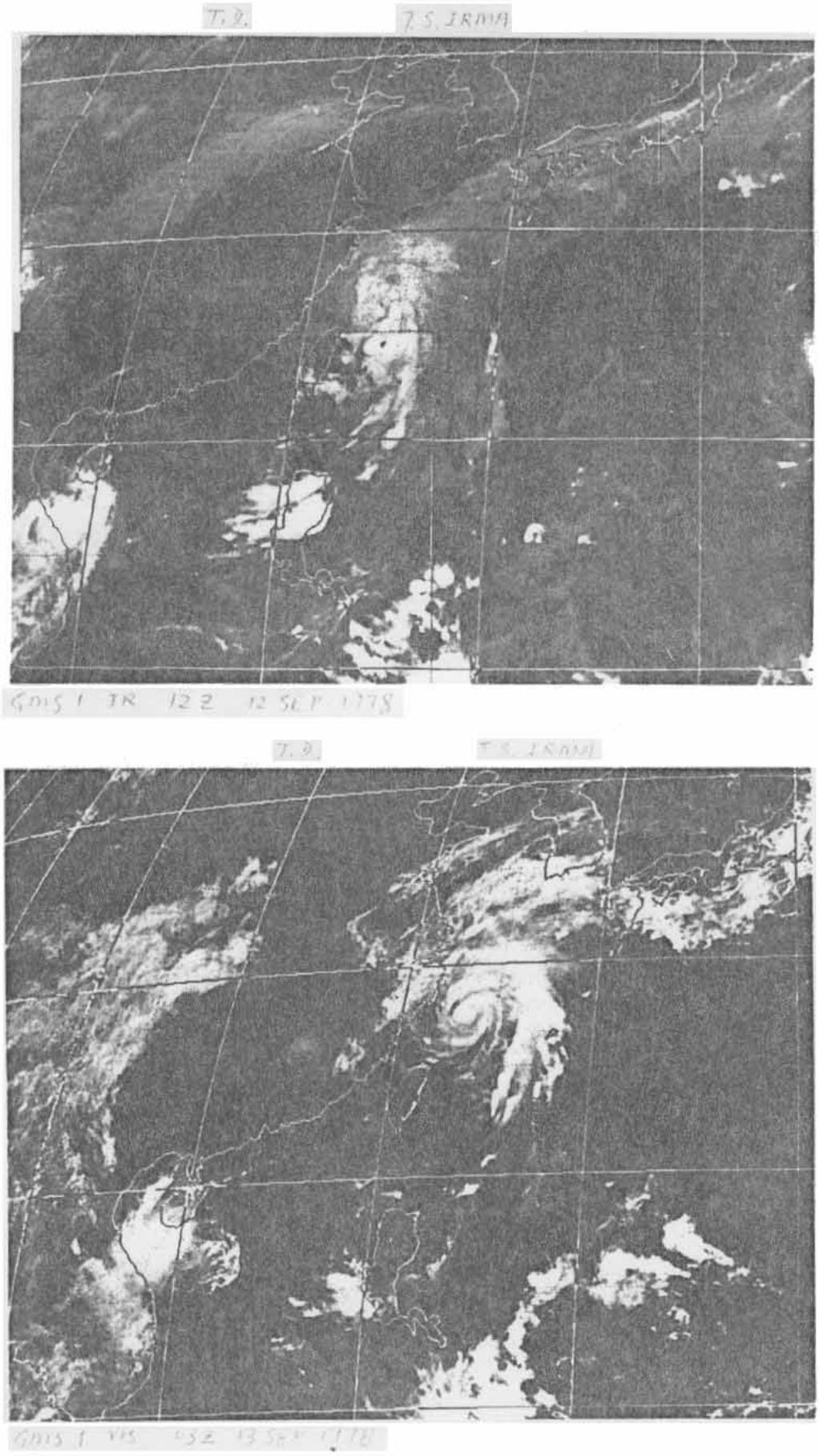

Fig. 6.4.4(1). Typhoon Irma 1978 centred just to the north of Taiwan with an associated rain area over Luzon. The images are from the GMS 1 low resolution channels. The upper picture shows the I.R. image for 12 GMT on 12 September and the lower image is from the visible channel at 03 GMT on 13 September.

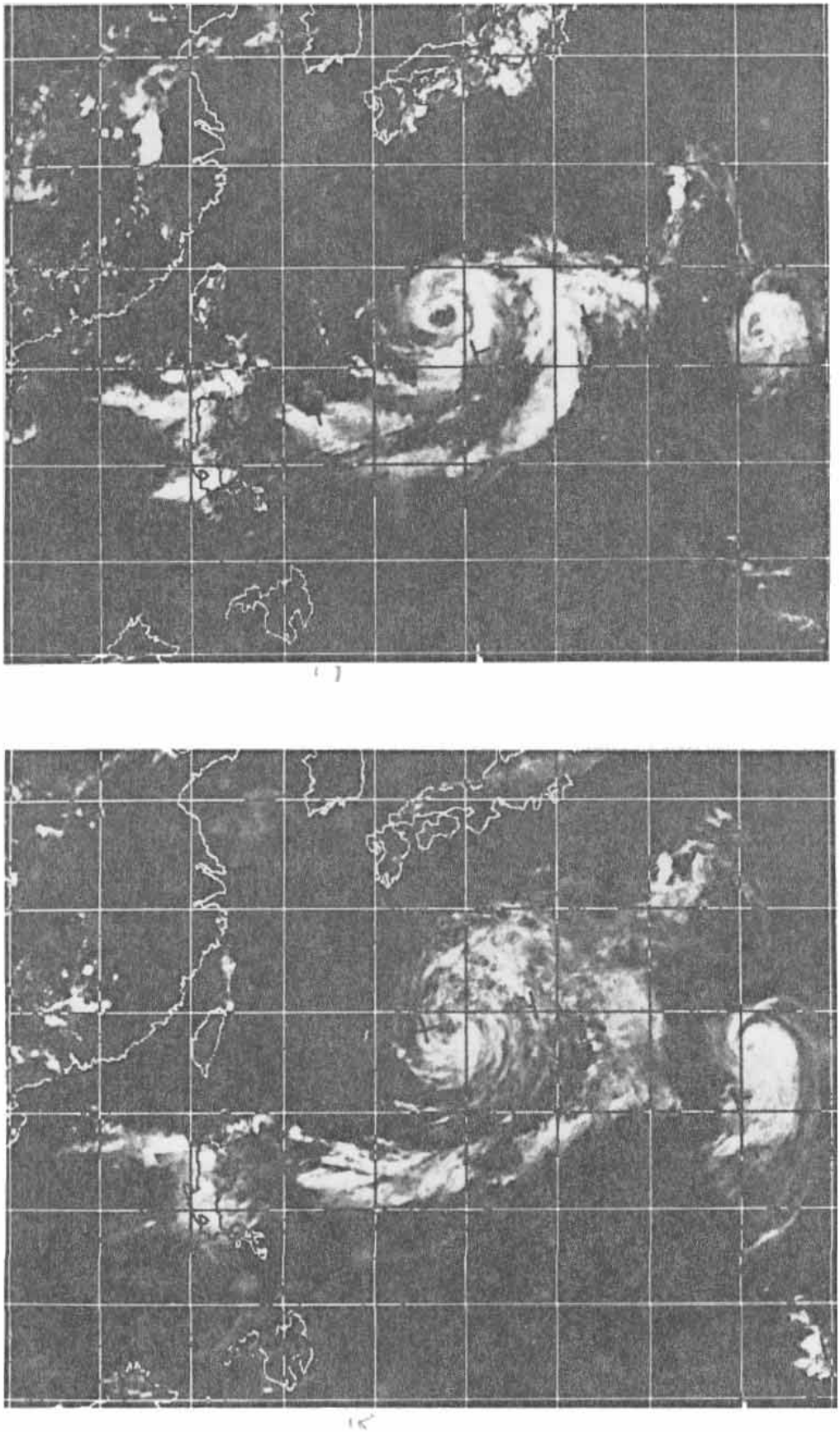

Fig. 6.4.4(2). Inflow towards typhoon Rita 1972 and associated rainstorms over the Philippines. The digitised Essa 9 images are for 17 July 1972 (upper) and 18 July (lower).

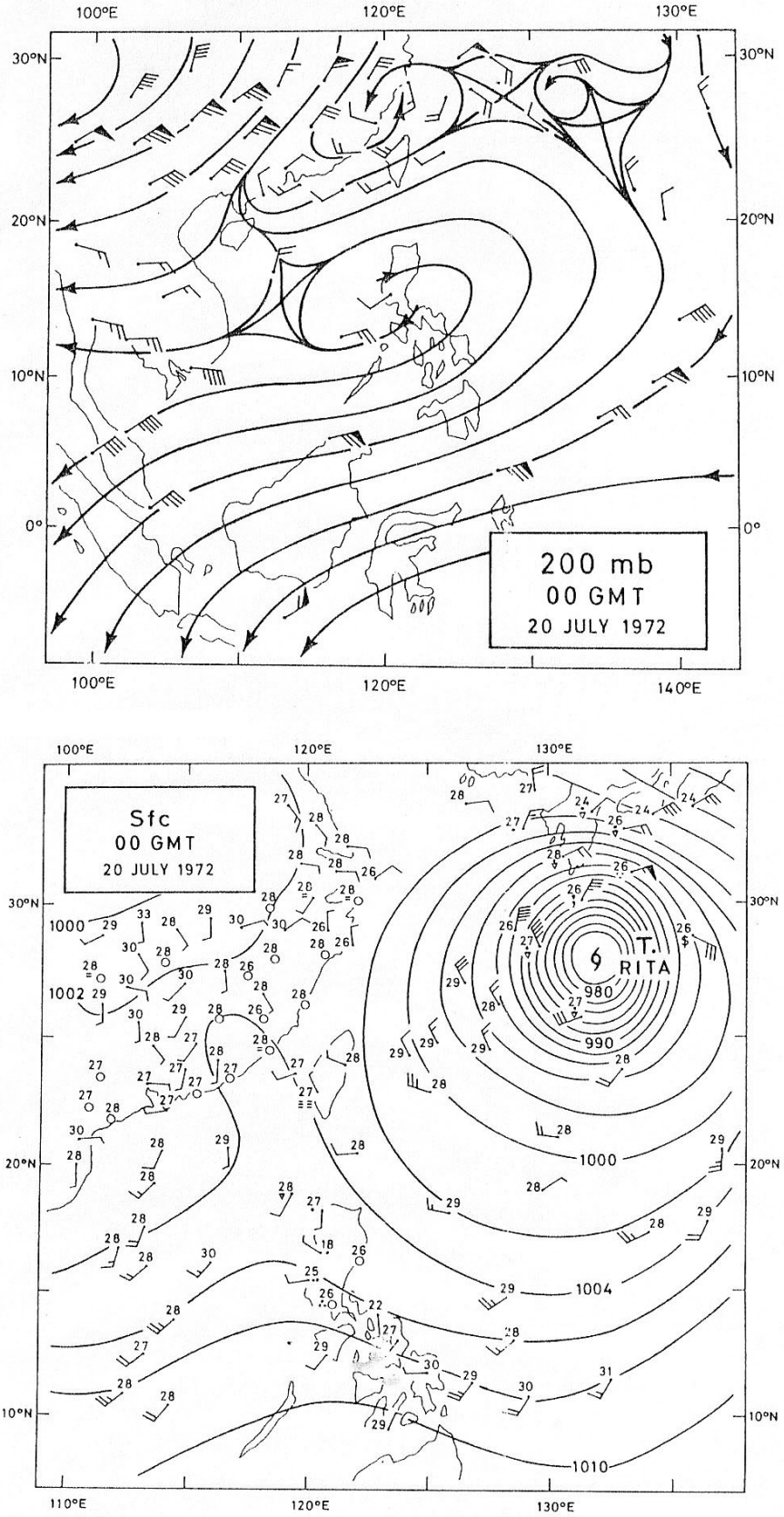

Fig. 6.4.4(3). Charts showing the mean sea level pressure (mb) and 200 mb streamlines at the time of the heavy rains over Luzon.

days 16-20 July with an amount of 479.6 being received on the 17 July. Although the 16-20 July was the wettest spell at Baguio, the whole month was abnormally wet with a total of 4 724.5 mm being recorded. This amount exceeds the average annual total. The frequency of occurrence of peak rates of fall during successive intervals of 15 minutes throughout the month is shown in Table 6.3.6(2). The average daily rainfall at Manila when tropical cyclones are located at various places in the region in the months of July and August is shown in Fig. 6.4.4(5). From the smoothed isohyets for July and August it is clear that tropical cyclones north of Taiwan are associated with average daily rainfalls at Manila which are similar to those experienced when tropical cyclones are near that city. Indeed, in August, tropical cyclones north of 23°N are, on average, associated with double the rainfall (at Manila) than is caused by those nearby.

Gordon (1973) discussed some of the contributions to vertical motion in the south-west monsoon and north-east trade currents. They are listed in Table 6.4.4(1). It is seen that several of these dynamic and thermodynamic factors favour ascent in a moist south-west flow. The importance of orography is clearly shown in the satellite pictures. However, heavy rains will not occur unless there is divergence in the upper troposphere (see sect 6.4.6). Often the divergence is associated with the easterly jet which carries off the cumulonimbii tops towards the west. There is then a strong vertical shear between the south-westerly inflow and north-easterly outflow, a feature found in many of these wet situations. However, more study of the mechanisms involved is required. In Fig.6.4.4.(3) it will be noticed, for example, that the surface winds at west Luzon stations are calm or nearly so and cannot therefore contribute directly to the oreigenic influences. Winds at 850 mb are usually westerly at 10-12 m/s in these wet situations.

In Japan, heavy rainfall occurs on the east side of Honshu and around Tokyo when a typhoon is approaching the western islands of Japan from the south. Japan is then swept by a strong easterly flow. The centre of the typhoon may be about 800 km away to the west or southwest during these heavy rain situations and satellite images look very much like those in Figs. 6.4.4(1) and 6.4.4(2) rotated [illegible] through 180°. There is often no rainfall, or only insignificant amounts, between the rainy areas over the east of Japan and the rains near the storm centre in the west. The same kind of rain shadow appears to the east of Luzon in Figs. 6.4.4(1) and 6.4.4(2). Typhoons Polly and Shirley of 2 August - 2 September 1974 and 4-9 September 1974 respectively, were good examples of this effect. Indeed, Typhoon Rita brought heavy rains to both Luzon and eastern Japan simultaneously with relatively rain free areas between the storm and the two affected areas.

Table 6.4.4(1). Contributions to vertical motion in south-west monsoon and north-east trade currents. (After Gordon 1973)

Mechanism	South-west Monsoon	North-east Trades
Coriolis term	upward	downward
horizontal cyclonic shear	upward	upward
horizontal anticyclonic shear	downward	downward
cyclonic curvature	upward	upward
anticyclonic curvature	downward	downward
Beta effect	upward	downward
conditional instability	upward R.H. 70 per cent	weak upward R.H. 80 per cent
convective instability	upward	weak upward
orography	upward in the western catchments and vice versa	upward in the eastern catchments and vice versa

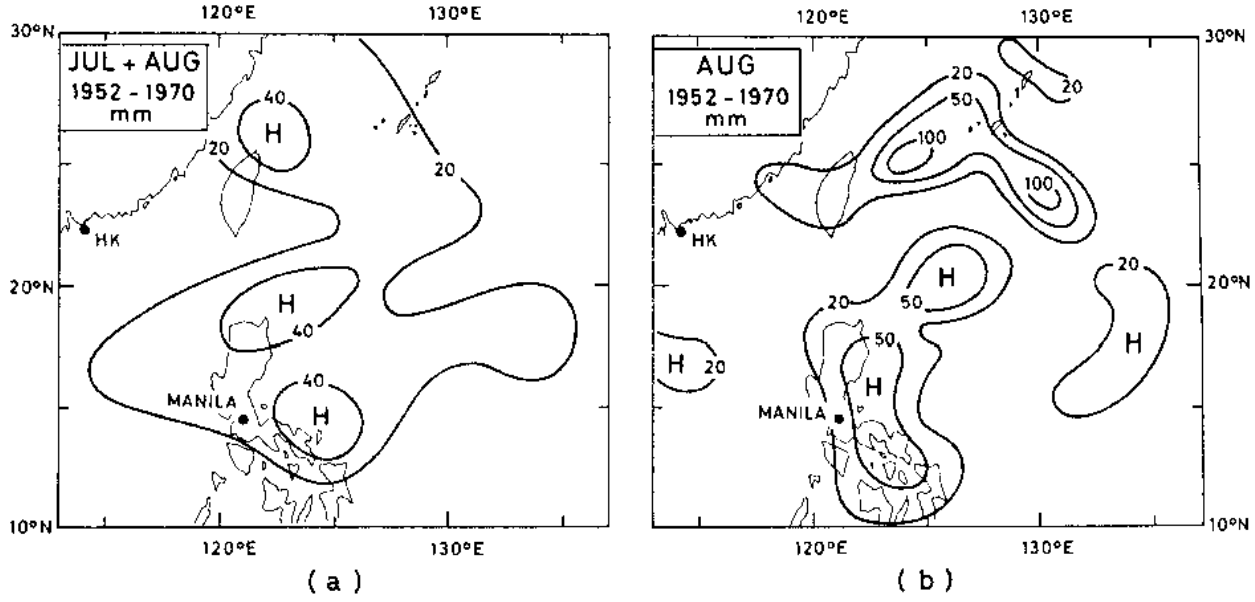

Fig. 6.4.4(5). The average daily rainfall at Manila, when a tropical cyclone is located in a particular one degree square at 00 GMT, is indicated - in mm - in that square. The isohyets in (a) are based on readings averaged over nine, non-overlapping, one degree squares for the months July and August; those in (b) are based on non-smoothed averages for the month of August.

Typhoons which enter China in summer on tracks north of Taiwan or across the island decay ~~in their lower levels~~ weaken as they move westward. However, ~~but activate~~ south of the centre and inflow are intensified the SW monsoon so that an isotach maximum is found ~~south of the centre~~ (S.W.) at levels from 850 mb to 500 mb (Lam 1975). This speed maximum in the south westerlies moves westward with the storm bringing heavy rainfall to stations on the south China coast which may be 800 km or more from the centre of the decaying typhoon. In the two cases studied by Lam (1975) daily rainfall totals of 220.0 mm and 189.3 mm occurred at Hong Kong in August 1969 and August 1972, when the remnant storms were approximately due north of the station three days after crossing Taiwan. Although rain fell on three days in each case, over 65% of the total was recorded on the second day as the isotach maximum in the south westerlies crossed the station. There was, in both cases, a relatively rain-free area between the coastal maximum and the more direct sotrm rainfall. This is illustrated for the case of the 1969 storm in Fig. 6.4.4(6). Indeed, the relatively dry region between the rain areas, already mentioned in connection with the Luzon and Japan rains is a common feature of ~~tropical cyclone~~ distant rain areas associated with E-C-S ~~rain areas~~ and is evident in the satellite image of Fig. 6.3.4(3) and even shows up in the average chart in Fig. 6.4.4(5)(b).

Occasionally, instability storms occur elsewhere in the outer circulation of tropical cyclones than in precursor bands. For example, Tao (1978) described two small cloud clusters which formed on the northern edge of the circulation of typhoon Amy on 21 August 1977. The two cloud clusters are marked A and B on the left hand image in Fig. 6.4.4(7). Typhoon Amy over 1 000 km away is centred near the bottom left of the figure at 20.5°N 118.4°E. The two clusters moved westward at 5-6 m/s in the mid-tropospheric easterly flow around Amy and crossed the China coast at night near Shanghai as shown in the image on the right of Fig. 6.4.4(8). (A) The outflow from cluster B ~~can be seen~~ to streaming towards the east relative to the cluster. A severe and record rainstorm started at Shanghai at 10 p.m. (1256 MT) bringing 540 mm in 8 h and 150 mm in 1 h. The distribution of rainfall from these cloud clusters is shown in Fig. 6.4.4(9). The fact that these storms formed over the sea and persisted for much longer than the usual heat thunderstorms suggests that they had some dynamic cause. The strong shear between the winds at 200 mb and the easterlies at lower levels is characteristic of such long-lived severe storms (see sect 15.7).//

(A) The winds at 200 mb ——→ were 25 m/s from the west, being about 1000 km ahead of an approaching trough, causing

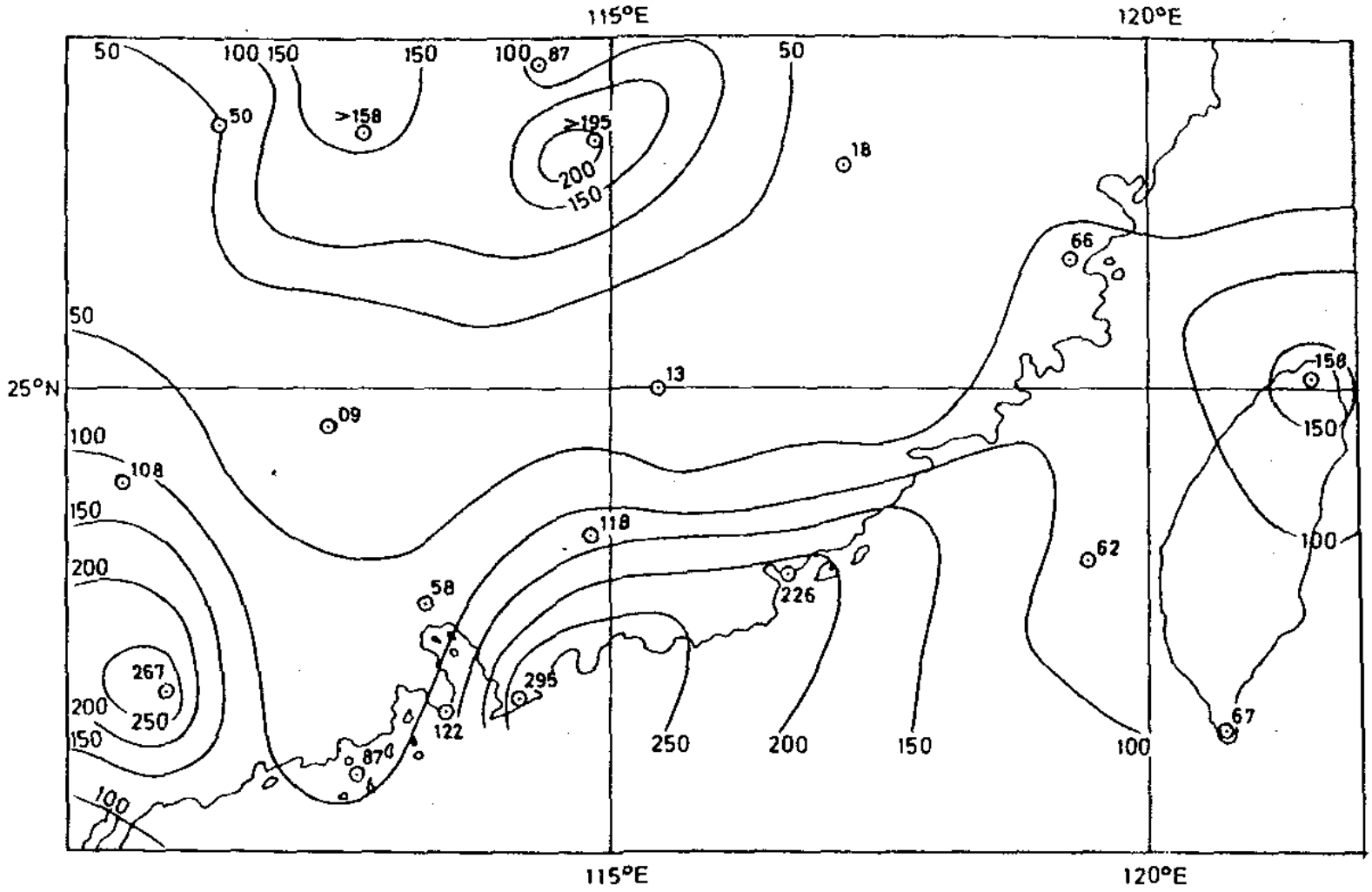

Fig. 6.4.4(6). Total rainfall in period 1(10-12 August 1969) (isohyets and rainfall figures in mm). (After Lam 1972)

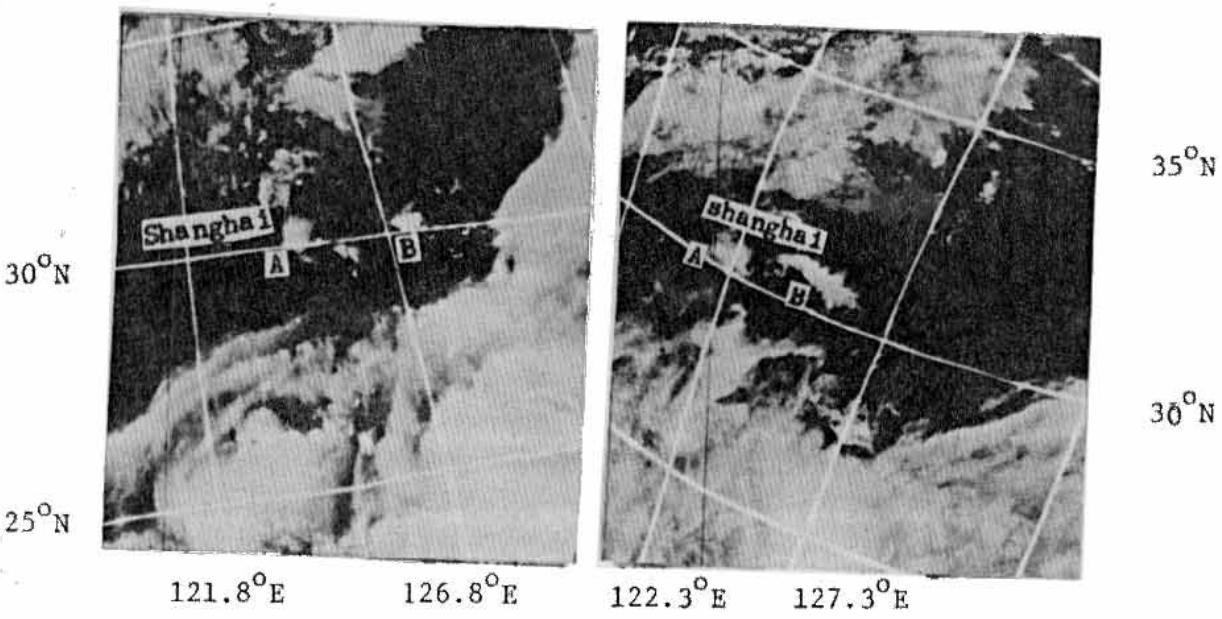

Fig.6.4.4(7). I.R. images from Noaa 5 VHRR received at Peking on 21 August 1977 at 00GMT (left) and 12GMT (right). The small cloud clusters, marked A and B, moved westward to inundate the Shanghai area. In the 00GMT image some of typhoon Amy's outer rainbands are visible to the south of cloud A but, the cyclone centre is well to the south of bottom left corner of the picture.

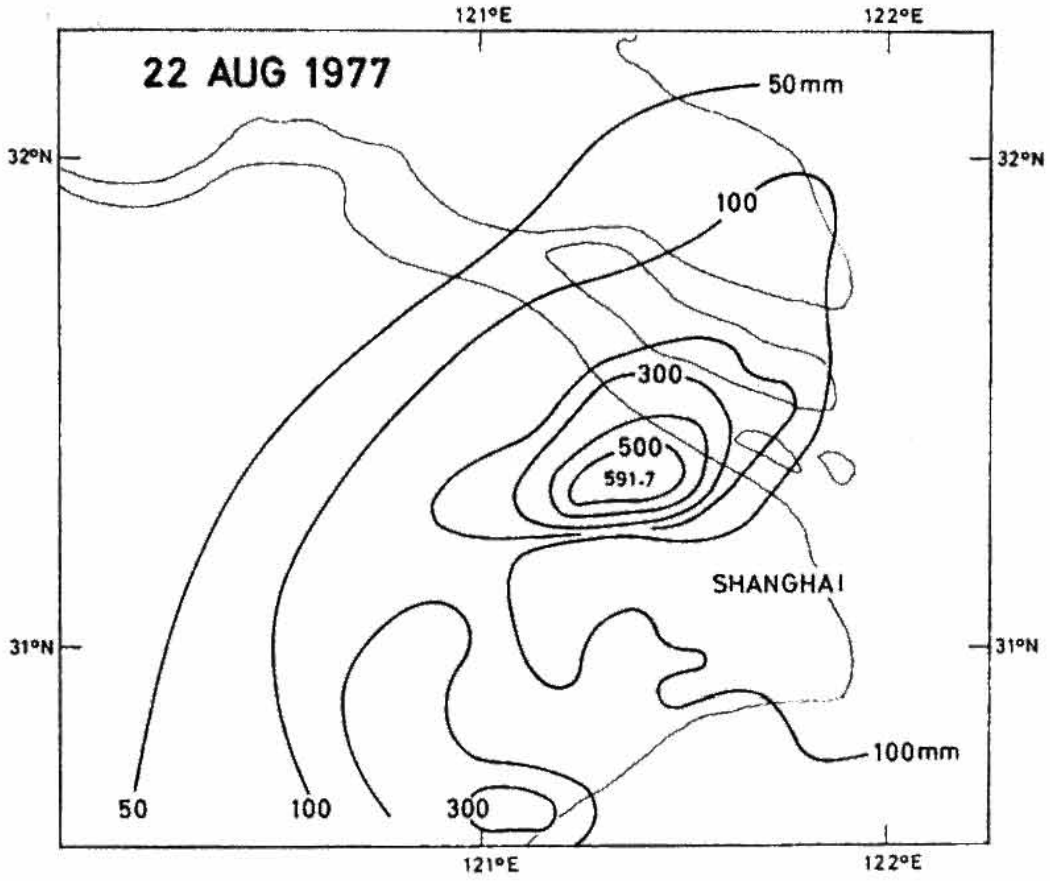

Fig. 6.4.4(8). Isohyets of rainfall on the 22 August 1977 following the convective rainstorms which moved in the easterly flow on the northern periphery of typhoon Amy. The typhoon was centred near Taiwan.

6.4.5 Monsoon effects on precipitation

The interaction of tropical cyclones and the monsoons is discussed in sect 13.2 but we can here consider the effect of the interaction on rainfall and its distribution.

Fig. 13.2. shows how the NE monsoon can be intensified in the autumn as a tropical cyclone approaches the high pressure area over the China mainland. Cold air is entrained into the lower levels of the storm circulation as illustrated by the soundings in Fig. 13.2 . Rainfall may then be widespread in the eastern parts of the circulation where if rides up over the gently sloping upper surface to the cold air (Bell and Fong 1980) to give enhanced rainfall. The phenomenon is illustrated in Fig. 6.4.5(1) which shows the rainfall distribution on the approach of severe tropical storm Nina to the South China coast on 16 October 1978. The cold air reduced the storm to a low pressure area with central pressure of about 1011 mb during the 16 September. No spiral bands could then be seen on radar or satellite pictures. Nevertheless, severe tropical storm Nina become the twelth wettest tropical cyclone to affect Hong Kong as shown in Table 6.3.7(3). A total of 420.2 mm of rainfall were recorded at the Royal Observatory Hong Kong and, of this total, 105.2 mm fell in the three hours between 16 GMT and 19 GMT on 17 October.

In the summer months tropical cyclones interact with the SW monsoon. Typhoons moving into the China mainland enhance the SW flow over the China Sea yielding increased rainfall on the left side of the storm. Typhoon Viola (1969) is shown over south China in Fig. 3.19 The 25 m/s south-westerly flow around an extensive inner area with lower wind speeds is clearly seen. Heavy rainbands - illustrated by Fig. 6.4.5(2) - form in the south-westerlies at such times leading to a rainfall distribution similar to that shown for the case of Nadine 1971 in Fig. 6.4.5(3). These heavy rainbands in the south-westerlies can persist for several days as a typhoon decays over the China mainland. At Hong Kong the heaviest rainfall usually occurs some three days after a typhoon has crossed Taiwan and entered the mainland.

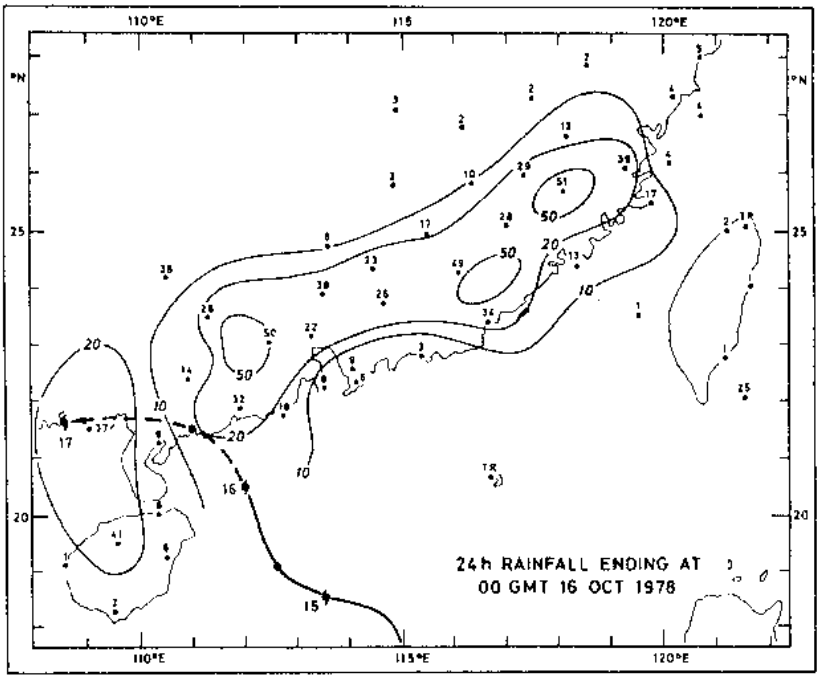

(a)

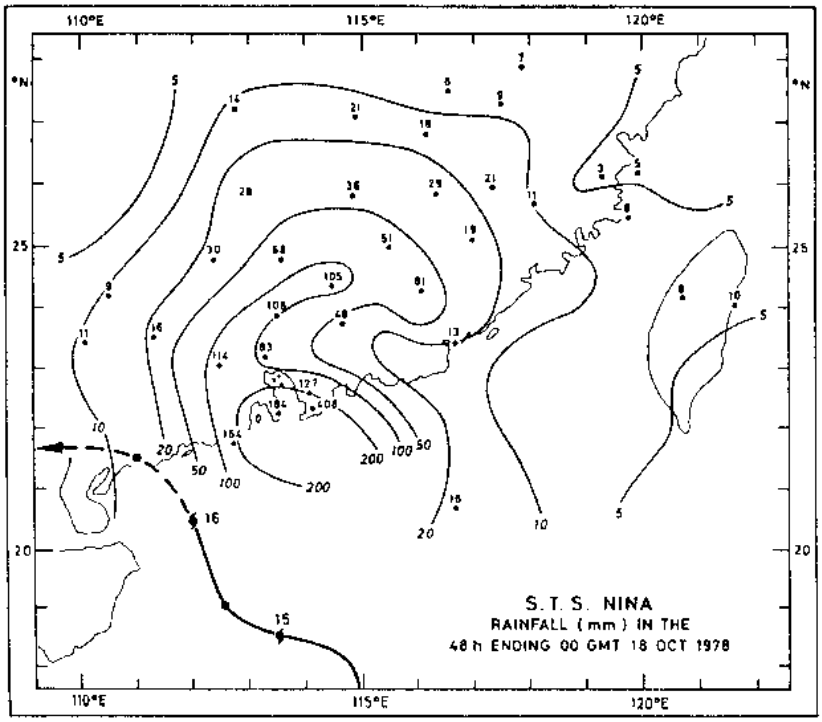

(b)

Fig. 6.4.5(1). The rainfall distribution (a) during the 24 hours in which severe tropical storm Nina approached the coast and an advancing NE monsoon and (b) in the 48 h after the storm had weakened to an area of low pressure and lost the characteristics of a tropical cyclone.

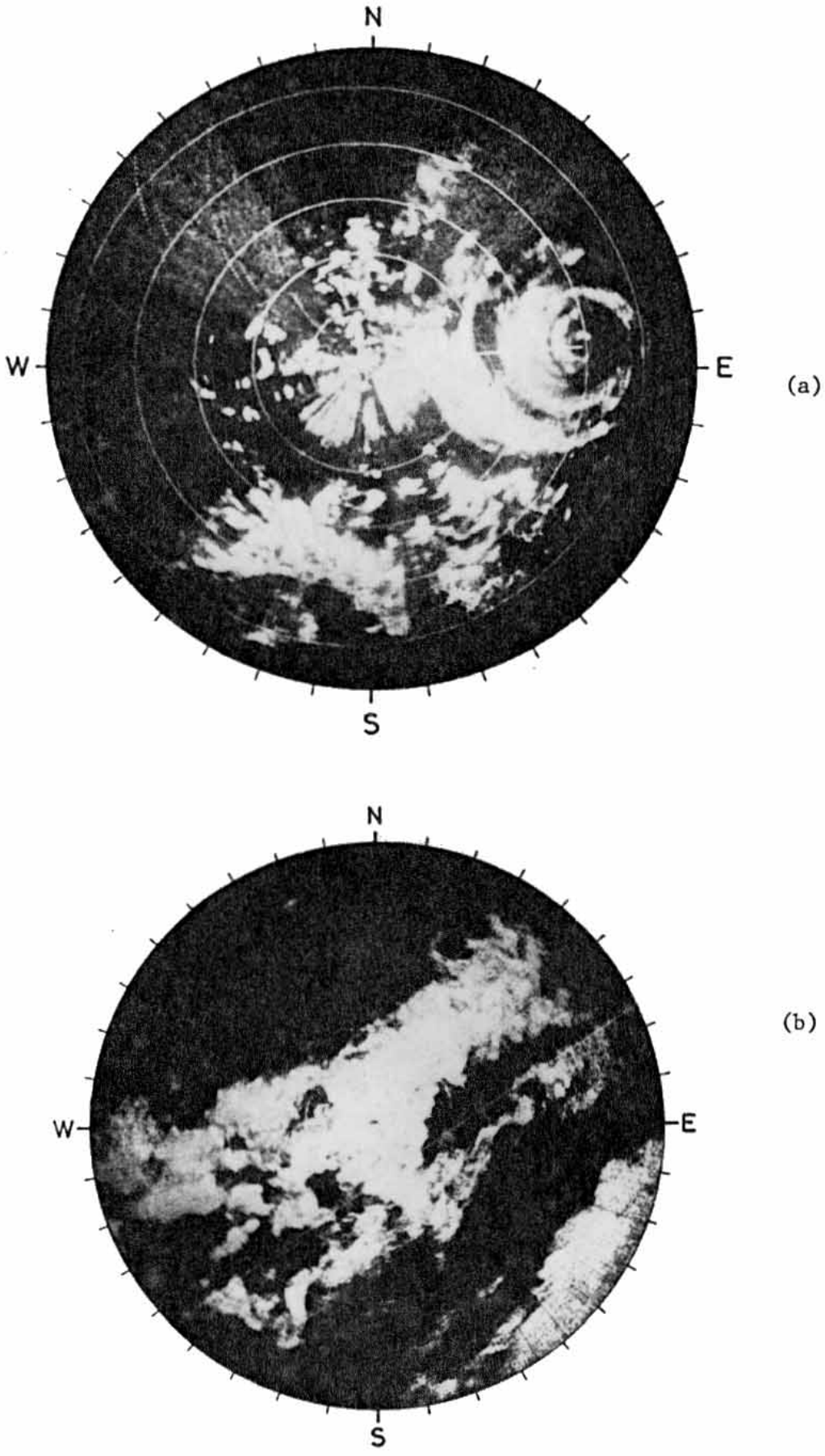

Fig. 6.4.5(2). The intense typhoon Viola approaching the China coast is shown in (a) while in (b) the eye-wall remnant can be seen about 100 km NNW of the radar rogether with a broad band of heavy rain in the SW'ly inflow. Photographs from ROHK radar on the 440 km range (a) at 0157 GMT on 28 July and on the 110 km range (b) at 1550 GMT on 28 July 1969.

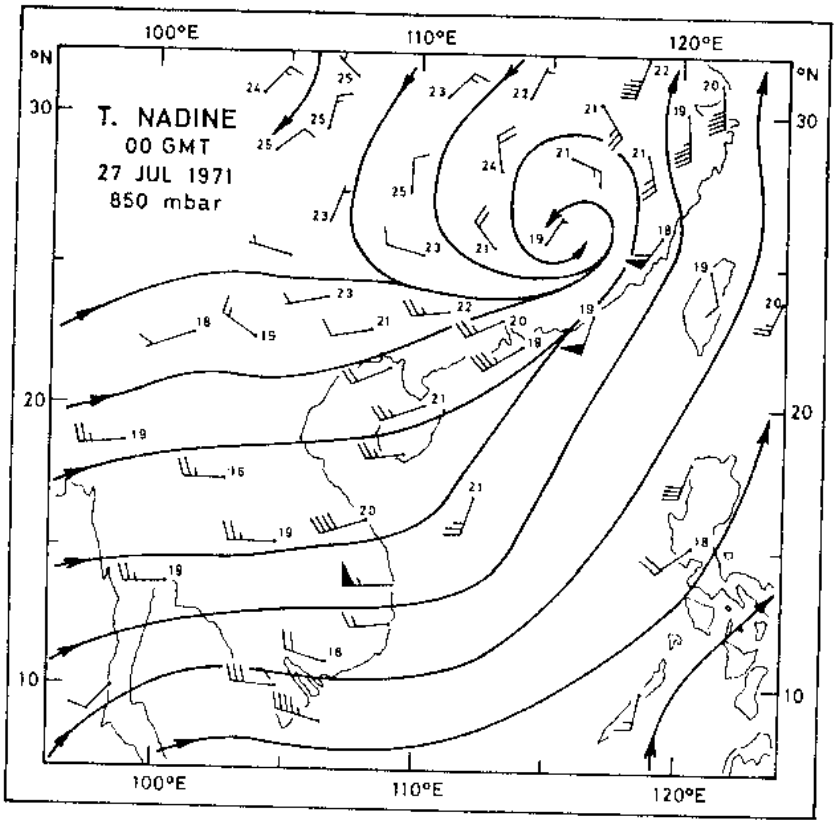

(a)

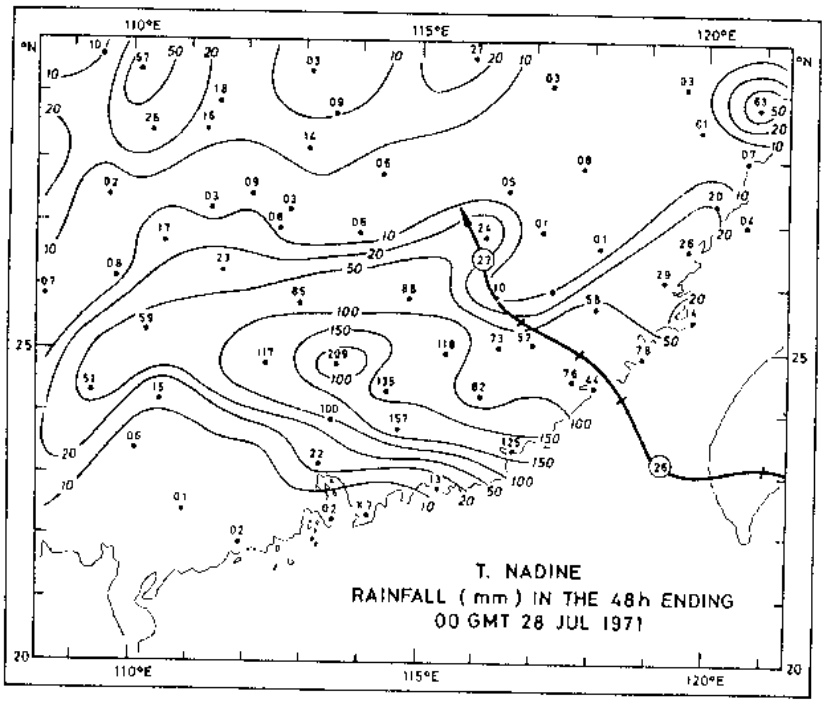

(b)

Fig. 6.4.5(3). The strong SW flow around typhoon Nadine as it moves inland (a) and the associated rainfall pattern (b) showing a maximum to the left of the track.

6.4.6 T.C. intensity and rainfall

Tropical cyclones depend upon the release of latent heat of condensation to warm their central regions and so develop large gradients of surface pressure and high wind speeds. Warmer cores are associated with deeper typhoons (sect 4.) and it is therefore expected, and found, that deeper i.e. more intense, tropical cyclones contain more rain. Table 6.4.6(1) gives an indication of the amount of rain and heat released and its variation with typhoon intensity.

Because of the widely varying speeds of movement, size and assymetries in tropical cyclones the rainfall at a station is not well related to storm intensity. For example, a week storm like Mac (1979) with central pressure of about 995 mb moved so as to keep Shanmei under one of its rainbands (sect 6.4.3) so inundating the area with 477 mm. On the other hand, the intense (951 mb) and fast-moving typhoon Hope (1979) passed over nearby Hong Kong bringing only 287.4 mm (Bell 1980). In addition to these complications there are others deriving from the varying oreigence effects attributable to similar storms but on different tracks.

Kwong (1974) correlated the rainfall at the Royal Observatory Hong Kong - 24 h , 3 d and total - with the minimum hourly mean sea level pressure there for 143 tropical cyclones which passed within 185 km of the station in the period 1884-1939 and 1947-1970. The correlation coefficient was -0.49 for the 24 h - rainfall, and -0.37 for the other two. Although these relationships are significant at the 0.001 level it is clear that variation of station pressure accounts for only 25% of the variance, at best.

Table 6.4.6(1). The total precipitation in some typhoons and model typhoons (after Watanabe 1964)

Name			p(min)	p(Current)	Total rainfall	Liberated energy
			mb	mb	10^9 t/h	10^{14} W
Nancy	(1961)	I	890	904-912	1.21	8.31
"	"	II	"	911-191	1.55	10.64
"	"	III	"	919-923	2.31	15.86
"	"	IV	"	925-940	1.50	10.28
Vera	(1959)		895	920	2.19	15.03
Sarah	(1959)		905	905	1.74	11.94
Tess	(1953)		900	915-975	2.34	16.03
Alice	(1958)		925	970-980	1.27	8.69
Della	(1960)		967	970	1.19	8.14
Ellen	(1959)		965	970	0.91	6.25
Flossie	(1958)		970	970-980	1.08	7.42
Amy	(1959)		980	980	0.47	3.25
R.W.Longley	(1949)					2.19
L.A.Hughes	(1952)					5.06
B.I.Miller	(1958)					6.97

6.4.7 Rainfall from dissipating T.C.

It has already been noted that the rain falling at coastal stations from passing tropical cyclones is poorly correlated with the storms' central minimum pressure (sect 6.4.6). Slow moving, relatively weak tropical storms have caused very heavy rainstorms. Tropical storm Agnes (1965) and tropical storm Ellen (1976) both caused more than 500 mm of rain at Hong Kong and are the third and fifth wettest storms ever to occur there (Table 6.3.7(5)). Similarly, a weak tropical storm with central minimum pressure higher than 1005 mb brought an unprecedented 594 mm of rain while ~~near~~ almost stationary over the relatively flat Florida panhandle (Davies & Bridges 1972). Further inland the relationship between rainfall and central pressure is even weaker. While the heaviest precipitation from a tropical cyclone is apt to occur near the coast high rainfall rates in inland mountainous areas have been caused by the remnants of both strong and weak tropical cyclones that barely show as weak low pressure areas on surface weather charts. It is rainfall from ~~these weak~~ such storm remnants with which we are here concerned. ~~The~~ An essential ingredient for ~~those~~ such this type of extreme rainfall ~~events~~ situation is the large mass of water vapour ~~which is~~ carried inland within the remnant vortices. ~~and which~~ The moisture supply is ~~also~~ often enhanced by the associated poleward flow patterns which may be established on the~~ir~~ eastern sides of the vortices. ~~This~~ The abundant moisture ~~may be released by~~ is condensed in vertical motions triggered by oreigenic effects, cold fronts, waves in the westerlies and upper divergence or, more usually, ~~as a result of~~ a combination of these factors.

When a tropical cyclone moves inland it soon looses its hurricane force winds and the subsidence in the lower and middle troposphere within the eye. Frictional convergence of low-level winds into the eye region results in ascent there and erosion of the tropical cyclone's warm core. Above the surface The remnant storm circulation is able to maintain much of both its vorticity and accumulated moisture as it moves in a generally north or northeast direction towards the westerlies. For example, remnants of tropical cyclones which have recurved in the Bay of Bengal have, on occasion, retained their identity as lower tropospheric vortices for several days while travelling right across China to the East China Sea and have there served as embryos for cyclogenesis. Should such remnant vortices encounter high ground or a cold front and interact with an upper westerly wave then a major rain-

producing situation can result. The situation is exacerbated, and widespread flooding may result, if a blocking situation prevails in the westerlies. In this event, the near stationary flow pattern at 500 mb can both maintain the conditions favourable for rainfall and reduce the speed of translation of the rain area. Without a blocking situation westerly waves, fronts and remnant vortices are free to progress and reduce the accumulation of rainfall at points on the ground.

The type of storm under discussion is well illustrated by the examples of the major flooding which ~~was~~ were caused over the eastern U.S.A. by the dissipating hurricanes Agnes and Eloise on 20-25 June 1972 and 22-25 September 1975. Both hurricanes moved northward out of the Gulf of Mexico. Agnes then veered more to the east to move up the east coast whereas Eloise travelled along the Appalachian mountains. The isohyets associated with the passage of these storms across Pennsylvania are shown in Fig. 6.4.7(1). They show that both remnant storms yielded heavy rainfall after travelling more than 1 500 km across land. The mean 500 mb charts in Fig. 6.4.7(2) show the omega (Ω) shaped blocking situations which prevailed on these two occasions. The Eloise block was well developed before the hurricane crossed the coast but the blocking pattern for Agnes did not develop until after the hurricane had entered land. As can be seen from Fig. 6.4.7(2) the 500 mb winds during the passage of Eloise were much stronger than during the passage of Agnes. This would tend, inter alia, to cause Eloise to move faster than Agnes - in such baroclinic situations the low level centre tend to moves at about half the speed of the 500 mb winds - and so lessen the accumulation of rainfall at points on the ground. Agnes moved at 7-9 m/s while Eloise progressed at 13-16 m/s and its moisture-laden tropical air rode up over the hills and a cold front. The remnant Eloise ~~to~~ flooded parts of Pennsylvania and New York with up to 305 mm of rain. The slower moving Agnes dropped up to 508 mm of rain over ground already near saturation and caused greater flooding than Eloise which arrived when the water in the rivers and streams was still low.

A study of the excessive rainfall associated with hurricane Agnes has been made by Bosart and Carr (1978a). They show that there were two areas of rain, one on the north eastern flank of the remnant vortex and the other further to the north ~~where moisture was carried to~~

on the east side of the westerly wave. Both rain areas were sustained by the advection of moisture around the east side of the remnant storm. Bosart and Carr (1978a) point to different physical mechanisms at work in the Agnes and Eloise rainstorm. The latter was associated with a major baroclinic trough in the westerlies with the resulting thermal advection playing a dominant role in controlling the vertical motion in the lower and middle troposphere.

The remnant of the deep hurricane Camille caused similar extreme flooding as it moved across Virginia in the night of 19-20 August 1969. When Camille crossed the Gulf coast the highest rainfall recorded was 239 mm at Picayune, lesser amounts were recorded inland until the remnant storm approached the Blue Ridge mountains in Virginia. The rainfall then increased greatly with 689 mm being recorded at Massies Mill. A possible, but unconfirmed, 787 mm fell at a station near the Type and Piney rivers. The rains from this storm came to within 80 to 85% of the probable maximum precipitation (sect 6.9.2) for durations of 12 h and areas up to 2 590 km^2 (Schwarz 1970). As ~~was~~ in the cases of hurricanes Agnes and Eloise, very high dew points prevailed in the lower troposphere and were maintained by the south easterly flow around the remnant low and across the mountains. Haggard et al (1973) carried out a statistical analysis of the maximum point rainfall from tropical cyclone remnants which crossed the Appalachians in the 70 year period 1900 to 1969. They fitted the maxima to a gamma distribution to give the probabilities of point rainfall amounts exceeding specified amounts during the ~~specified~~ situations.

In conclusion, the movement of a remnant tropical cyclone into a relatively mountainous area - or towards a cold front - ahead of a slow moving upper disturbance creates a potential for heavy rainstorms and possible flooding. Such situations should be carefully monitored especially if the high level flow is divergent. There are difficulties in adequately modelling the processes involved so as to derive useful rainfall forecasts by dynamical means (Carr and Bosart 1978b). In addition, the relatively low latitude troughs in the westerlies which trigger these heavy rainfalls are not always clearly indicated by the contours indeed, even the remnant storm itself is unlikely to be adequately resolved using conventional reports and objective analysis methods (Bell 1980).

Fig. 6.4.7(1). The total rainfall caused by hurricanes Agnes and Eloise over eastern Pennsylvania (centred about 41°N 77°E). Isohyets originally marked in inches are here labelled in millimetres (Redrawn from Schlegel 1976).

Fig. 6.4.7(2). Mean 500 mb contour heights for 21-35 June 1972 (left) and for 22-25 September 1975 (right) during the heavy rainstorms due to hurricanes Agnes and Eloise respectively. (Redrawn from Schlegel 1976)

6.5 The Properties of Rain

6.5.1 Temperature of Rain

A falling raindrop can be considered as an ideal, ventilated wet-bulb and its temperature will be determined by the local ventilated wet-bulb temperature of the atmosphere. If this changes, raindrops require about 10 s to achieve a new equilibrium temperature, but this time will vary widely with drop size, temperature and humidity. In typhoon conditions the wet-bulb temperature of the atmosphere ~~will~~ rises by about 1°C in the last 100 m of a drop's fall to the sea or to ground near sea level. Since even the largest drops have free fall speeds of less than 10 m/s it would be expected that typhoon rainwater would have a temperature close to the surface wet-bulb temperature indicated by standard observations. I have measured the temperature of rainwater passing through the funnel of ~~the~~ a Jardi gauge in typhoons and tropical storms and the results are given in Table 6.5.(1). They show that the rain was never cooler than the wet-bulb temperature prevailing in the screen. On average the rain had a temperature of 25.1°C, being 0.5°C cooler than the air temperature and 0.4°C warmer than the screen wet-bulb.

Table 6.5(1) Temperature of rain in typhoons and tropical storms at Hong Kong

Date	Tropical cyclone	Temperature (°C)			Difference (°C) Rain - Wet-bulb	JARDI Rate of rainfall mm/h	Remarks
		Dry-bulb	Rain	Wet-bulb			
16 Jul 1970	T.S. Ruby	25.7	25.6	24.8	0.8	48	Centre to E 74 km
16 Jul 1970	T.S. Ruby	25.6	25.4	24.9	0.5	42	Centre to E 74 km
16 Jul 1970	T.S. Ruby	25.4	25.0	24.7	0.3	60	Centre to NE 130 km
16 Jul 1970	T.S. Ruby	25.1	24.7	24.7	0	62	Centre to NE 140 km
16 Jul 1970	T.S. Ruby	25.5	24.4	24.4	0	18	Centre to NNE 170 km
17 Jul 1973	T. Dot	25.4	25.1	24.3	0.8	42	In eye wall
14 Oct 1975	T. Elsie	22.4	21.5	21.4	0.1	17	Taking in cold air Centre to SW 78 km
26 Jul 1976	S.T.S. Violet	26.3	25.5	24.7	0.8	60	Centre to WSW 320 km
6 Aug 1976	S.T.S. Clara	26.6	25.2	25.2	0	72	Centre to SSW 190 km
20 Jul 1977	T. Sarah	27.0	27.0	26.3	0.7	120	Centre to SSW 500 km
20 Jul 1977	T. Sarah	26.8	26.3	26.0	0.3	108	Centre to SW 450 km
AVERAGE		25.6	25.1	24.7	0.4		

6.5.2 Chemistry of rain

The processes involved in the formation of tropical cyclone clouds and rain lead to the chemical purity of their water approaching natural limits. The electrical conductivity of a water sample is a measure of the dissolved ionic material it contains. The conductivity of laboratory distilled water is typically less than 2 μmhos/cm while the usual value for cloud water lies between 50 and 1 000 μmhos/cm. Much lower values obtain in tropical cyclones. At a site atop Whiteface Mountain in New York State, some 300 km from the Atlantic, Falconer and Kadlecek (1980) found conductivities of 2-10 μmhos/cm and 10-20 μmhos/cm in hurricanes David and Frederick respectively in September 1979.

Measurements of pH values do not provide explicit clues on the degree of contamination of water. The water in precipitating clouds usually has a pH in the range between 5 and 4. Similar values were found during the passage of hurricanes David and Frederick.

6.6. Areal Rainfall

The amount of rainfall which falls on a catchment as a tropical cyclone passes is usually strongly dependent on the track of the storm. In particular if the topography of the basin or its environs is mountainous then the rainfall associated with storms on different tracks can be greatly different. For example, Kuo et al (1979) studied the rainfall on the Tam-sui watershed in north Taiwan during the passage of 67 typhoons. The areal-average rainfall over this basin was estimated in the usual way by dividing the watershed into Thiessen's polygons bounded by lines equidistant from neighbouring rainfall stations and using the areas of the polygons as weights to apply to gauge readings. Three branches, of the watershed were treated separately. The region concerned has an area of 2 726 km^2 and is indicated in Fig. 6.6(1) along with the selected eight classes of typhoon tracks. The mountains in the upper reaches of the rivers rise to over 3 000 m.

Fig.6.6(2) shows the hourly catchment rainfall for each of the 12 hours before and 12 hours after the greatest hourly total, expressed as a percentage of ~~this greatest~~ the storm's hourly total. This normalised presentation is shown for westward moving storms called type 2 (Fig.6.6(1)) and for those which move up the east coast - type 5. These two tracks cause the most rainfall in the watershed. However, the probability of damage from type 5 storms is much less because of the smaller peak hourly rainfall. Some rainfall amounts from the three areas are given in Table 6.6(1). The average rate of rainfall over Ta-han Chi - western branch of the watershed - for typhoons in various locations is indicated on the right of Fig. 6.6(1).

Table 6.6.1(1). Maximum observed rainfall depths in 24 h over specified areas in different regions

Area km^2	Australia mm	India mm	U.S.A. mm	Maximum mm
259	826	813	894	894
1 295	737	765	831	831
2 590	673	711	767	767
12 950	467	478	394	478
25 900	389	366	307	389
129 500	⩾ 170	160	159	170

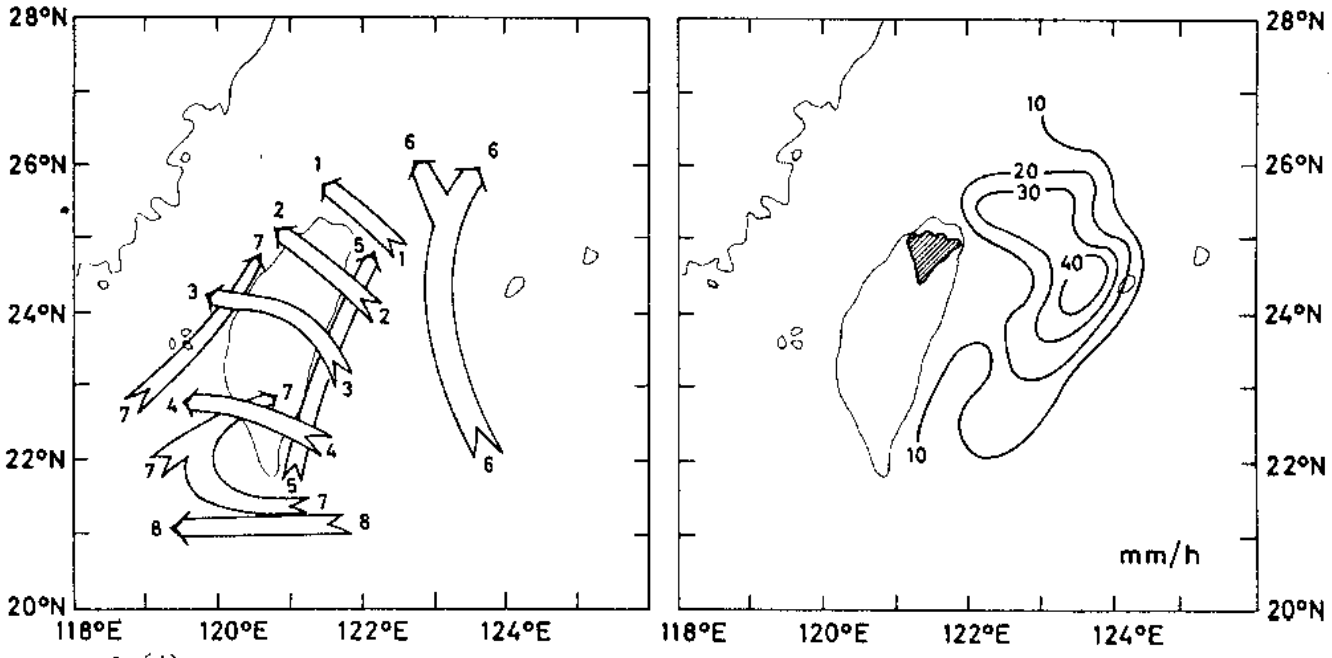

6.6.(1)

Fig. ~~6.8.5~~(1). The eight classifications of typhoon tracks (left) which give rise to characteristic rainfalls in the Tam-sui river watershed (shaded area on right). The average rate of rainfall in the western Ta-han Chi branch of the watershed from typhoons centred in various locations is indicated by the isopleths (right). (Redrawn from Kuo et al 1979).

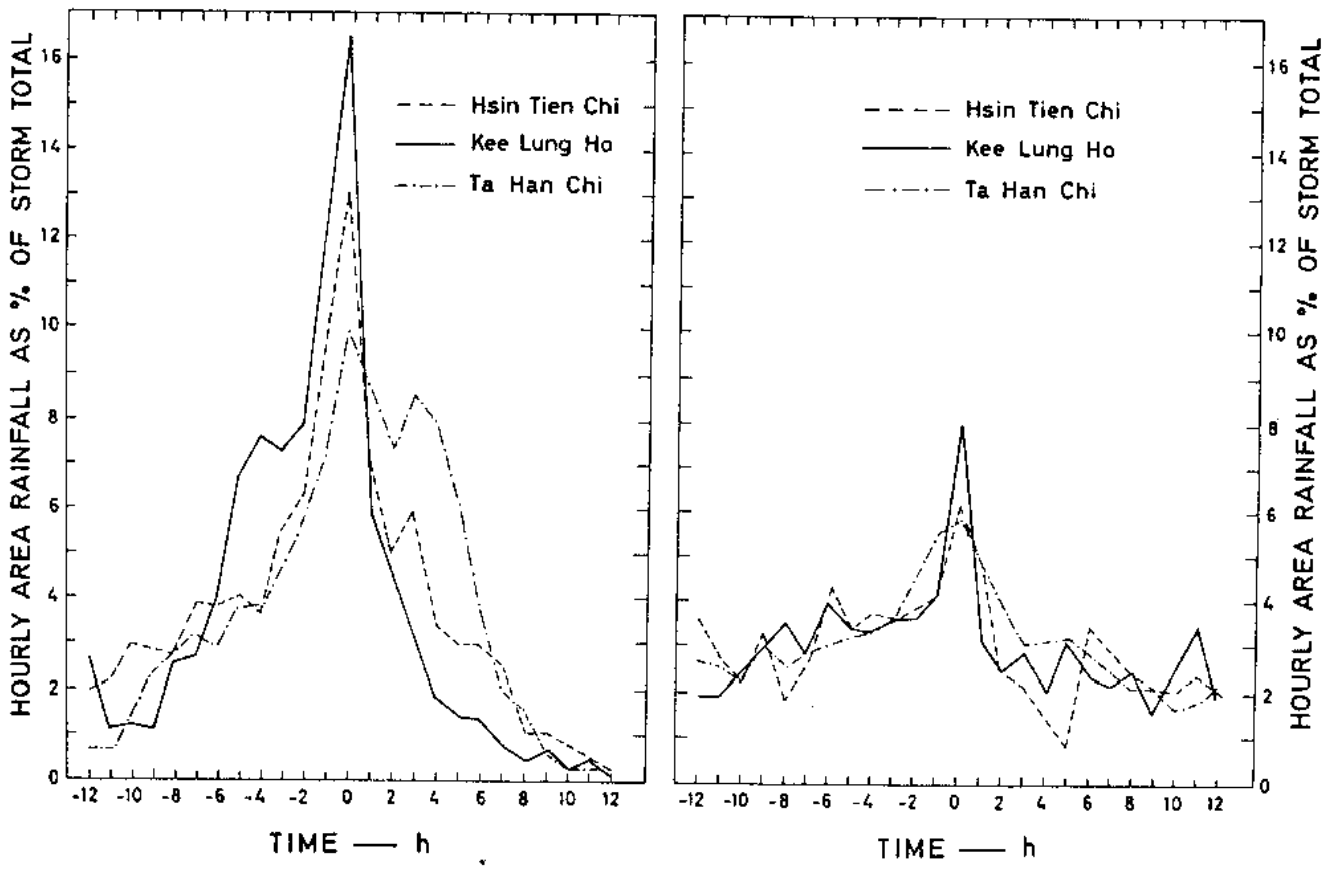

6.6.(2)

Fig. ~~6.8.5~~(2). The normalised hourly catchment rainfall over each of the three branches of the Tam-sui river watershed - about the hour with the greatest fall - for passing typhoons of Type 2 (left) and Type 5 (right). (Redrawn from Kuo et al 1979)

Table 6.8.5(1)

Track	Area rainfall in each of 3 branches	Maximum 1-h total	25-h rainfall / storm total
	mm	mm	%
Type 2	388.4	38.8	97.1
No. of	176.5	29.0	94.5
T.C. = 4	355.5	46.5	96.0
	Total: 920.4		
Type 5	175.0	10.4	79.5
No. of	213.9	17.3	78.3
T.C. = 2	254.3	16.1	76.0
	Total: 643.2		

6.7 Floods

For the major proportion of any one year the flow of water in the lower reaches of most rivers is constrained within well defined alluvial channels. The surrounding alluvial plain is agriculturally rich and is adjacent to a water supply which can also be used for transportation. If the country is mountainous then the montane alluvial plains are particularly attractive for the development of communities. In Japan, for example, 52% of the people live on the rich alluvial plains which constitute only 10% of the total area of the country. Communities in such areas are at risk because, after heavy rain storms, the alluvial plains serve to absorb, and in some measure to pass, the resulting flood waters. In the case of an infrequent extreme rainfall event heavy flooding and horrific loss of life - in some cases amounting to several thousands persons - can result.

In many areas the most devastating floods are associated with the passage of tropical cyclones. The relatively high and sustained rates of rainfall within the storm and the large area bearing rain are two factors which, together, are capable of providing extreme flood discharges in both small and large river basins. At such times catastraphic flooding is often accentuated by the high water levels from storm surge (sect 12), high tides, big waves and wind set-up along the coast and in river mouths which hold back the discharge of rain-flood water.

The size of the catchment usually governs the character of flooding. Very large rivers such as the Mekong are relatively slow to change in their down stream reaches. Water levels there rise slowly in response to the accumulated contributions from rain storms in the upper areas of the catchment and flood levels are slow to fall; they can remain high for what is often an uncomfortably long period. Because several major rain events are needed for these rivers to flood, the event is usually seasonal. At the other end of the size spectrum are the small mountainous catchment areas such as abound on the South China coast, in the Philippines and Japan. In these catchments "flash floods" occur with very little time delay between the start of the flood and the peak discharge. This type of flood owes its particularly dangerous nature to

the suddenness and speed with which it can occur especially if the catchment slope is such as to accelerate the runoff. Although thunderstorms are most frequently the cause of flash floods in small catchments, rains associated with tropical cyclones are also a frequent cause. Runoff of the heavy continuous rains in the central parts of a tropical cyclone is particularly rapid if the ground has been saturated by earlier rains in the outer parts of the same storm or from other prior rains. Decaying tropical cyclones (sect 6.4.7) moving inland and encountering high ground, cold fronts or westerly waves are particularly prone to produce major flash floods. In the U.S.A. the flash flood in the James River Basin, Virginia caused by decaying hurricane Camille in August 1969 and the extensive flooding from the decaying hurricane Agnes from Virginia to New York in June 1972 were particularly damaging; 153 and 120 lives were lost in these two events, respectively.

Flash floods have been increasing in frequency and intensity in many areas due to urbanization. The replacement of trees and vegetation by buildings and road works decreases the permeability of the ground and increases both the amount and the speed of the runoff. Improved drainage channels facilitate the rapid transport of water to the lower reaches where bridges, culverts and buildings often impede drainage to the sea.

Graphs showing the variation of the river stage or discharge with time are known as "hydrographs". They are used in Fig. 6.7(1) to illustrate the effect of urbanization on a catchment. The Tsurumi river catchment has an area of 235 km^2 and drains into Tokyo Bay. Four hydrographs which result from a design rainstorm of 308 mm in two days are shown for different degrees of urban development in the catchment. The time of concentration decreases and the peak flood discharge increases as the catchment becomes more urbanized. It is expected that the maximum flood discharge, due to the design storm, will rise from 630 m^3/s for natural conditions to 1 350 m^3/s when 80% of the catchment is developed.

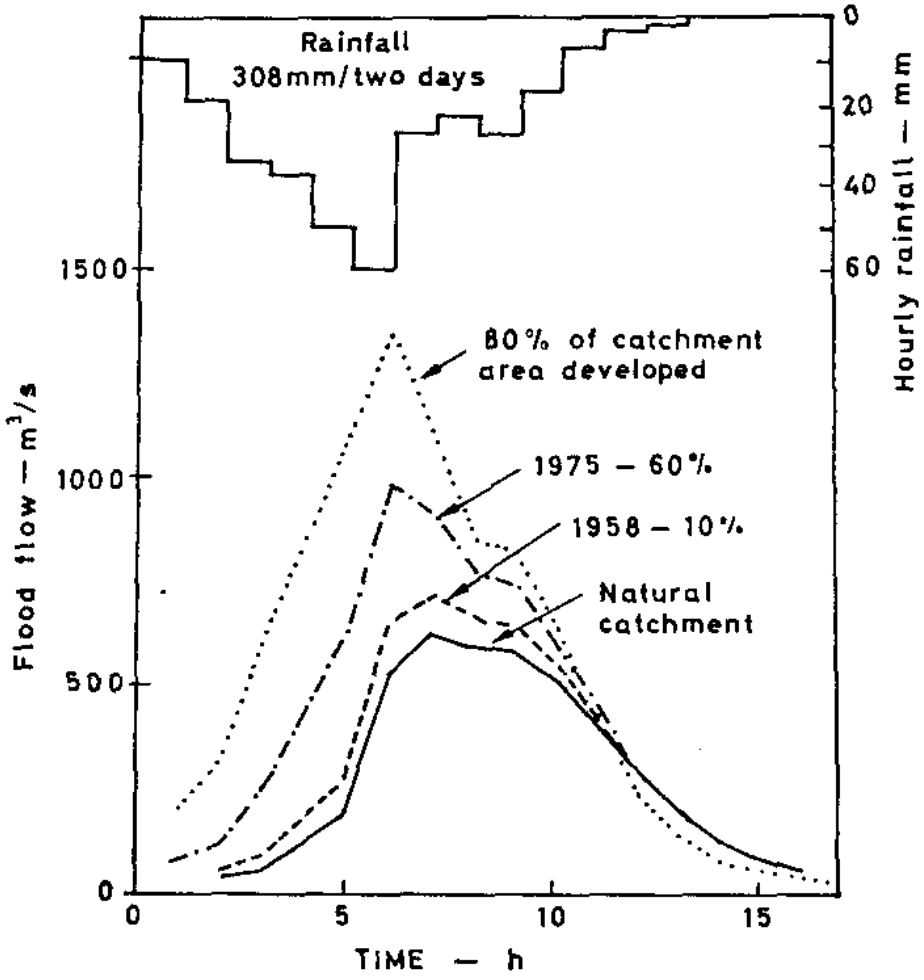

Fig. 6.7.(1). Hydrographs from the Tsurumi river, which drains into Tokyo Bay, showing how the peak flood from a 308 mm two-day storm has increased in volume and peaked earlier as development has taken place in the catchment. (From Japanese Ministry of Construction 197)

6.7.1 Flood hazard

Flood hazards depend on a number of different factors namely:

a) Duration - The degree of damage, dislocation of transport and public services and the life of vegetation are critically dependent on the duration of a flood.

b) Depth of water - Flood barriers, building stability against flotation and foundation failure and vegetation survival all have a limited tolerance to water depth. Survival of persons and livestock is greatly dependent on this factor.

c) Speed - High water speeds create erosive forces and hydrodynamic pressure on obstacles which can destroy structures and bring down mud and debris. Fast flows greatly increase the difficulties of survival for people and livestock and increase the difficulty of rescue operations.

d) Rate of rise - A fast rise of water level decreases the possibility of giving adequate warning. Flood risk planning is therefore necessary to save life and damage in ~~these~~ areas prone to flash floods.

e) Frequency of occurrence - Is an important factor in land use and flood risk planning. The total damage and loss of life in a flood plain depends on the cumulative effects of depth, duration and speed of floods over many years.

f) Time of flood - The season in which floods occur can be critical. Flooding during the growing season can have a catastrophic effect on food production with results on the affected communities as severe as those due to prolonged drought.

The mitigation of flood disasters depends firstly on the estimation and mapping of flood risks including the frequency of occurrence, maximum possible severity, rates of rise of water level and duration of critical stages i.e. height of water above some fixed datum. Historical flood levels are used by hydrologists in this process along with considerations based on meteorological inputs. In areas where tropical cyclones are the prime cause of severe flooding the effect of storm surge in the lower reaches of large tidal rivers must also be studied.

Having first estimated and mapped the flood risks then methods of reducing them by engineering measures can be evaluated and controls can be placed on flood plain occupation, land use and building. When the described protective measures against floods are unable to cope with extreme conditions then emergency measures have to be pre-planned and brought into operation after flood warnings have been issued. People and livestock may then have to be evaculated and temporary action taken to reduce the ingress of water or to strengthen river banks and any structures that may be at risk.

6.7.2 Flood warnings

Meteorologists and hydrologists work together in flood prediction but, the relative degree to which each is involved depends on the size of the relevant catchment. The prediction of flash floods in small catchments is almost entirely a meteorological problem based on quantitative precipation forecasts (QPF) or the extrapolated movement of rain areas observed by radar or satellite. For predicting floods in very large catchments hydrologists use standard methods based on river stages and the runoff from snow-melt or rainfall in the upper reaches of the basin. Normal synoptic precipitation reports are often adequate for this task. Numerical models are used to assimilate the information and predict a hydrograph for some location on the river. However, the tidal reaches of such rivers in tropical cyclone prone areas may be vulnerable to flooding by storm surge - the prediction of this phenomena, because of its time scale, is predominantly a meteorological problem but it can be an important input into the hydrological model for predicting flooding further inland. In rivers which peak in 12 to 24 hours, storm surges can have a significant effect on their flood flows and depth over coastal plains. During the passage of a tropical cyclone, flooding in tidal rivers can thus be due primarily to storm surge - as in wide rivers flowing over coastal plains - or from rainfall - as in short, narrow, fast rivers - or from a combination of the two phenomena.

Disaster prevention or mitigation using emergency measures depends on an organizational system in which both the flow of environmental information and forecasts and the responsibility for specific activities are clearly identified. During the approach of tropical cyclones all environmental information from land and remote sensors is assessed by meteorologists and hydrologists working together. Flood forecasts whether caused by rain or surge or a combination of both are prepared and disseminated as tropical cyclone warning bulletins to centres responsible for taking and controlling the necessary emergency action.

6.8

6.9. Landslips

6.8.1 mud avalanches ?

6.9.1 The prolonged and heavy rainfall associated with tropical cyclones frequently causes severe landslips in hilly or mountainous terrain. In many areas the damage and loss of life from this cause is often greater than that due to wind or flooding. Particularly damaging are the slips known as flowslides or mud avalanches which occur suddenly and with considerable destructive energy. They are of great consequence in Japan and Hong Kong where the high density of population necessarily leads to some building development on hillsides. The phenomenon occurs there in both tropical cyclones and the heavy rains in May and June associated with the surface monsoon trough or Bai U (plum rains). The heaviest rain during the passage of a tropical cyclone occurs over the hills and mountains (Figs. 6.8.1(1)) which are, of course, the places having the greatest potential for landslips. Although serious slips occur every year in the hilly terrain of South Asia only a few cases have been well studied. Details of some of the major landslip events in Japan and Hong Kong are given in Table 6.8.1(1). Similar disasters occur, of course, in the Philippines, China and the mountainous regions around the head of the Bay of Bengal. However, casualties are usually less there because of the lower density of population. In these areas the accompanying floods usually take a larger toll of life. Landslips are not limited to coastal areas but can occur well inland in association with remnant tropical cyclones. It is not unknown for decaying storms to cause landslips in the Himalayas between Nepal and Assam. For example nearly 100 people were killed as a result of such a landslide at Darjeeling on 13 June 1950 and many lost their lives from similar causes in West Assam in October 1968 although in this case the loss of life from flooding was much greater.

6.9.2 The exceptionally heavy rainfall at Hong Kong in tropical storm Ellen 1976 is of special interest because firstly, the storm was weak and ill defined with heavy rain in the outer rainband far from the storm centre and secondly, the storm led to a special investigation into the stability of filled slopes. Figs. 6.6(a) (6.8.1(2)(a)) and 6.7 (6.8.1(3)) show how weak was the storm. The investigation of the mud avalanche was carried out by a panel of six soil engineers who were internationally renowned for their expertise in this field. They attributed the avalanche to the fill being incorrectly layered and inadequately compacted and they made recommendations on the design and construction of such slopes (Hong Kong Government 1977).

6.9.3. The variation in rainfall rate during the passage of tropical storm Ellen over Hong Kong is shown in Fig. 6.1 while its distribution in space is shown in Figs. 6.2 and 6.6(b). The heavy rain persisted at Hong Kong until the storm's centre was 450 km distant to the northwest; by this time the minimum central pressure had risen from 992 mbar at landfall to over 1002 mbar. The down pour continued until 0200 GMT on 25th August at about which time the disastrous mud avalanche shown in Fig. 6.5 occurred. A total of

Table 6.8.1(1)- Severe Landslips in Japan and Hong Kong

Place	Date	Cause	Deaths	Remarks
Kobe, Japan	July 1938	Bai U	461	A rocky mud avalanche from granitic mountains to low lands. 100 000 houses destroyed.
Mt. Soumzan Hakone, Japan	26 July 1953	Bai U	10	A slide of 700 000 m^3 of volcanic altered clay.
Hong Kong	12 June 1966	Monsoon trough	64	More than 500 slips costing US$ 6 x 10^6 to repair. 24 h rainfall 401 mm (See Fig. 6.2). 1 h rainfall 157 mm.
Hong Kong	16-18 June 1972	Monsoon trough	138	185 slips (See Fig. 6.3) 200 mm of rain fell on each of the three days (See Fig. 6.2) 24 h rainfall at Tytam was 547 mm.
Kure, Japan	17 Sept. 1945	Makurazaki typhoon	1 154	Avalanche in a narrow valley in the lower slopes of a granitic mountain.
Tokyo, Yokohama, Japan	26 Sept. 1958	Kanogawa typhoon	61	1 029 slips 24 h rainfall 393 mm.
Hong Kong	12-13 Oct. 1964	Typhoon Dot	26	Numerous landslips. One mud avalanche from a filled slope in Kuntong (Fig. 6.4). 330 mm of rain fell in two days. 24 h rainfall 304 mm.
Hong Kong	25 Aug.1976	Tropical Storm Ellen	27	Many landslips. A disastrous mud avalanche flowed into the lower floors of a block of flats (Fig.6.5) killing 18 people. 24 h rainfall 416 mm.

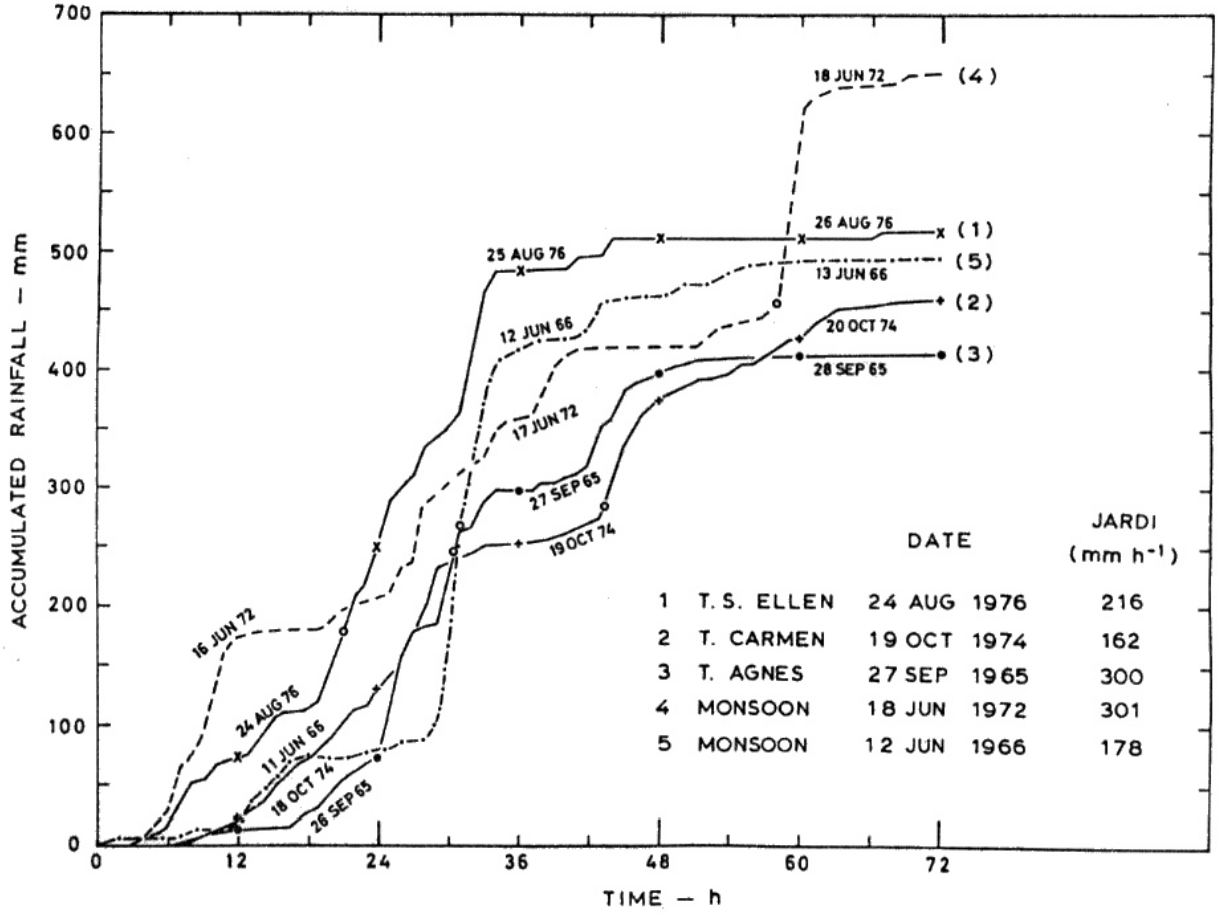

Fig.6.8.1(4). Plots of the accumulated rainfall at the Royal Observatory Hong Kong on five occasions on which local landslides occurred. The highest instantaneous rates of rainfall as recorded by a Jardi gauge are listed and the points at which they occurred are indicated by open circles.

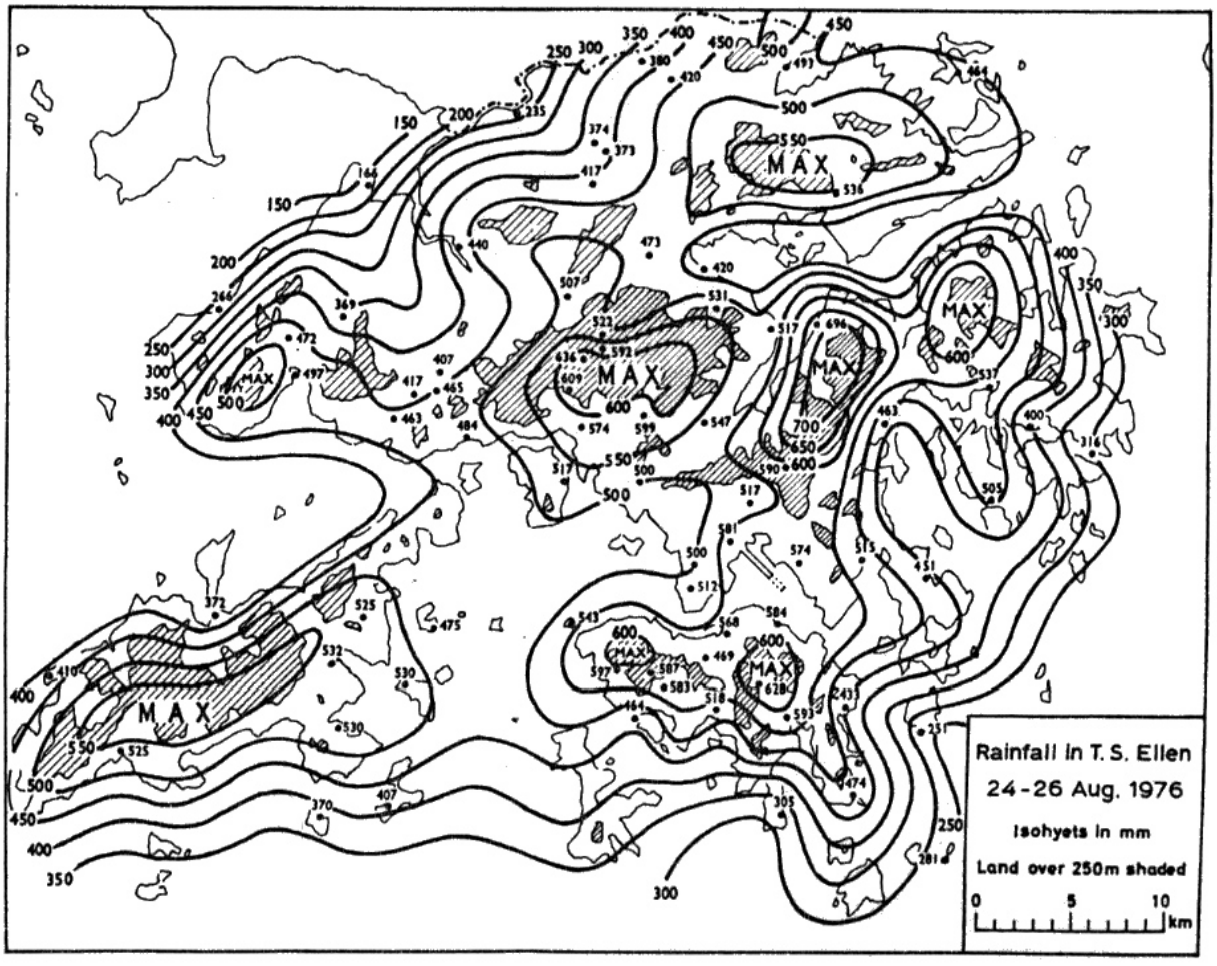

Fig. 6.8.1(1). The distribution of rainfall over Hong Kong caused by the passage of tropical storm Ellen.

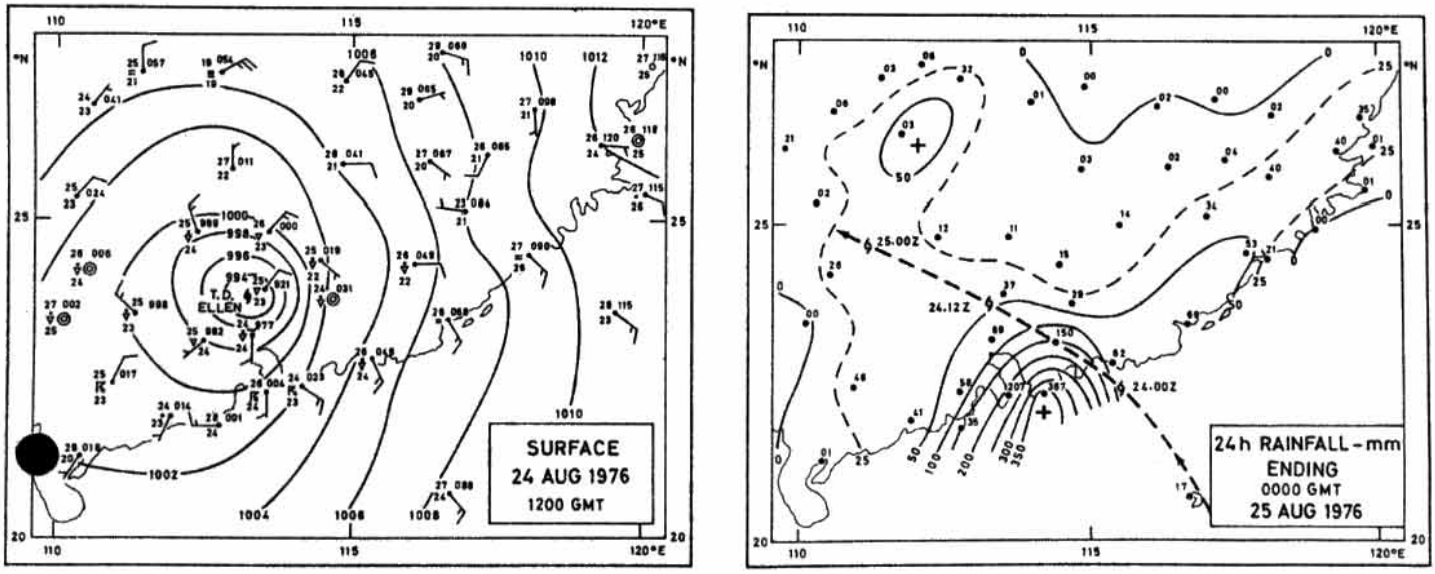

(a) (b)

6.7.(2)

Fig. 6.6 (a) T.S. Ellen over southern China and (b) the 24 h rainfall distribution and track of the storm.

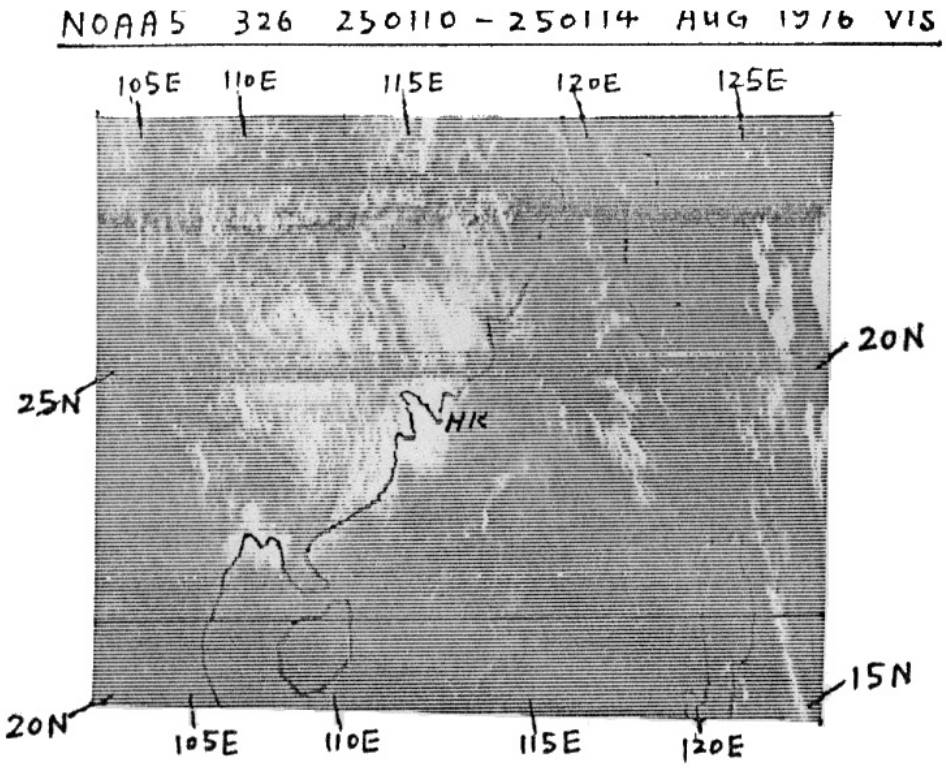

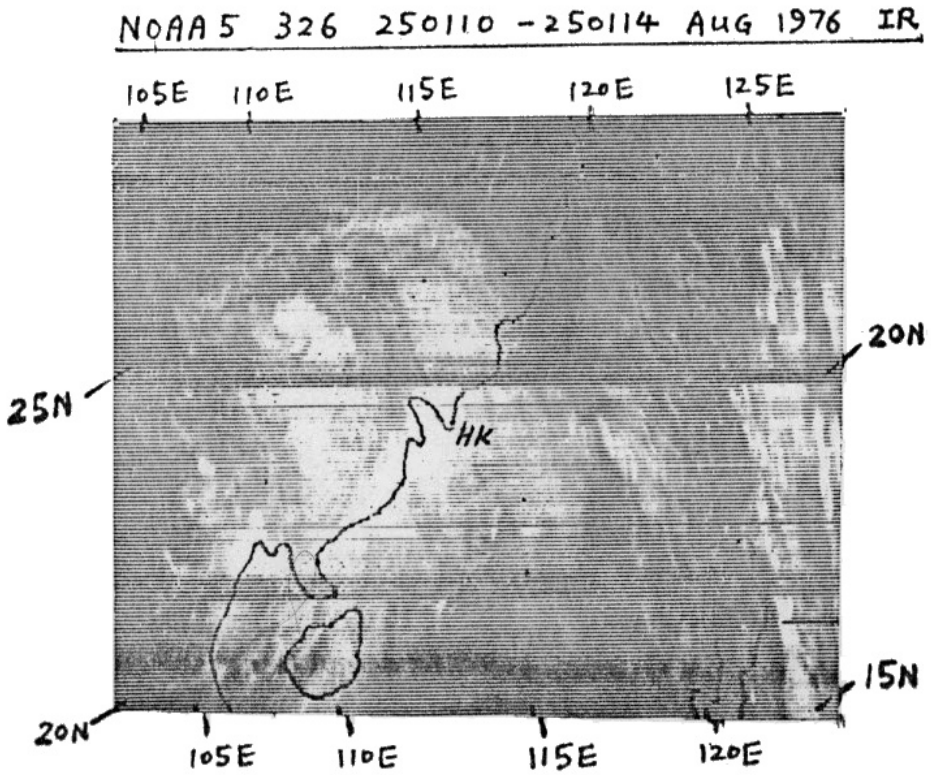

Fig. 6.8.1.(3) APT pictures from NOAA 5 on pass 326 over tropical storm Ellen at 0110-0114 GMT on 25th August 1976. The black bands across the pictures and due to radio interference from a plastics welding machine.

6.8.1(1)

Fig. A mud avalanche in Kungtong, Hong Kong caused by typhoon Dot on 13th October 1964.

Fig. 6.8.1(2) A mud avalanche in a filled slope at Sau Mau Ping. Hong Kong caused by tropical storm Ellen on 25th August 1976. (Hong Kong Standard.)

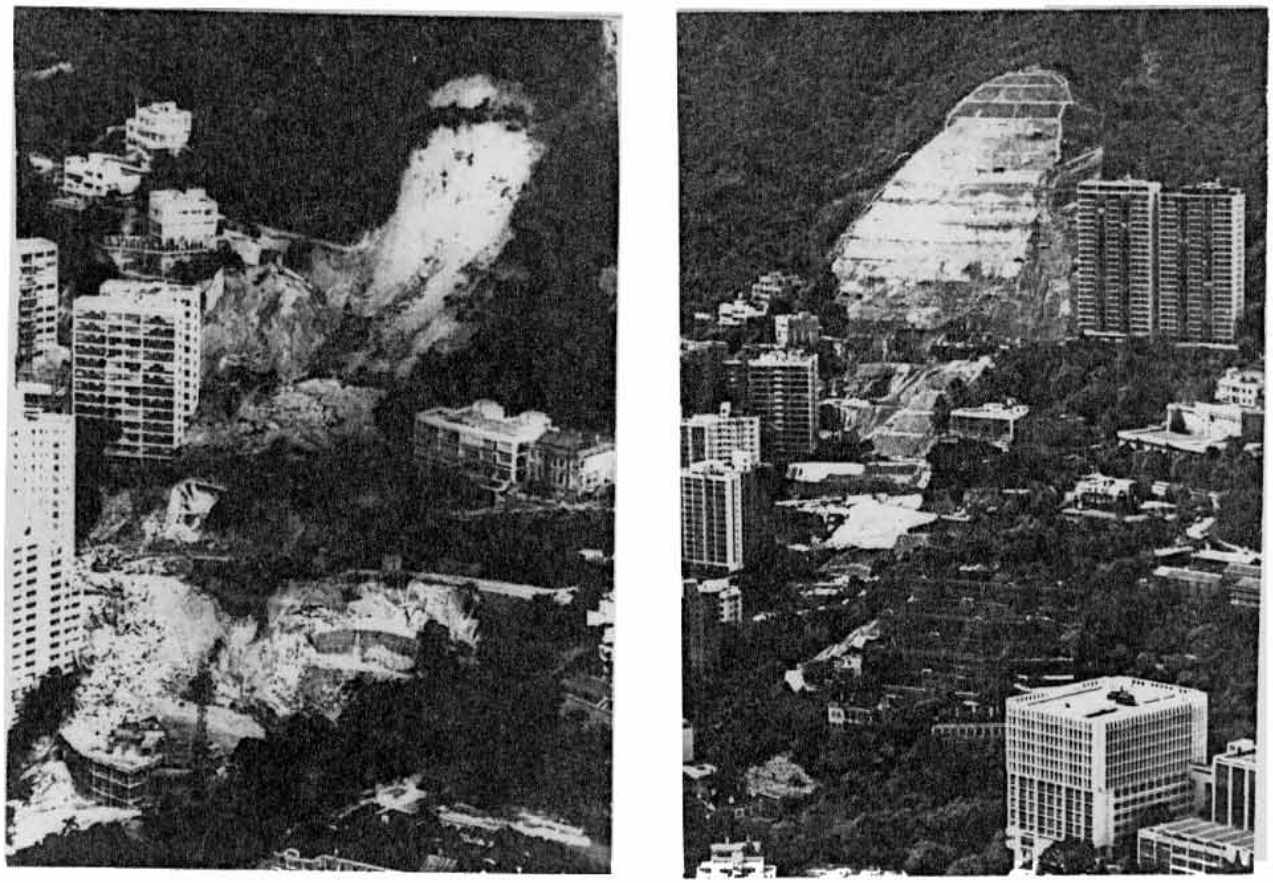

Fig. 6.8 (8). The Po Shan Road landslide on Hong Kong Island on 18th June 1972 before and after repair. (Hong Kong Government Information Services).

416.2 mm of rain had fallen in the prior 24 hours and the "instantaneous" rate of rainfall had reached 415 mm/h as shown in Fig. 6.8.1(4). The raingauge at the radar station reported 89 mm between 0005 and 0105 GMT on the 25th August. The visible and infra-red pictures received from NOAA 5 satellite (Fig. 6.8.1(5)) show the outer spiral band to be bright over Hong Kong but much weaker nearer the centre. This rainband was almost stationary near Hong Kong for many hours and was the direct cause of the deluge. The situation is a good example of those in which a locality remains under a rainband because the latter's movement away from the storm centre is compensated by the movement of the storm as a whole (Sect. 6.4.3). The two radar photographs in Fig. 6.8.1(6) show the rainband at 1359 GMT on the 24th August and 5h 27 min later during which period it remained essentially stationary just to the east of the radar station. Heavy rain cells moved along the length of the rainband and, from time to time, other additional bands formed to either side.

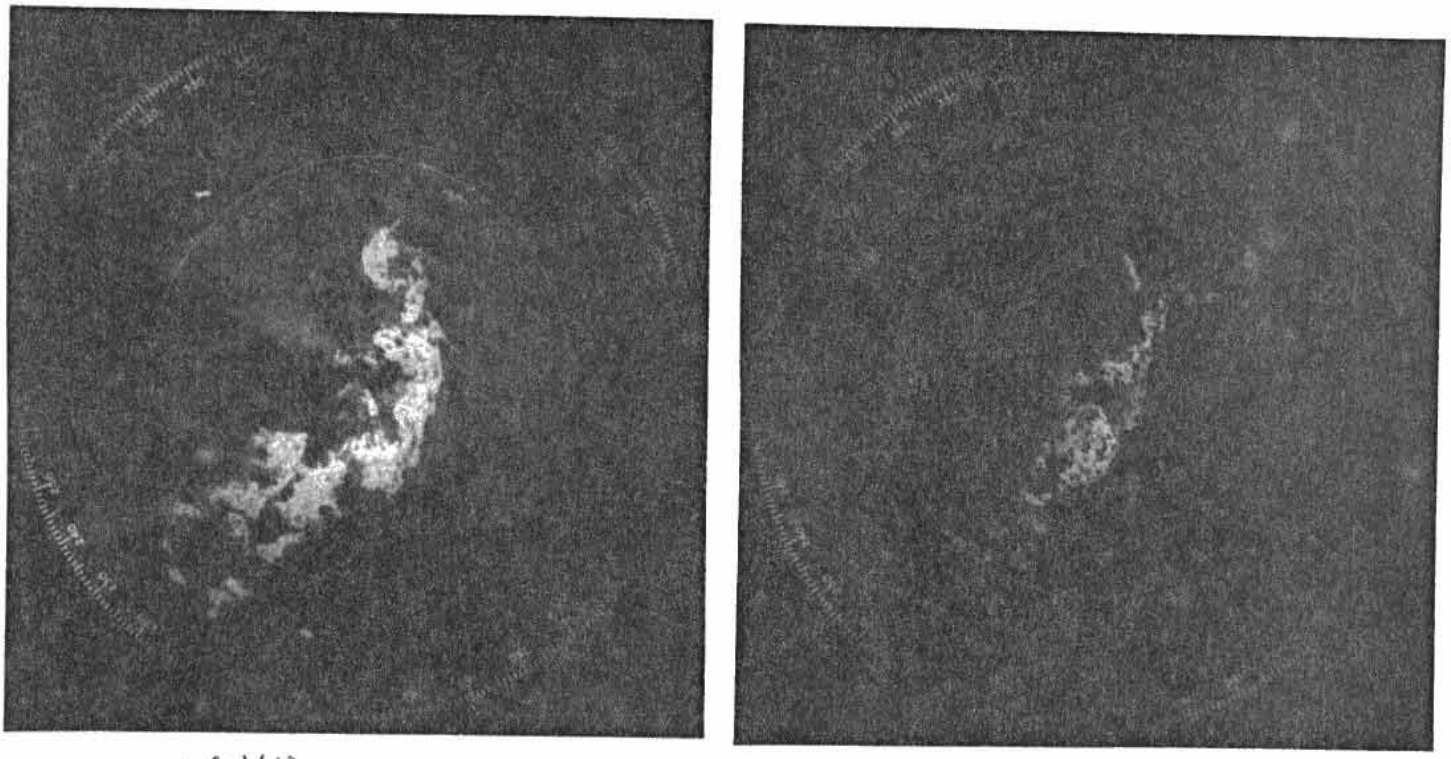

6.8.1(6)

Fig. 6.8. Hong Kong 43S radar photographs (range ring at 74 km) showing a near stationary rainband in tropical storm Ellen on the 24th August 1976 at 1359 GMT (left) and 1926 GMT (right). Isoecho circuits show only rainfall rates greater than approximately 1 mm/h and black cores show rates greater than about 100 mm/h. The elevation of the beam is 2°. The after glow of returns from rainfall less than 1 mm/h is also visible.

Photographs of other notable H-K-land slips are shown in Figs. 6.8.1(7) and 6.8.1(8).

6.7.1 The cause of mud avalanches

.1 The rocky outcrops which form hills, decompose at the surface and along joint planes to produce silty and clayey materials containing many boulders. These rocks and materials tend to creep down the face of the parent rock as colluvium (slopewash) to take up more stable slopes at lower levels. This process continues year after year and is accelerated by the many slips which occur during the passage of tropical cyclones. In Hong Kong the slope of the hillside formed by the insitu decomposition of the bed rock and the overlying colluvium from the peaks can be as high as 36° from the exposed rock to levels typically around 150 m above sea level. At this altitude there is a well defined change of slope to about 18° which continues down to the coast. The determination of the stability of natural and man-made (filled) slopes in rainstorms is a complex problem in soil mechanics, a simple outline of the main features of the problem is given below.

.2 The gravity forces tending to move a sloping soil mass downhill are related to the angle of the slope. The soil strength - shear strength - which resists these forces is dependent on the type of material, its degree of compaction or density and whether it is wet or dry. Where the gravity forces exceed the strength of the material failure occurs resulting in a slip. In loose dry granular soils the critical slope angle will be about 33°, or 1 in 1.5, and is independent of height. If the soil is compacted to increase its density the critical angle will increase to at least 37°. In practice soils contain some moisture and are termed partially saturated soils. The forces of adsorption between soil and water cause the strength and therefore the critical angle for partially saturated soil to be greater than for a dry soil. However, as more water enters the soil and it approaches a saturated state the strength reduces to a value of the order of that in perfectly dry soil.

.3 Water can enter the slope by infiltration from the surroundings and from the surface and also, in some cases, by rising ground water. Should more water continue to enter the soil during heavy rainfall, conditions in the soil itself, such as layers of different densities, may cause seepage forces and down hill flow to develop, further reducing the strength of the soil and the stability of the slope. Should the strength fall below that required to resist the gravity forces some deformation of the soil will occur, and if the soil is loose, the deformation will tend to produce a decrease in volume i.e. the soil contracts. If the soil is nearly saturated, then this contraction is resisted by the water in the soil pores, causing a rapid build up of pore pressure and seepage forces. The soil will then flow in a liquid state and may move at a velocity as great as 30 m/s. These mud avalanches are very destructive. The depth in which liquefaction occurs is limited to the wetted zone - which in Hong Kong conditions is typically about 4 m. If, in contrast, a dense soil deforms it will tend to increase in volume i.e. expand. This expansion prevents a collapse and even though the slope may fail, there is no liquefaction. The material will move until stability is restored and the movement arrested. Such a slip is known as a "debris slump".

.4 From the foregoing it is clear that the stability of a slope will depend on 1) the angle of the slope 2) the type of material 3) its degree of compaction or density and 4) the degree of saturation of the soil. When there is no cohesion between the soil particles, such as in clean dry sand, the shear strength (due to friction) depends upon the loading which increases linearly with depth so that the stability of such a slope is independent of depth. This is illustrated by sand piles which retain a constant slope regardless of their height. For a cohesive material such as clay the shear strength depends entirely upon cohesion; as a clay slope is cut higher a level will be reached at which the gravity forces exceed the fixed shear strength and the slope fails. Most soils have both cohesion and internal friction. Lumb (1965) has shown that the cohesion of residual soils in Hong Kong drops rapidly with increased degree of saturation and attains zero or a very small value at saturation. Soils derived from volcanic rocks have less shear

strength than those derived from granites. In man-made or filled slopes the degree of compaction of the soil and the way in which it is laid down is all important for the stability of the slope. Compaction increases the shear strength and reduces the permeability of the soil, while laying down the soil in horizontal layers limits the depth of infiltration and increases hill-side seepage.

.5 Man-made slopes are usually protected from runoff and some vertical infiltration of water by drainage culverts set in about 0.5 m from the face and laid around the upper boundary of the slope or cutting. It is also usual for large cuts to be made in steps or berms and to provide each berm with a drainage channel. The face of the cutting is often covered with chunam plaster to reduce infiltration. Retaining walls are usually provided with drainage holes at a density of about one per square metre. Jets of water can sometimes be seen issuing from these holes during and after heavy rain. (Fig 6.8.2(.)) Similar holes in chunam plaster are of doubtful value as water seldom issues from them unless they are connected to special drain pipes in the slope. There are other techniques, beyond the scope of this text, for protecting both natural and man-made slopes. However, surface drains are of no use unless kept clear and in good repair indeed, they can become the cause of slips if they are broken or blocked with debris. People living below slopes should therefore ensure that all drains are kept in good repair and that they are cleared whenever the approach of a tropical cyclone is warned.

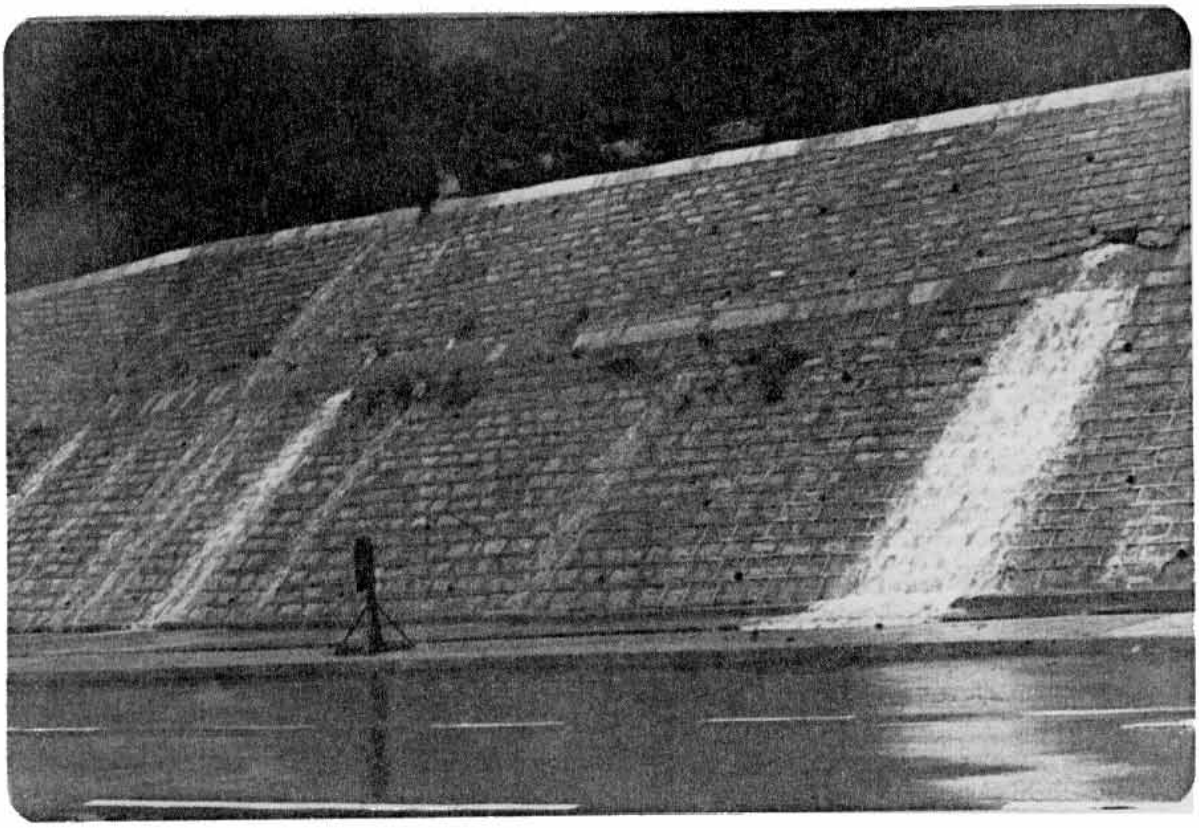

Fig. 6.32 (1) Water issuing from a few of the drain holes in a cutting after S.T.S. Agnes (1978) passed Hong Kong. On the right, water pressure is seen to have lifted the facing stones above the berm where drainage to relief holes must have been blocked or inadequate.

6.7.2 Predicting slope failures

.1 No slope steeper than about 25° is absolutely safe, there is always a finite risk of failure during an earthquake or a period of heavy rain. Earthquakes can trigger slides in marginally stable slopes and also cause avalanches by liquefaction of the soil. The latter phenomenon arises because the cyclic loading or shaking of the soil by the tremors causes a reduction in its volume thereby increasing the pressure of the water in the pores so inducing liquefaction. Slides due to liquefaction have occurred on slopes of only 1.5°. Lumb (1975) analysed the stability in heavy rain of Hong Kong slopes composed of residual soils. On the basis of his experience he was led to postulate that infiltration from above was the dominant factor controlling the pressure of water in the pores. The stability of slopes in heavy rain then depends on the infiltrative capacity of the soil. The percolating water produces a zone of saturation and, provided that the rainfall rate is at least as great as the infiltration rate, the saturated zone penetrates further into the soil with time as a "wetting-front". Lumb found that the probability of receiving enough rain in Hong Kong to saturate the mantle to a depth of 4 m was 2.5% for decomposed granite (400 mm in 14 h) and 20% for decomposed volcanics (400 mm in 3 days).

.2 The residual soils in Hong Kong vary greatly in strength both laterally and vertically on any given slope so that there is a probability of a given sample having a certain strength. Lumb (1975) determined the probability of failure of cuttings of various slopes and heights in decomposed granites and decomposed volcanics. The decomposed volcanic slopes are intrinsically more stable than the granites. However, when he expressed the probability of failure in terms of the combined probability of the slope receiving sufficient rain for saturation and having a sufficiently high infiltrative capacity the decomposed volcanic slopes were found to be four times as likely to fail as the granites. This is in broad agreement with the observed occurrence of landslips.

.3 Lumb (1975) also examined the time distribution of rainfall at the Royal Observatory, Hong Kong, which preceeded some 65 local landslides. He found that the slips correlated best with the total rainfall over

15 days and the total rainfall on the 16th day. Severe landslides occurred after more than 200 mm of rain had fallen in the prior fifteen days with more than 100 mm on the sixteenth day, the day of the slip. Therefore, if it is possible to predict when the daily rainfall will be more than 100 mm, the probability of landslide occasions could also be predicted and precautions taken to avoid loss of life near critical slopes.

.4 Lumb's method has been refined at the Royal Observatory to enable an operational landslide warning system to be established. It has been found that, in general, 3-day quantitative rainfall forecasts are currently more accurate than those for the individual days. Accordingly, the graph of Fig. 6.8 (a) is used each day to determine whether the rainfall total over the past 13 days and that forecast for the next three days indicates a probability of a landslide situation. If the answer is affirmative an "amber" alert is issued to indicate that some slips are probable during the next three days. The graph of Fig. 6.9 (b) is next entered on the basis of a 24-hour rainfall forecast and the total rainfall over the preceeding 15 days. A "red" warning is issued if the graph indicates that a slip is probable. In addition to rainfall there are other factors involved in determining the stability of a given slope. These include the state of the drainage system, and other protective works and the state of completion of work in progress on the slope and the inhomogeneities and faults within the slope itself. It is not possible therefore to be precise, landslide warnings have to be taken as indicating that the probability of some unspecified slopes slipping is high. The historical rainfall record at the Royal Observatory (the rainfall on a given local slope may differ greatly from that at the Royal Observatory, see e.g. Fig. 6.8) indicates that the graph of Fig.6.8 (b) would lead to the issue of a "red" warning about 4.0 times per year on average and that the probability of the warning being followed by a landslide would be about 44.6 %.

.5 The Ministry of Construction in Japan estimated in 1969 that there were some 13 300 surveyed slopes which were designated as dangerous because they had i) a slope greater than 30° ii) were more than 5 m in height and iii) would affect at least 5 households or 1 school, hospital etc. in the event of failure. The warning system used there is a particular case of the more general system used in Hong Kong and is shown in Table 6.

Table 6.8.3(1). Landslip Warning Criteria - Japan (Ministry of Construction 1977).

		Rainfall during the past 14 days		
		100 mm	40 - 100 mm	Nil
Alert	Rainfall on the 15th day	50 mm recorded	80 mm recorded	100 mm recorded
Warning		50 mm recorded and 30 mm in one hour forecast	80 mm recorded and 30 mm in one hour forecast	100 mm recorded and 30 mm in one hour forecast

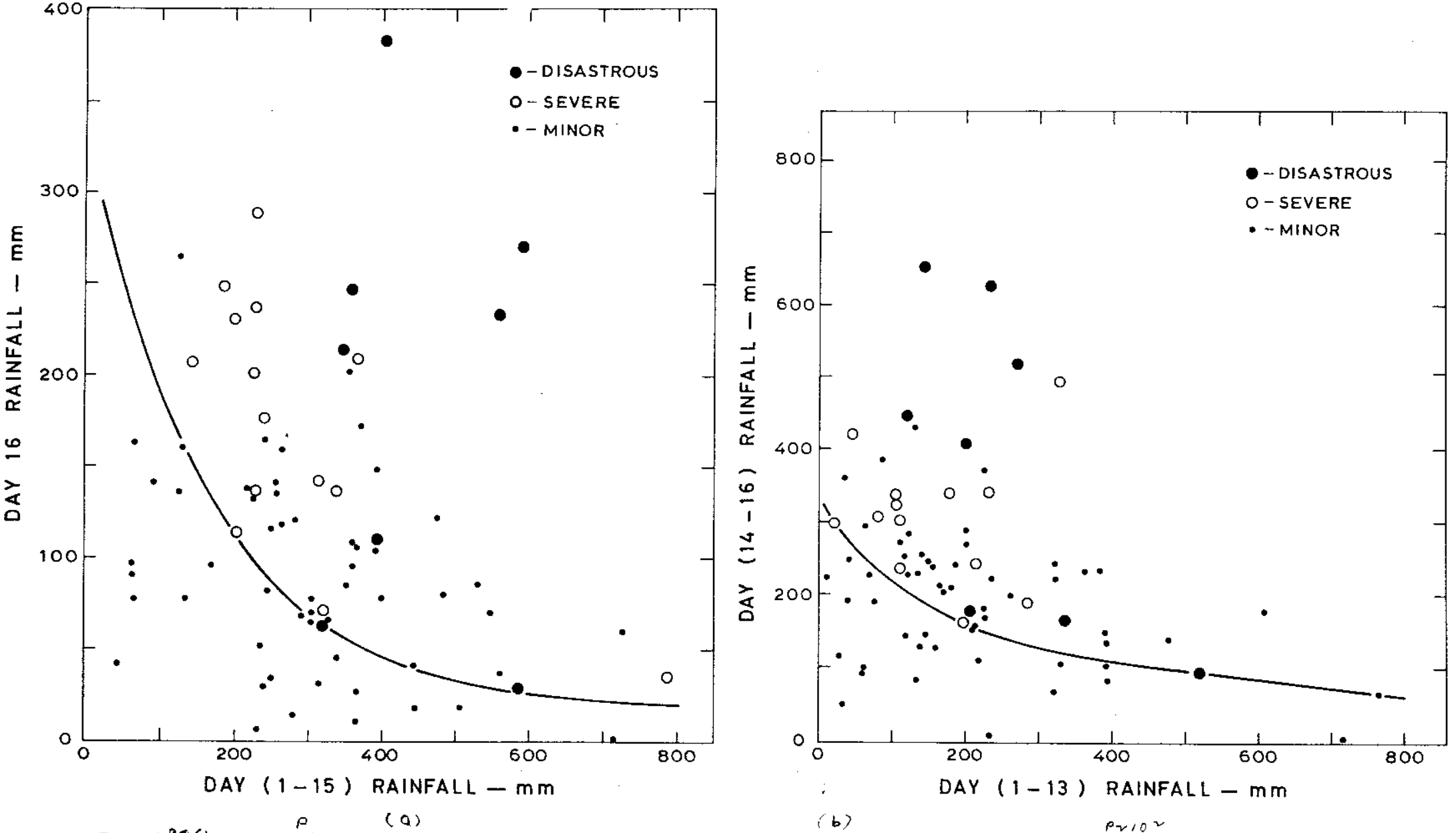

Fig. 6.83(1) Landslide occurrences in Hong Kong between 1930-1940 and 1946-1973 and the associated rainfall patterns. Slips occur on day 16.

.6 Tropical cyclone rainfall frequently arrives after a period of relatively dry weather. The critical rainfall total of 150 mm to 200 mm may then accumulate over two or even one day right at the end of a 15 day period so that the landslide warning criteria are quickly attained. The "alert" and "warning" situations may then arise almost simultaneously. In practice, this should not give rise to problems because a community should go into preparedness whenever the approach of a tropical cyclone is warned.

.7 Finally, the inherent variability of residual soils and their weakness under stress-relief conditions impose strict limitations on the reliability of design calculations so that there is always a finite risk of failure of any steep slope (Lumb 1975). Even when a slope is heavily instrumented and under close observation it is not possible to be sure of its stability. For example, in November 1971 Japanese engineers were saturating a hillside with water in an experiment to study the mechanism of slope failure when it slipped unexpectedly, killing fourteen research workers, invited guests and a television-camera crew. If the risk of failure of a slope is known to be high then attention should be given to ameliorating the consequences by constructing wide berms and relocating sensitive down-slope structures. If, however, the consequences are irreducibly grave then the project should be abandoned.

6.9.1 Rainfall probabilities

Engineering structures are usually designed to stand against heavy rain events of some specified probility. If the failure of the structure is likely to lead to major losses of life and property, then rare events that will on the average occur once in a few hundred years will have to be allowed for. However, quantitative rainfall record of such length is in general not available. In order to obtain an estimate of rainfall amounts of specified probabilities, the techniques based on the statistics of extremes such as those given in Gumbel(1960) may be employed. Hong Kong rainfall data have been so analysed by Bell and Chin (1968) and Kwong (1974).

According to the Gumbel distribution, the probability P(x) of the extreme value of a parameter in a sample being equal to or less than x is given by the equations:

$$P(x) = \exp(-\exp(-y)) \qquad 6.9.1(1)$$

$$y = \alpha(x - \mu) \qquad 6.9.1(2)$$

where α and μ can be determined empirically from the observed extremes of a number of samples. In practice, annual maximum values are analysed but longer periods may be used. The equations can be re-written as

$$x = \frac{1}{\alpha} y + \mu \qquad 6.9.1(3)$$

$$\mu = - \log_e[- \log_e P(x)] \qquad 6.9.1(4)$$

If a particular series of annual extreme rainfall values conforms to the Gumbel distribution, then when they are plotted on extreme probability paper, where the abscissa is related to P(x) by equation 6.9.1(4), they will lie close to a straight line given by equation 6.9.1(3). The plotting position P(x) is determined by

$$P(x) = 1 - \frac{m}{N + 1}$$

where m is the rank of the observed extreme and N is the total number of observed extremes. This procedure is illustrated by the following example.

The annual extremes of tropical cyclone rainfall were compared with rainfall due to other causes by Kwong (1974).It was found that there were one or two years in which no tropical cyclone

passed within about 550 km (300 nautical miles) of Hong Kong and the annual extreme rainfall value was quite unconnected with tropical cyclones. Hence extreme hourly rainfall values recorded at the Royal Observatory Hong Kong were extracted from groups of three consecutive years. Fig. 6.9.1(1) shows the results of the analysis plotted on extreme probability paper. The extreme hourly rainfall amounts due to tropical cyclones corresponding to return periods of 100 and 1000 years are about 95 and 130 mm respectively. Both values are roughly 20 mm lower than the corresponding values for non-tropical cyclone rain. Kwong (1974) noted that there was very little difference between the instantaneous rainfall rates in tropical cyclone and non-tropical cyclone situations corresponding to the same specified probabilities. The lower hourly rainfall amounts in tropical cyclones was attributed to the faster movement of rain cells in tropical cyclones.

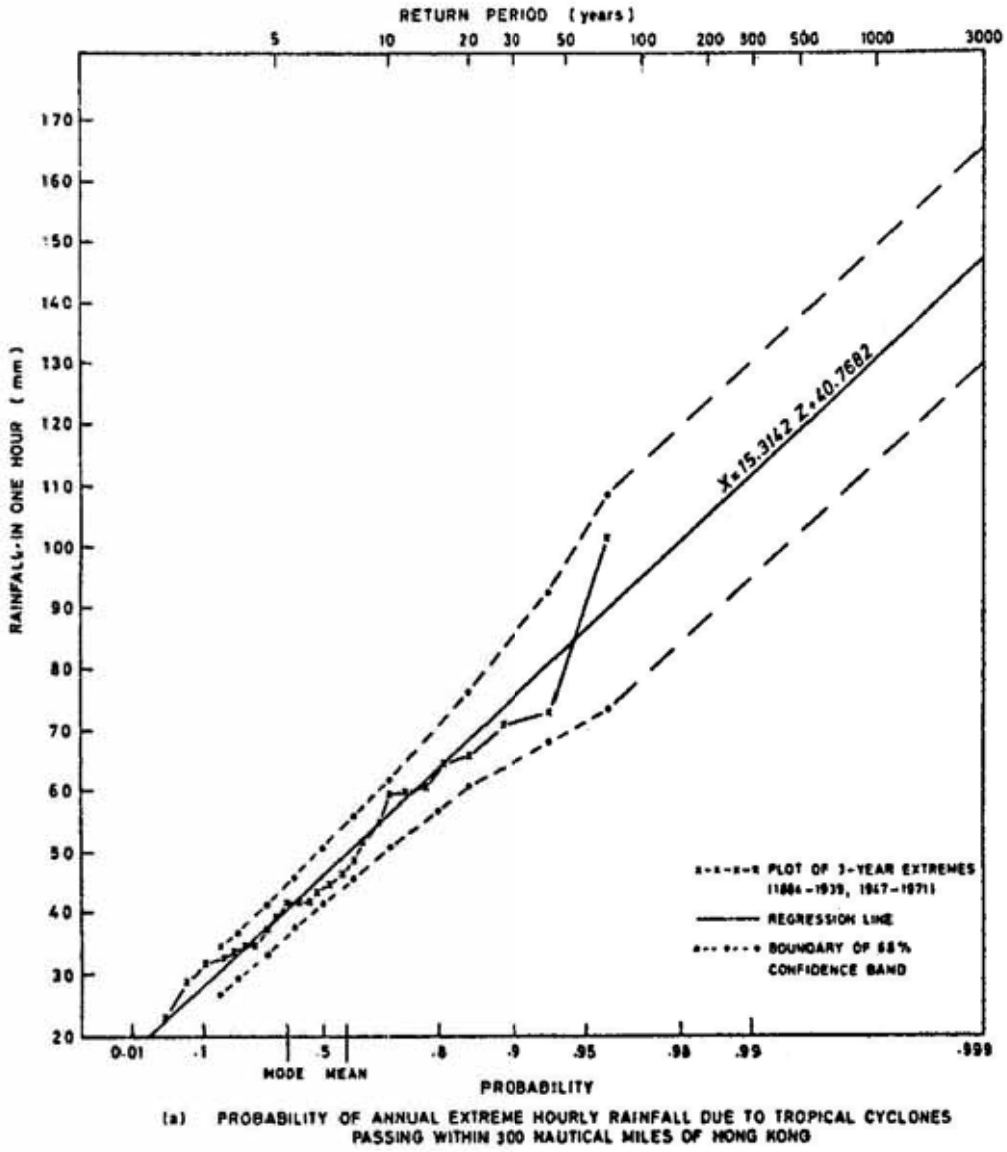

(a) PROBABILITY OF ANNUAL EXTREME HOURLY RAINFALL DUE TO TROPICAL CYCLONES PASSING WITHIN 300 NAUTICAL MILES OF HONG KONG

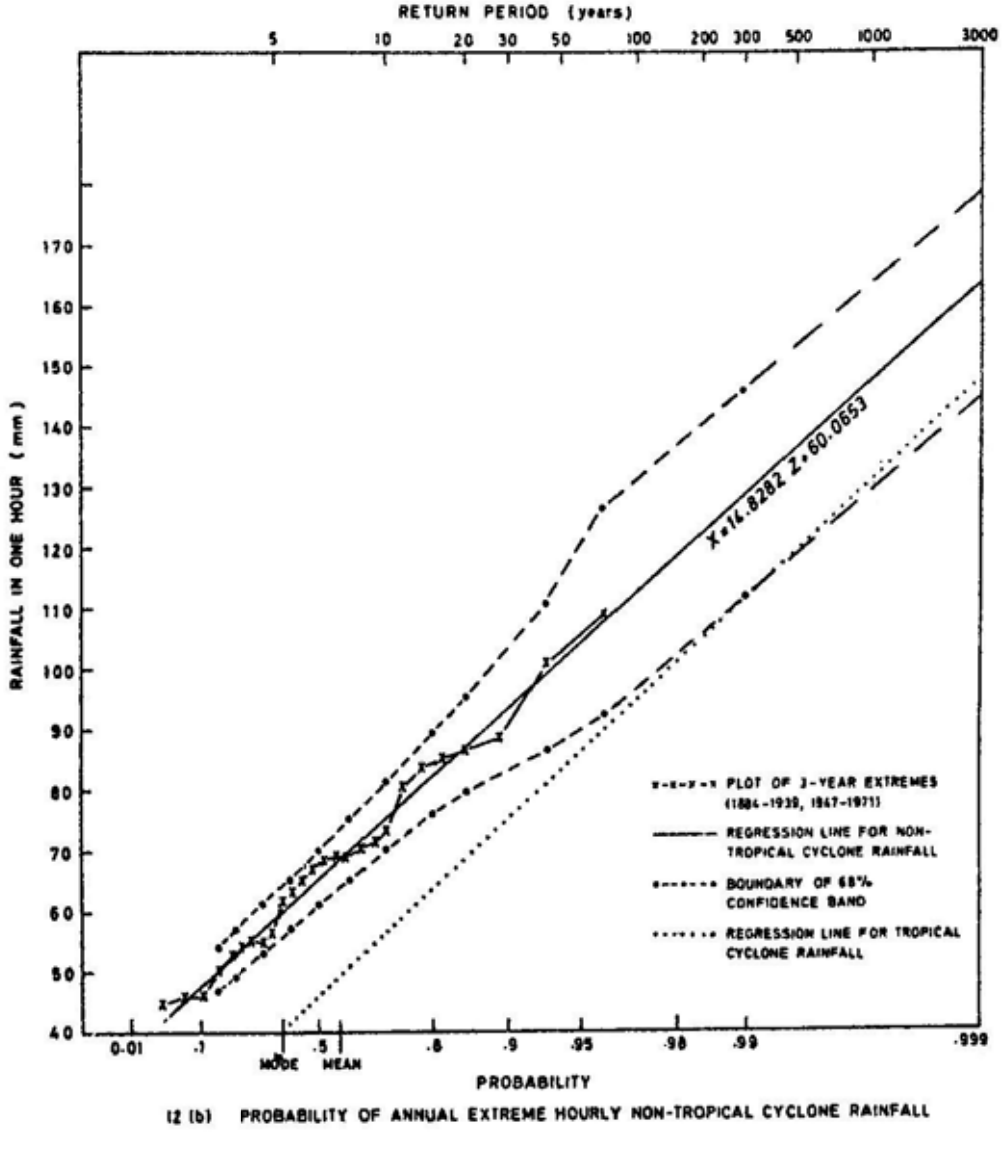

12 (b) PROBABILITY OF ANNUAL EXTREME HOURLY NON-TROPICAL CYCLONE RAINFALL

Fig. 6.9.1 (1) Probability of annual extreme hourly rainfall at the Royal Observatory, Hong Kong, estimated using the Gumbel Distribution (after Kwong 1974)

6.9.2 The Probable Maximum Precipitation (PMP)

Engineers often require knowledge of the magnitude of the most severe rainfalls likely over a given area. This information is required to assist in the safe and/or economic design of ~~catchwaters~~, spillways, dams and other rain-sensitive structures. To meet this requirement, hydrometeorologists compute the "probable maximum precipitation"(PMP) for the area concerned. P.M.P. has been defined as the theoretically greatest depth of precipitation for a given duration that is physically possible over a particular drainage area at a certain time of year. There are difficulties with this definition and ~~those~~ with that which defines PMP as the quantity of precipitation that is close to the physical upper limit for a given duration over a particular basin. Our knowledge of the complicated and interrelated processes in storms is limited, PMP values must therefore be estimates. We cannot answer the questions as to how "probable" or how "close"are the values given. To avoid these problems a more operational concept of PMP is often used in which "the definition of probable maximum is given by the operations performed on the data." (WMO 1974).

For practical details the reader is referred to the excellent WMO (1974) manual on the subject.

It is not proposed to go into all the details of methods used to estimate PMP but only to present an outline of them and highlight some of the features particular to tropical cyclones. Because of inadequacies in our understanding of rain mechanisms the starting point for determining the PMP is to obtain depth/area/duration data for all extreme storms in the region of interest. The rainfall is then maximised on the assumptions that firstly, rainfall can be expressed as the product of available moisture and the combined effect of storm efficiency and inflow winds and secondly, that the most effective combination of storm efficiency and inflow has either occurred or been closely approached in relevant extreme storms on record. On these assumptions three main steps are taken to maximise storm precipitation in areas without significant orographic effects. The steps are called "moisture maximisation", "transposition" and "envelopment".

Moisture maximization involves increasing the precipitation in the observed extreme storm to a value that is consistent with the maximum moisture in the atmosphere for the storm location and month of occurrence.

It is usually found that in tropical cyclones the moisture content is nearly always near maximum. A distance-from-coast adjustment (sect 6.9.2.1) may then be used. If the 12 h persisting dew point at 1 000 mb in the storm is less than that on record for the same location then the rainfall is increased by a moisture adjustment factor equal to the ratio of the maximum observed 12 h precipitable water to the storm 12 h precipitable water. The precipitable water in an atmospheric column is obtained from the 1 000 mb dew point and tables for a pseudo-adiabatic atmosphere.

Transposition involves considering extreme storms in other regions which are homogeneous relative to terrain and meteorological characteristic. By this means - transposition - the amount of data for a particular catchment can be greatly increased. Tropical cyclone rainfall may have to be adjusted for distance from the coast ~~when transposed~~.

Envelopment is the process of smoothly interpolating between derived rainfall maxima for different durations and/or areas. Such smoothing will yield greater values for some durations/areas than are derived from only moisture maximisation and transposition. The process also smooths the derived maxima from many storms and compensates for the random occurrence of extreme rainfalls because the available storms may not have had equally efficient rainfall mechanisms for all relevant areas and durations. Envelopment also gives values of PMP which are regionally consistent - anomalous values should be avoided unless they can be explained on topographic or meteorological considerations.

PMP estimates may be made for specific catchments or they may be generalised i.e. prepared for many places and mapped over a large area by drawing isolines. In many regions the PMP for the areas and durations of prime interest are attributable to tropical cyclones. Additional adjustments can then be made to the generalized PMP to allow for orographic effects within a catchment, ~~area and to compensate for distance of the catchment from the coast. Tropical cyclone~~ rainfall has been maximised for many places including the Mekong

river basin (Hydrometeorological Branch 1970), the U.S.A. (Schreiner and Riedel 1978) and Hong Kong (Bell and Chin 1968). The first study relates to a very large basin and the last to a very small one. ~~When a~~ In some cases, and particularly when a ~~very~~ long series of records is available for a raingauge network, ~~then~~ statistical - as opposed to physical - maximisation techniques can be used ~~to back-up standard methods of estimation~~ (Herschfield 1965, Bell and Chin 1968). At most locations where tropical cyclones determine the PMP it is found to be equivalent to ~~a~~ rainfall ~~of~~ amounts having a return period of several thousand years.

6921

6.9.2.1 Distance-from-coast adjustment

The general decrease in tropical cyclone rainfall with distance inland is attributable to the weakening and changing nature of the vortex and its distance from the moisture source. The normal transposition methods provide no decrease in storm rainfall with transposition inland because in most tropical areas the maximum low-level (1 000 mb), 12 h persisting dew points show little or no variation within about 1 000 km of the coast. Schreiner and Riedel (1978) adjusted for this effect using the graph shown in Fig. 6.9.2.1(1) This is based on a studies of the decrease of tropical cyclone rainfall with distance from the coast (Schwarz 1965, Schoner 1968) and has been extended to greater than 500 km using additional data. The graph is used to both increase the rainfall - for all areas and durations - for storms transposed closer to the coast and to decrease rainfall for tranpositions further inland.

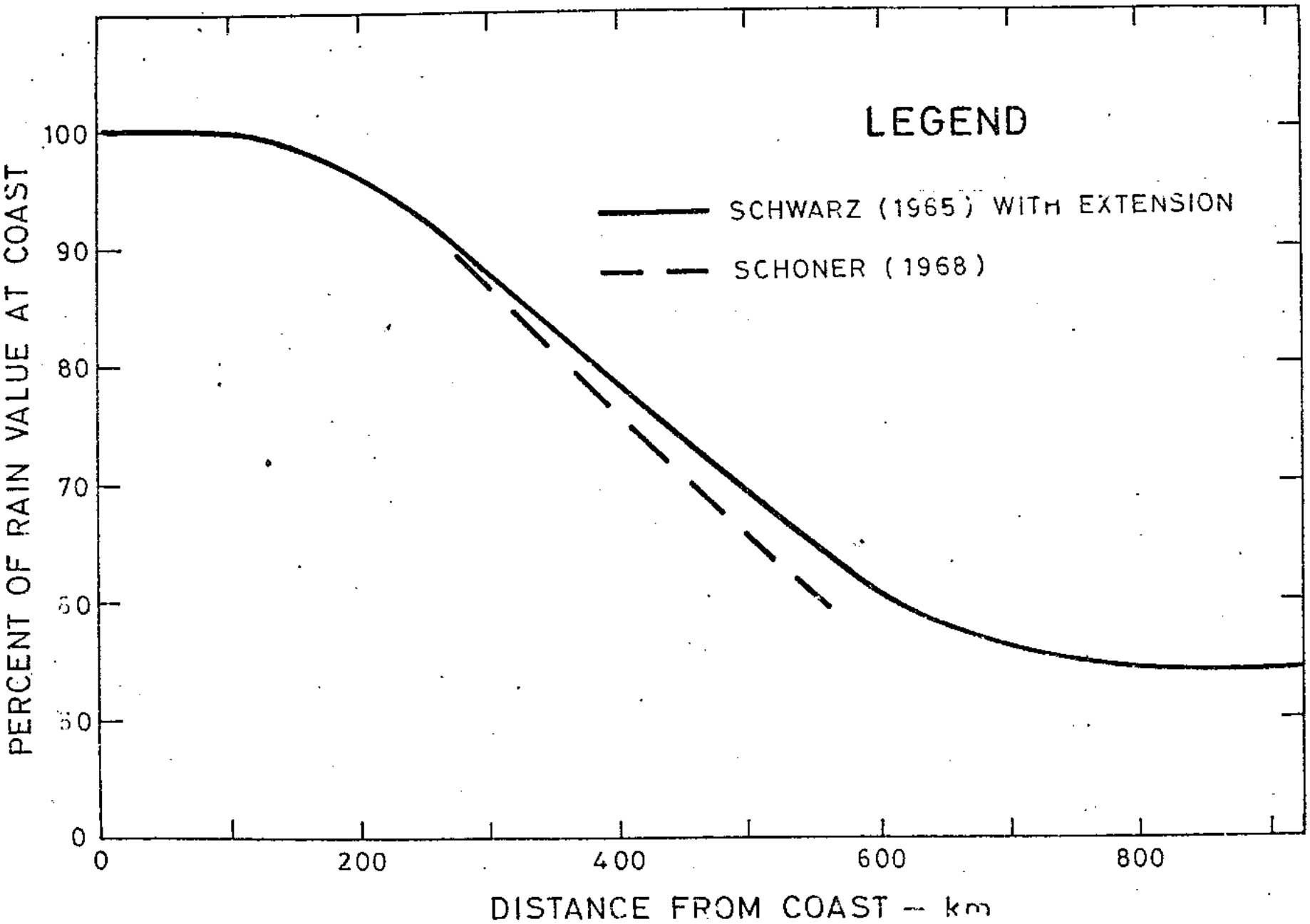

Fig. 6.9.2.1(1). The percentage reduction of tropical cyclone rainfall with distance inland from the coast (After Schreiner and Riedel 1978).

6.9.2.2 Topographic adjustments

When tropical cyclones encounter high ground it is found that firstly, there is an increase in rainfall with elevation on windward slopes (sect 6.4.2). The magnitude of the effect varies with the direction and speed of the moist low-level flow and with the extent, height and regularity of the mountain barrier. There is also a concomitant decrease of precipitation on these areas. Secondly, foot hills or first slopes provide enough lift to stimulate convective activity in the moist air in tropical cyclones. Thirdly, over an extensive area of gently rising terrain - such as to the west of the Mississipi - rainfall depths over areas greater than 2 590 km^2 decrease with elevation (Schreiner and Riedel 1978). There are two factors working in opposition to modulate the rainfall in such circumstances. Firstly, the gentle lifting intensities vertical motion and rainfall and secondly, as elevation increases the column of moisture available to rain producing mechanism is decreased. Schreiner and Riedel (1978) introduced an adjustment to be used in transposition of storm rainfall up or down such slopes. This was based on the variation in precipitable water with height in the atmosphere for maximum 12 h persisting dew points for the storm location and in the transposed location. The adjustment ranges between 6 and 10% per 305 m change in elevation, depending on the elevation of the storm and dew point values.

There are difficulties in seperating the orogenic from the convergence components of tropical cyclone rainfall. However attempts are made to estimate the former using single or multiple level models. If it is assumed that the airflow perpendicular to a mountain range is squeezed between the crest and some undisturbed upper nodal level, that the air is saturated and that its temperature decreases along rising streamline at the moist adiabatic rate , Then the rate of precipitation is given by the storage equation

$$R = \frac{\overline{V}_1 \left(W_1 - W_2 \frac{\Delta P_1}{\Delta P_2}\right)}{Y} \qquad 6.9.2.2(1)$$

where R is the rainfall rate in cm/s; $\overline{V}_1$ the mean inflow wind speed perpendicular to the ridge in cm/s and W_1 and W_2 are the liquid water

equivalents in cm of the inflow and outflow precipitable water; Y is the horizontal distance in cm over which the air rises and Δp_1 amd Δp_2 are the pressure differences in mb between the top and bottom of the inflow and outflow, respectively. Using the relationship between specific humidity q and precipitable water W

$$W = \frac{\bar{q}\ \Delta p}{g e} \qquad 6.9.2.2(2)$$

or the approximate relationship between W and the mean mixing ratio $\bar{w}$

$$w \approx 0.0102\ \bar{w}\ \Delta p \qquad 6.9.2.2(3)$$

we can derive the storage equation for a layer as

$$R \approx \frac{0.0378\ V_1\ \Delta P_1\ (\bar{w}_1 - \bar{w}_2)}{Y} \qquad 6.9.2.2(4)$$

where R is in mm/h, $\bar{V}_1$ in m/s, Y in km, Δp_1 in mb and $\bar{w}$ in g/kg. The total precipitation is obtained by adding the rainfall rate from all layers up to the nodal surface. Allowance has to be made for the trajectory of raindrops which will be displaced by the strong tropical cyclone winds. Some precautions are necessary to ensure that the addition of the oreigenic and convergence contributions do not over-estimate the PMP. Attempts have to be made to ensure that the convergence component contains no orogienic contribution and vice versa.

6.9.2.3 Other considerations

The potential of looping or slow moving tropical cyclones to cause extreme rainfalls was illustrated in sections 6.3.2 and 6.3.6. Another example important for PMP studies in the USA and elsewhere, is that of hurricane Easy. This storm moved in a slow loop just off the west coast of Florida between 3-7 September 1950. The resulting rainfall over relatively flat terrain at Yankeetown - near 29°N on the west coast of Florida - constitutes the greatest observed rainfall in the USA for area from 26 to 5 180 km^2 and durations from 18 to 72 hours. When the forward speed of other major rain-producing hurricanes was reduced to the speed of Easy and their rainfall recomputed then the resulting non-oriegenic rainfall depths were of approximately the same magnitude as in the Yankeetown storm (Schreiner and Riedel 1978). Maximisation of tropical cyclone rainfall by reducing the speed of movement to the lowest speed on record for the region - usually a recurving or looping situation - is a technique that could be applied also in other tropical cyclone areas.

When preparing PMP for the Meking River Basin (Hydrometeorological Branch 1970) adjustments were made for latitude. It was considered that tropical cyclones have full potential for rainfall production when northward of 15°N but that this decreased southward with no typhoons having affected Malaya (Watts 19) The rainfall potential was therefore scaled down from 100% at 15°N to zero at 5°N.

Mountain ranges can act as a barrier to the inflow of moisture from the ocean. For example the mountains to the east of the Mekong basin cut off moist inflow from the China Sea to the lee areas. To adjust for this an effective barrier height is chosen. The ratio of [illegible] content above the barrier to the total moisture content above sea level, before the barrier is used as a barrier adjustment.

In transferring the Yankeetown hurricane northward Schreiner and Riedel (1978) considered that reduction of the sea surface temperature offshore would limit the inflow of moisture and call for some reduction in rainfall amounts. The sea surface temperature was averaged within circles of diameter 644 km as this was considered representative of the area from which a large tropical cyclone could process the moisture within

a 24 h period. The average temperature of the offshore circles determined the precipitable water, this was expressed as a fraction as that at the latitude of the Yankeetown hurricane (29^{o}N) to get adjustment factors for reducing rainfall with northward (colder sea) displacement.

When using the PMP to develop a critical flood hydrograph it is necessary to consider the initial height of the stream flow and terrain conditions. For large catchments it is necessary therefore to consider the effects of a tropical cyclone having occurred prior to the PMP. The larger the drainage the more probable it is that two tropical cyclones should be separated by a relatively short interval of time and the less critical is the similarity of their tracks indeed, it was found that a displacement of one track relevant to the other may produce a more critical hydrograph. A close sequence of tropical cyclone was particularly important in estimating the probable maximum flood at sites on the Mekong river. The probability of storms following one another at certain displacements over the Mekong basin is given in Table 6.9.2.3(1). The question of what severity should be allocated to the antecedent storm to be used with the PMP is difficult to answer. The passage of one storm is not known to influence the rain potential of the next. The probability of sequences of wet storm is best decided by examining the data worldwide. The north American experience is that one storm can produce up to 70% of the rainfall of the greater of the two with a time interval of 3 days. Two couplets were adopted for the Mekong, the first being an interval of 3 days between storms with the first having yielding rainfall 50% of that of the PMP. The second pair had a four day interval with the prior storm being 65% of the PMP.

6.9.3 Buildings and T.C. rainfall

Large raindrops carried by winds of hurricane force impact on window panes with a frightening noise as if each drop were made of stone. The volume of rain intercepted by a window or other vertical surface perpendicular to the wind increases with wind speed. At speeds of hurricane force the intercepted rainfall will be several times that falling on a horizontal surface of the same area. Wind pressure forces any accumulated water through window surrounds - it then enters the building as a jet - or it may soak through some walls. The intercepted rain drains off such vertical surfaces under the primary control of drag forces set up by the local airflow. In this way water on the upper windows of tall buildings may be seen to "drain" away upwards, against gravity, but in accordance with the pressure distribution and wind flows shown in Fig. 5. The flow of water falling onto terraces or flat roots is similarly controlled by airflow and not by gravity. Drains - even at the highest points of such surfaces - can therefore help to prevent excessive flooding.

In the free atmosphere, raindrops fall vertically at a terminal speed determined by their sizes and they are carried along horizontally by the mean wind over one second or more. The ratio of the flux of rainwater through the horizontal plane F_h to that through the vertical plane perpendicular to the wind, F_v, is equal to the ratio of the fall velocity of the drops, w, and the wind velocity, v, so that:-

$$F_h / F_v = w/v \qquad (6.9.3(1))$$

F_h is, of course, the rainfall, R, so that the flux of water through the vertical plane is given by

$$F_v = R \frac{v}{w} \qquad (6.9.3(2))$$

In practice, the catch by a vertical wall will depend on the drop-size distribution - larger drops have greater w - and on the efficiency of deposition on the wall e.g. some drops, especially small ones would be carried around the edges of a wall of small dimensions. To determine experimentally the relationship between F_v and R, Ishizaki et al (1970) measured the rainfall intercepted by a wall 4 m high and 7 m wide and

compared the catch with that of a standard 20 cm raingauge fitted with wind shield. They found that the ratio of the rainfall on the wall (F_v) to that in the gauge was given by

$$F_v / R = 0.14\ v \qquad (6.9.2(3))$$

up to wind speeds of about 30 m/s at which point the ratio was about four. The constant of proportionality, 0.14 s/m, corresponds to the reciprocal of a fall speed, w, of 7.14 m/s. This fall speed corresponds to that of raindrops with diameters of about 2.3 mm - a size close to that of drops of median volume, Do, in heavy ($\geq$100 mm/h) tropical-cyclone rain. The size of median volume drops in heavy rain is illustrated in Figs. 10.4(2) and 10.4(4).

It is of interest to use eqn (6.9.2(3)) to calculate how much water will be intercepted by a wall or window in typhoon conditions. Rainfall rates of 150 mm/h are frequently sustained over several minutes as is shown in Fig. 6.3.6(1). If this rainfall is driven by winds of 30 m/s perpendicular to a wall it would yield about 10.5 $\ell/m^2/min$. Heavier bursts of rainfall having a rate of say 300 mm/h would yield 21$\ell/m^2/min$. It is easy to appreciate that, during the combination of high wind speeds and heavy rain in the ~~eye~~ regions ~~wall~~ of tropical cyclones, walls need not be very extensive in order to intercept several thousand litres of rainwater per minute.

REFERENCES

Cheng, T.T. 1971. "Response of a Jardi-rate-of-rainfall Recorder". Tech. Note (Local) No. 13, Royal Observatory, Hong Kong.

Government of Hong Kong, 1977,"Report on the Slope Failures at Sau Mau Ping August 1976"

Lumb, P. 1965. The residual soils of Hong Kong. Geotechnique 15, 180-194.

Lumb, P. 1975. Slope failures in Hong Kong. Q. J. Engng Geol. 1975, 8, 31-65.

Murayama, N. and Fukatsu, H. 1969. Limit of detection of rainfall over Owase by Nagoya Weater Radar. Tokan Gijutsu News, 10, 20-25.

Sakakibara,H and Takeda, T. 1973. Modification of typhoon 7002 rainfall by orographic effect. J. Met. Soc. Jap., 51, 155-166.

Staff Members, Division of Meteorology, Tokyo University. 1969. Precipitation bands of typhoon Vera in 1959 (part I). J. Met. Soc. Japan, 47, 298-309.

1970. Precipation bands of typhoon Vera in 1959 (part II). J. Met. Soc. Japan, 48, 103-117.

Takeda, K. and Motoda, Y. 1965. Effect of orography on typhoon rainbands. Tenki, 12, 371-376.

Takeda, T., Moriyama, N. and Iwasaka, Y. 1976.
A case study of heavy rain in Owase
area. J. Met Soc. Japan, 54, 32-41.

Yanagisawa, Z., Aoyagi, J. and Kambayashi, N. 1974.
Radar analysis on the precipation around
Owase. Met. & Geophy. 25, 51-79.
(In Japanese)